Optimization of Perceptual Steganography Capacity Using the Human Visual System and Evolutionary Computation

Raniyah Abdullah Wazirali

B.Sc. in Computer Science (Taif University)
M.Sc. in Information Technology (University of Technology, Sydney)

Supervisor: Dr. Zenon Chaczko

A Dissertation submitted to
The University of Technology, Sydney
In fulfillment of the requirements for the degree of
Doctor of Philosophy

School of Computing and Communications
University of Technology, Sydney
Sydney, NSW, AUSTRALIA

March 2016

Dedication

I dedicate this to my parents Abdullah and Afnan for their endless support, sincere prayers and encouragements throughout my life and my PhD

I dedicate this to my husband Abdulrahman and my son Battal for their continuous love, sacrifices and patience throughout my years of study

اهداء

لحظات يقف فيها المرء حائرا عاجزا عن التعبير كما يختلج في صدره من صدره من تشكرات لأشخاص أمدوه بالكثير و الكثير ، لحظات صار لابد أن ينطق بهما اللسان و يعترف بفضل الآخرين اتجاهه لأنهم و بصراحة كانوا الأساس المتين الذي بني عليه صرح العلم و المعرفة لديه، و أناروا سبيل بلوغهما

فأهدي ثمرة جهدي التي طالما تمنيت إهدائها و تقديمها في أحلى طبق

إلى التي حملتني وهنا على وهن، و قاست و تألمت لألمي، إلى من رعتني بعطفها وحنانها و سمعت طرب الليل من أجلي، إلى أول كلمة نطقت بها شفتاي أمي الغالية أفنان.

إلى الذي عمل و كد و جد فقاس ثم غلب حتى وصلت إلى هدفي هذا، إلى المصباح الذي لا يبخل إمدادي بالنور، إلى الذي علمني بسلوكه خصالا أعتز بها في حياتي والدي العزيز.

إلى شريك حياتي و توأم روحي الذي شجعني بحبه و حنانه و دعمه الغير محدود على مواصلة مسيرتي العلمية، إلى زوجي الحبيب عبدالرحمن

إلى صغيري الذي كان دافعي و مصدر اصراري و قوتي، إلى ابني و فلذة كبدي بتال

وإلى رياحين حياتي في الشدة و الرخاء إخوتي وأسرتي جميعاً.

ثم إلى كل من علمني حرفاً أصبح سنا برقه يضيء الطريق أمامي.

وفي الأخير أشكر كل من ساهم في إنجاح هذه الرسالة من بعيد أو من قريب.

Originality Statement

I certify that the work in this thesis has not previously been submitted for a degree nor has it been submitted as part of requirements for a degree except as fully acknowledged within the text.

I also certify that the thesis has been written by me. Any help that I have received in my research work and the preparation of the thesis itself has been acknowledged. In addition, I certify that all information sources and literature used are indicated in the thesis.

Signed .....

Date .....

Acknowledgments

All praise is due to Allah (Glorified and Exalted is He), without his boundless favours and blessings none of this work could exist.

Throughout the course of this Thesis, there have been several people who have afforded me with direction, motivation and provision for finishing this work. Firstly, I am indebted to my supervisor Dr. Zenon Chaczko for his continual guidance, support and suggestion. Without his insight, this work would not be possible. I would like also to thank Dr. Roman Danylak for his encouraging comments and suggestions throughout the reviewing stage. His participation was vital to the completion of this thesis.

On the personal front, I would like to express my appreciation to my parents, husband, brothers and sisters, for their nonstop love, truthful prayers and support during the research. I must also express my thanks to all my colleagues and friends in the Department of Computing and Communications at the University of Technology, Sydney.

Lastly, I would like express my thanks to the late King Abdullah of Saudi Arabia for the King Abdullah Foreign Scholarship Program and the Saudi Arabia Culture Mission for providing a chance and funding to engage this research.

Abstract

Efficient solutions for the purpose of delivery of information are called for by the revolution of internet. However concerns and problems over security, distribution of digital content and encapsulation of media artifacts have arisen as a result of these phenomenal developments. Hence, it has become necessary to seek capabilities to transport and secure multimedia with its meta-data in a safe way. Steganography has evolved as an enabler of multimedia applications keeping secret communication and embedded captioning secure.

There is a tolerable outcome that occurs between imperceptibility and steganographic capacity that fit right into the mix. For instance, the more subtle elements are hidden within the cover object having higher capacity, the more degradation is exhibited towards the carrier file, resulting in an increase in the distortion attributed to the information being concealed and at the same time, decreasing the stego file quality.

Suitable use of Evolutionary Algorithm and effective use of the weaknesses of Human Visual System in steganography are investigated in this thesis. Firstly, two high capacity steganography approaches are developed with the use of aforementioned features. The first method aims to overcome the limit capacity of edge based steganography in the spatial domain. The second method proposes a proper threshold selection for each coefficient which increase the capacity of transform domain. An estimate of the embedding rate based on image complexity is also proposed. Moreover, since peak signal-to-noise ratio (PSNR) is largely used as a measure of quality of images of stego, the reliability of current quality assessment metrics for stego images is also

evaluated at the third stage. Follow by developing an Anticipatory Quality Assessment Metric for effective imperceptibility measurement.

All proposed methods are aimed to assist the optimization of the statical and visual characteristics in the cover images while hiding large size of information. To reveal impressive imperceptibility and capacity of the proposed method over the existing dilemmas, a broad range of requirements have been carried out. To indicate the utility and value of all techniques proposed, they all have been empirically validated. The main aspects of image steganography are improved by the suggestions and methods, and are revealed by the results.

Nomenclature

AQAM Anticipatory Quality Assessment Metric

BPCS Bits Plan Complexity Structure

BPP Bits per pixel

CSF Contrast Sensitivity Function

DCT Discrete Cosine Transform

DFT Discrete Fourier Transform

DoG Differences of Gaussian

DWT Discrete Wavelet Transform

EA Evolutionary Algorithm

EBE Edges based data embedding method

GA Genetic Algorithm

GP Genetic Programming

HVS Human Visual System

IQM Image Quality Metric

JND Just Noticeable Distortion

LOG Laplacian of Gaussian

LSB Least Significant Bits Substitution

LSBMR LSB Matching Revisited

MOS Mean Opinion Scores

MSE Mean Square Error

NVF Noise Visibility Function

OPAP Optimal Pixel Adjustment Process

PLCC Pearson Linear Correlation Coefficient

PM1 Plus Minus 1 Algorithm

PSNR Peak Signal to Noise Ratio

PSO Particle Swarm Optimization Algorithm

PVD Pixel Value Differencing

ROI Region of Interest

RPF Random pixel embedding method

SDoG Summation of Differences of Gaussian

SQE Subjective Quality Evaluation

SROCC Spearman Rank Order Correlation Coefficient

SSIM Structural Similarity Index

UIQI Universal Image Quality Index

WPM Watson's Perceptual Model

wPSNR Weighted Peak Signal to Noise Ratio

Terms and Definitions

- **Steganography** is the science of concealing information within another non-secret information in an invisible way. It is derived from the Greek “steganos”, meaning "covered”. Graphos is also Greek meaning "writing". Steganography mainly aims to hide the presence of the message.
- **Steganoalysis** is the science of detecting hidden message using steganography.
- **Watermarking** is a pattern of bits inserted into a digital image, audio or video file that identifies the file’s copyright information (author, rights, etc.).
- **Cryptography** is the science of transforming information into an unreadable format.
- **Embedding/Insertion** is the process of mapping one file into another.
- **Extracting** is the process of obtaining the hidden message.
- **Cover-image/carrier** is the name of the original file that used to hide the message inside it.
- **Stego-image** is the name of the file after the embedding process. The cover image and the stego image must be identical.
- **Multi-dimensional media** is the integration of several types of media into one.
- **Encapsulation** is the process of packing multi-media into a single media.
- **Imperceptibility** is the quality of non perceptibility of the hidden file.
- **Capacity** is the number of allowable bits which can be inserted safely without any visible or statistical degradation.

- **Secret Message** is the name of the file or information that is hidden from general view.
- **Metadata** is a set of data that gives details about other data.
- **Optimization** is the process of enhancing and improving the stored results as best possible.
- **Fitness Function** is an objective measure of how close one is to a given solution.
- **Perception** is the ability of noticing something through the senses.

Contents

List of Figures

List of Tables

Chapter 1

Introduction

1.1 Overview

Recently, information communication technologies, including multimedia, have become increasingly complex, powerful and popular. The Internet connects a rapidly expanding audience through a wide array of services using corresponding delivery methods that are efficient and effective. However, the rapid expansion and diffusion of the Internet has not only made communication, commerce, and education accessible, but has also led to significant concerns related to the content and handling of multimedia. The challenge is to protect media content and its meta-data to deliver advance multimedia structures. With the need for protection, the technique of steganography has proliferated. Steganography aims to combine information and data to secure communication, especially through multimedia.

In short, steganography is the science of concealing information through a certain process of hiding an object within another object in the image (Figure 1.1). This is primarily based on the idea that the information that is hidden should not be visible to the human eye, often referred to as the Human Visual System (HVS) by embedding objects within an appropriate carrier.

Two essential criteria are required for any steganographic system: image imperceptibility; and payload capacity. However, these are a conflicting cri-

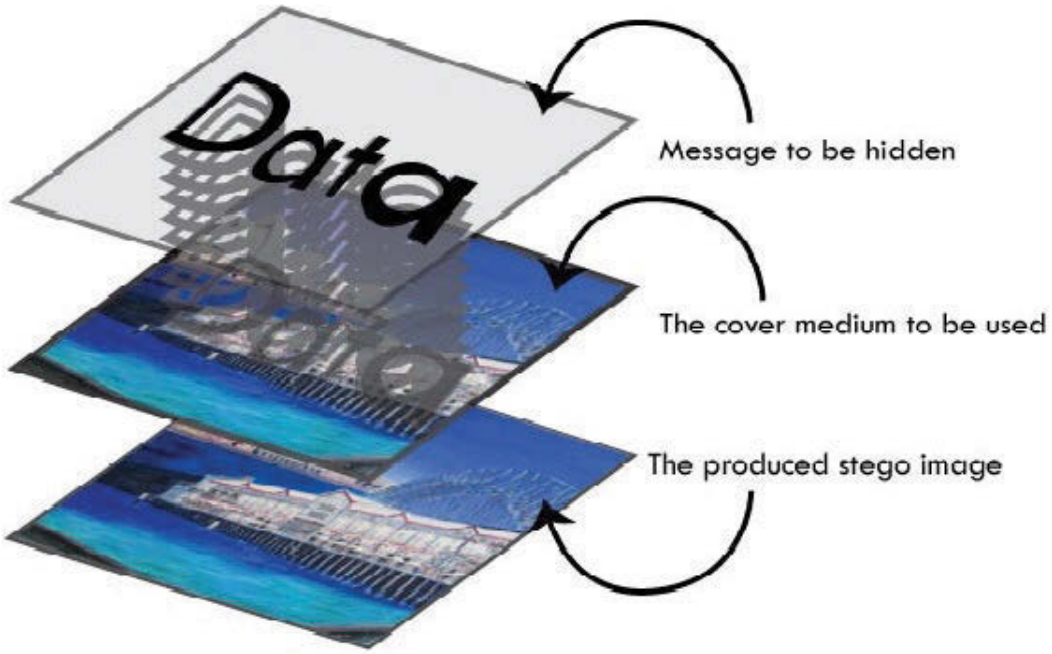

Fig. 1.1: Steganography concept

teria. The more data inserted into the carrier, the more noise added. The effectiveness of steganography and the hiding of digital data is measured by the volume of data hidden. However, the cover image should be embedded at an optimum level, which is seen as a tradeoff in the process. Steganography therefore can be seen as an optimization problem to achieve effective levels of image embedding (Khan et al., 2004; Ohnishi and Matsui, 1996; Wang et al., 2001; Fard et al., 2006b; Dasguptaa et al., 2013; Mandal, 2000; Wazirali et al., 2014; Westfeld and Andreas, 1999).

1.2 Research Motivation

Steganography can either be text based or media (images, audio or video) based. Media-based steganography is considered to be stronger and more effective than the one which is text based. Steganography is stronger and safer compared to cryptography as the sent message hardly arouse attention that can subject information being disseminated to suspicion and scrutiny.

Plain text, even if unbreakable, will easily arouse suspicion and this may lead to problems especially in countries where encryption is not allowed (Shi, 2005).

While the main purpose of steganography is information security, it can also be applied in a variety of commercial and scientific fields where multimedia tools are used; advanced data structure; document tracking tools: document authentication; smart ID; military agencies; and medical imagery systems. Similarly, it can also be used to devise data structures used in the embedding of description information within a file, resulting in system to system transmission of meta information while retaining the meta-data. To illustrate this, the simple embedding of details into a certain picture could compromise the process by adding more details about the image. This shows that multi-dimensional multimedia is capable of solving hard disk space problems related to the saving of media content. When applied to big data, the problem of allocating and requiring a certain volume of the hard disk in recording details and multimedia information can be solved through the proper steganographic system. For instance, there is a potential benefit of steganography in terms of reducing the traffic in a network.

Hence, there is a need to develop a highly efficient and effective service model for businesses and IT infrastructure that provides advanced multimedia structures. One way to provide this, is to integrate steganography and apply it to multimedia with the aim of producing new muti-dimensional multimedia.

1.3 Research Problem

The current media and communication domain is dominated by digital multimedia artifacts. In essence, digital content usage has turned out to be a reality to most individuals. Media has facilitated the access to essential resources, training of essential skills and efficient time management. However, the information processing tasks, which are performed by such media, still need to be developed significantly.

Most of the existing steganography approaches focus on the embedding process without considering the right position of inserting data or the content of the cover image. As a result, only few data can forms be hidden safely. The effectiveness of concealing data is dependent upon the balance of imperceptibility versus capacity. The conflict between these properties, which results in a more challenging problem for steganography, could consider the image content and complexity to effectively hold a balance between the conflicting tradeoff requirements. In order to resolve the conflict, techniques of steganography are used which supports a model vision in order to embed data in an invisible manner. Human Visual System (HVS) is a mathematical model simulating the human way of perception.

The weaknesses of human perception can be used in steganography to provide effective approaches. However, integration is not an easy task as it requires to understanding of the combination between vision science research and multimedia concept. Moreover, for the purpose of an optimum tradeoff between robustness and imperceptibility, optimum embedding level for every region of the image cover is required. Genetic Algorithm and Genetic Programming will be used and trained to achieve the below goal and to achieve the best possible solution.

1.3.1 Research Hypothesis

Is it possible to mitigate weaknesses of human perception to generate robust, highly imperceptible and large capacity steganogaphic multimedia artifacts using evolutionary approaches.

1.3.2 Research Aim

There is a need in advanced multimedia to address big data issues and produce better multimedia tools. Therefore, the research aim is to demonstrate effective solutions to address the problem of embedding multi dimentional information in multimedia objects. Steganography is an effective method to deal with encapsulation to allow embedding of information in multimedia

objects. Currently, there are many methods for the same purpose but a key limitation is that storage is very limited, which in turn limits the number of messages. However, through this thesis it is preferred to use potentially all available spaces of an image to store different meta-data with no visible distortion.

1.3.3 Research Objectives

In order to achieve the aim of optimizing the capacity while preserving the imperceptibility of the stego object, five main investigations will be accomplished. Each investigation will be direct a major research objective of this research. These are:

1. Increase capacity of edge-based steganography
2. Develop perceptual threshold for transform based steganography
3. Design an estimate payload capacity based on image complexity
4. Design an effective anticipatory quality assessment metric by integrating HVS characteristics
5. Develop of an image sharing application based on seganography

1.4 List of Publications

- **Wazirali, R.,** Chaczko, Z. and Kale, A., 2014, "Digital Multimedia Archiving based on Optimization Steganography System", In Asia-Pacific Conference on Computer Aided System Engineering (APCASE'14), (pp. 82-86) IEEE.
- **Wazirali, R.**, Chaczko, Z. and Carrion, L., 2015. "Bio-informatics with Genetic Steganography Technique", In *Computational Intelligence and Efficiency in Engineering Systems* (pp. 333-345) Springer International Publishing.

- **Wazirali, R.** and Chaczko, Z., 2015. "Hyper Edge Detection with Clustering for Data Hiding", *Journal of Information Hiding and Multimedia Signal Processing.*
- **Wazirali, R.** and Chaczko, Z., 2015. "Data Hiding Based on Intelligent Optimized Edges for Secure Multimedia Communication", *Journal of Networks,* Vol. 10, No. 8, pp.477-485.
- **Wazirali, R.** and Chaczko, Z., 2015. "EA based Heuristic Segmentation for Efficient Data Hiding", *International Journal of Computer Applications*, Vol. 118, No. 5.
- **Wazirali, R.** and Chaczko, Z., 2015. "The Use of HVS to Estimate Perceptual Threshold for Imperceptible Steganography", in the 30th International Conference on Image and Vision Computing, New Zealand, (IVCNZ'15).
- **Wazirali, R.** Slehat, S., Chaczko, Z., Borowik, G. and Carrion, L., 2015. "Objective Quality Metrics in Correlation with Subjective Quality Metrics for Steganography", Asia-Pacific Conference on Computer Aided System Engineering (APCASE), pp. 238-245 IEEE.
- **Wazirali, R.** and Chaczko, Z., 2016. "Estimating Optimum Embedding Capacity based on Image Complexity Using Human Visual System", *Multimedia Tools and its Applications Journal* (Submitted).
- **Wazirali, R.** and Chaczko, Z., 2016. "Anticipatory Quality Assessment Metric for Steganography Imperceptibility Evaluation", *Journal of Information Hiding and Multimedia Signal Processing* (Submitted).

1.5 Organization of the Thesis

The rest of this thesis is organized as follows;

- **Chapter Two** introduces the theoretical background adopted for this thesis and provides the literature, state of art and techniques.

- **Chapter Three** discusses the theoretical, mathematical and the methodological perspectives utilized in the thesis.

- **Chapter Four** develops a novel edge-based steganographic approach to expand the capacity of steganography, relying upon the edge with least modification in stego file. Differences of Gaussian (DoG), Contrast Sensitivity Function (CSF) and Genetic Algorithm (GA) features are prominent in the work. The goal is to strengthen the framework achieved by utilizing the perceptible edge from the DoG which directs the consolidated framework. Supplementary usage of both CSF and GA facilitate the optimization of the embedding capacity by developing the irregular edge visibility; this depends upon the size of the secret data.

- **Chapter Five** analyzes the DWT coefficient of the cover image to select a proper perceptual threshold for each coefficient based on the content of the cover image. This allows high embedding rate and ensures less distortion of the cover image. Moreover, the use of DWT in this proposed model is based on the threshold's multi-resolution hierarchical characteristics as well as its lower resolution embedding and low cost detection.

- **Chapter Six** proposes an estimation of optimal capacity of steganographic techniques used to combine Human Visual Model (HVS) with Genetic Programing (GP) to produce a proper embedding rate for each coefficient. The process aims to generate an embedding rate that is appropriate for each coefficient. The combination of HVS and GP enables the balancing of hiding capacity and imperceptibility in relation to perceptual mapping of secret data based on the cover image's components. Furthermore, the model is based on the objective of estimating the DCT's embedding capacity through an improved version of the Genetic Algorithm and Watson's Perceptual Model; this is done in order to offer minimum error distortion based on the measurement of image complexity through HVS.

- **Chapter Seven** proposes an objective quality evaluation on predicting the subjective quality using anticipatory objective. Anticipatory Quality Assessment Metric (AQAM) is an objective assessment metric that simulates the judgment of human perception. The primary objective of this chapter is to develop a systematic method of using HVS for image steganography quality assessment.

- **Chapter Eight** summarizes the research findings based on achieving the research objectives. Additionally, important future research avenues are suggested offering furthur progress to this major area of research.

Chapter 2

The Art of Steganography

As a practice, steganography is not new. Only recently it has become recognizable as field of study with a methodology for the design of multimedia digital systems. The chapter provides an overview of concept, characteristics, techniques and solutions that integrate various type of multimedia. The properties related to steganography are measured and explained in order to obtain a robust steganographic technique. This is followed by a discussion of the three categories of approaches used in steganography: frequency domain; spatial domain; and adaptive steganography, followed by a discussion of applications of the technique in practical and valuable ways.

2.1 Background

Digital artifacts often contain more information that can not perceived by human naked-eye. Therefore, the old saying "what you see is what you get" may no longer hold true. Parts of multimedia may not always be what can be seen by the human naked eye; they might conceal other images, sounds or texts that are embedded in media.

Steganography is the science of embedding elements within another element. It is aimed at concealing information or a file to avoid arising suspicion. There are three key criteria in the construction of steganographic system; robustness; stego image quality; and payload capacity. The interaction of

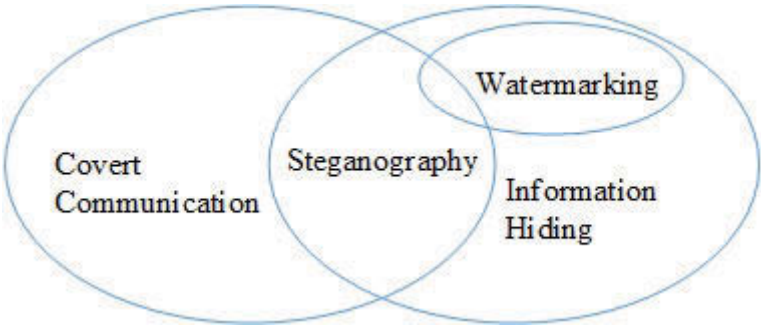

Fig. 2.1: Relationship between steganography and other fields

these criteria may determine the outcome of the image and embedding of the data. For instance, steganographic payload capacity plays a big role in relation to image imperceptibility. A higher capacity of embedded data could lead to a higher rate of distortion in relation to the carrier file. As a result, the stego image will have a low quality. Enlarging the steganographic system's capability and security is impractical because of its effect on various elements such as the embedded information, introduction of relics to the carrier, and the safety of the project in relation to the imperceptibility or modification of the stego file.

Steganography is different from cryptography as it aims to conceal the very existence of the secret message while cryptography aims to transfer the secret message to cypher text so it will be unreadable. The appearance of the cypher text rouse the attention of a secret message and this motivates attackers to try to break up the the cypher text. Even when the attacker is unable to extract the secret message, they simply could destroy the cypher text and therefore, the authorized receiver could not receive the message in time. This is one of the main important advantages of the steganography.

Steganography and watermarking achieve different aims. While steganography aims to hide the very existance of the secret file by embedding object within another, watermarking goals protect the digital right of digital media even if the copyright information is deleted. Watermarking works on proving the owner of the file even when some minor changes have been done on the watermarked file. A watermark can be visible or invisible and in both types,

Table 2.1: Comparison between steganography, watermarking and cryptography

Criteria	Steganography	Watermarking	Cryptography
Holder	any multimedia object	image/sound	text
Type of secret data			
Key	optional	optional	compulsory
Number of Input	at least two multimedia files		one
Output	stego-file	watermaked-file	ciphertext
Challenge	capacity and imperceptibility	robustness	robustness
Attackers	steganalysis	image processing	cryptalysis
Visibility	never	sometimes	always
Fails if	detected	removed or replaced	de-ciphered
Flexibility	free to select any media	restricted	none

it must impossible to delete the watermark object without causing distortion. Figure 2.1 graphically illustrates the relationship between steganography and other similar fields. The connection between steganography and image watermarking encompasses active steganography and certain types of watermarking related to authentication applications. Table 2.1 and Figure 2.2 illustrate the main differences between Steganography, watermarking and cryptography and may eradicate the confusion between the three techniques (Cheddad, Abbas et al., 2010).

Steganography can be used to support information security as a secret communication tool. It can be used to achieve most security requirements such as confidentiality, integrity and non-detection. Confidentiality can be achieved through the invisibility of the hidden information and only the authorized party can know the existence of the secret message. The integrity of steganography can be achieved by ensuring that hidden information can be extracted correctly and can be read easily without any concern of modification of the

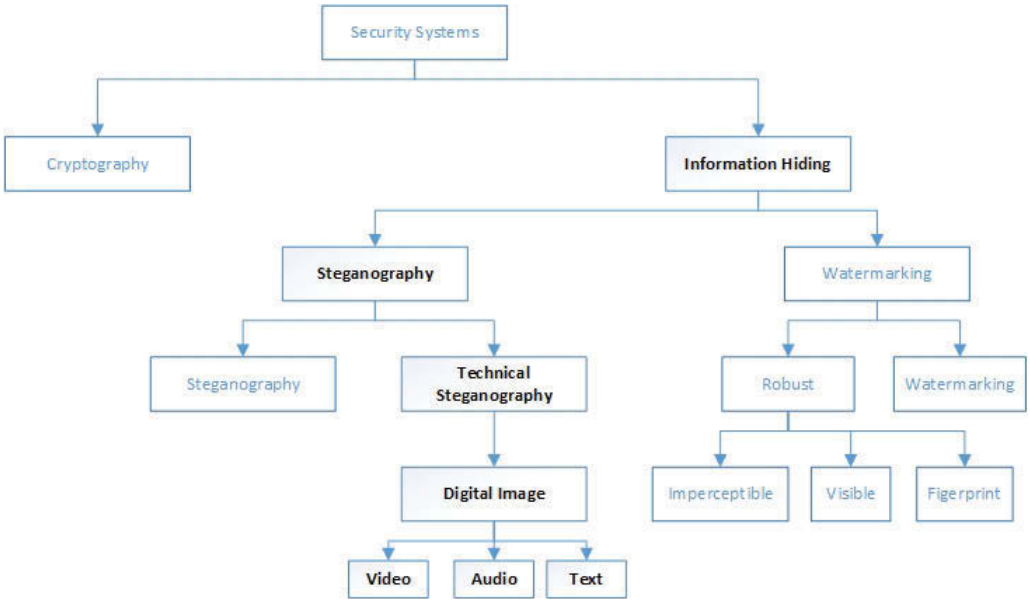

Fig. 2.2: Embodiment disciplines related to concealing information

hidden information. Lastly, steganography can hide information avoiding detection by anyone through visible or statical analysis.

The use of steganography is not limited to information security purposes. It is also used in scientific as well as commercial processes. This includes the concealment of data in multimedia tools, advance data structures, medical imagery systems, military intelligence, tracking and authentication of documents, and embedding in smart ID. When applied to devising data structures, steganography aids in the embedding of descriptive information. This is done in relation to the original file resulting in a smooth transmission of meta-information and meta-data from system to system. This would mean that the issue of the allocation of hard disk space is resolved through advance data structure. Problems related to big data can be addressed using steganography because of the lower rate of hard disk volume required when recording information and the details of multimedia being subjected to steganography.

2.2 Steganographic Architecture

Katzen and Petitcolas explain the methods of Steganography by presenting a single process as shown in Figure 2.3 (Katzenbeisser and Petitcolas, 2000). Alice the sender, needs to convey a message (m) to the recipient (Bob), using an appropriate carrier (c). Alice embeds the message (m) in the carrier (c) and most likely uses a stego key (k). Thus, Alice gets a stego file (s) which must be indistinguishable from the carrier (c) not by a human visual system or statical analysis. In this manner, the stego file (s) symbolizes the original carrier file (c) along with the secret message file (m) hidden inside the carrier.

At that point, Alice sends the stego object (s) to Bob over a public channel. The goal of the system is to evade Wendy (an outsider) from checking or understanding the imperceptible message (m). On the other part, Bob extracts the hidden message (m) since he knows the installing strategy and the stego key (k) utilized within the implanting method (Katzenbeisser and Petitcolas, 2000). The transmitter and the composed beneficiary should have the stego key. Subsequently, the greater part of steganographic strategies are to quickly offer clients a stego key or security watchword when they attempt to incorporate data in a secure smart phone or workstation record.

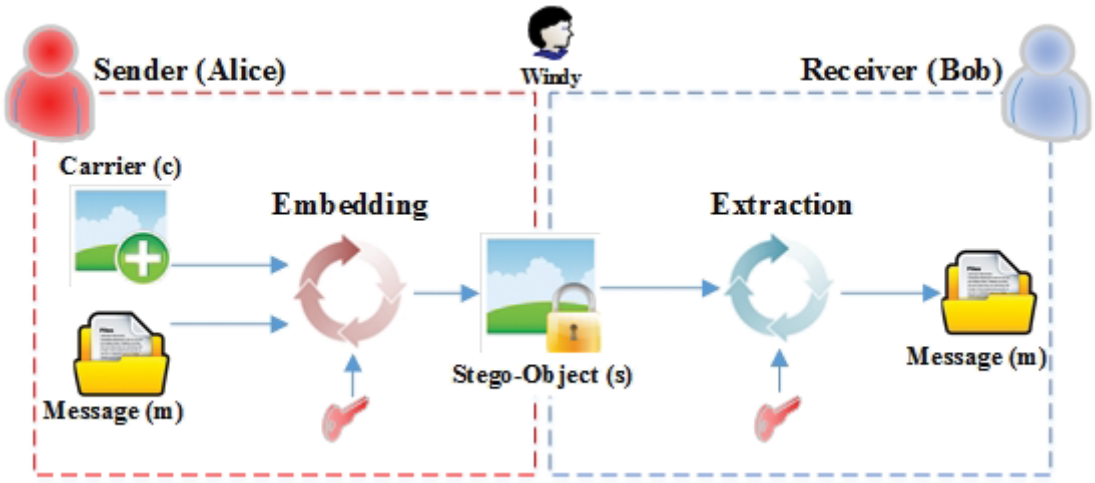

Fig. 2.3: Architecture of steganography

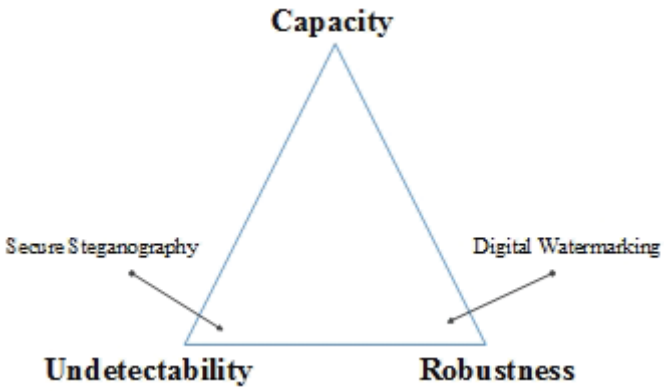

Fig. 2.4: Trade-off factors in steganography

2.3 Steganographic Properties

In its most essential form, three basic characteristics of a steganographic systems should be understood to undertake the evaluation: the security; imperceptibility; and hiding capacity (Wang and Wang, 2004). These should always be assessed in any steganographic project to ensure the system's effectiveness. According to Cole, three fundamental principles are also considered to determine a steganography technique's effectiveness, these are: imperceptibility, the volume of data to be embedded; and the difficulty level of detecting concealed data (Cole and Krutz, 2003). Figure 2.4 indicates the main trade off requirements for steganography. It shows that steganography approaches focus on achieving optimum imperceptibility as best as possible. However, watermarking mainly focuses on achieving maximum robustness against possible attack. The following subsections explain these properties in more details.

2.3.1 Robustness (Security)

Steganographic systems are unsuccessful if the secret message in an image is discovered by an attacker. Similarly, it is also the case if the technique used in the embedding of the message arouse suspicion of attackers. It is therefore imperative to make the system as secure as possible by ensuring that attack-

ers will have a difficult time in detecting a stego file despite applying various ways and means. It is then the aim of steganographic systems to make sure that similar statistics for both the stego file and cover file exists. According to Venkatraman et al., this could be guaranteed if the cover files' attributes and characteristics are consistent and without perceptible distortions occurring during the course of embedding (Venkatraman et al., 2004). However adversaries need to be addressed because it might still raise suspicion that a secret message is present in the image. Cox et al. relates that these adversaries include the existence of statistical anomalies such as histograms as well as other sorts of higher-order statistics (Cox et al., 2008).

2.3.2 Undetectability (Imperceptibility)

Many steganographic publications refer to security as a synonym to undetectability. Hence, Cox et al. believe that imperceptible steganographic systems are also known as secure steganographic systems (Cox et al., 2008). Accordingly, a highly secure steganographic system yields a stego image that has an optimum quality. Venkatraman et al. (2004), point out, however, that the most difficult thing known in the concealment of secret information is the presence of noise or the modulation of the cover image. Hence, to make the system more secure and effective, the introduced noise should not be contributing to the degradation of the stego image's perceived quality.

2.3.3 Payload Capacity (Embedding Rates)

Steganographic capacity refers to the largest amount of bits allowed for embedding in a certain cover file, at the same time presenting a slight chance to be detected by attackers. On the other hand, Cox et al. argue that steganographic capacity is smaller than the embedding capacity (Cox et al., 2008). This is supported by the concept of embedding rate or capacity. Venkatraman et al., mention that the embedding rate is known as the size of hidden information relative to the cover image size (Venkatraman et al., 2004). Hence, Wang and Wang argue that the objective of steganographic

systems is to maximize or increase steganographic capacity while minimizing recognition of hidden messages embedded in stego images (Wang and Wang, 2004). Furthermore, (Cole and Krutz, 2003) mentions that steganographic techniques could be affected when large volumes of data are hidden in the image (Artz, 2001; Rabah, 2004). Hence, steganography techniques can also be developed by expanding the volume of secret data to be concealed without an adverse effect to the characteristics of the stego files.

2.3.4 Trade-off Between Steganography Properties

Steganography aims to augment the capacity and imperceptibility of a secret message (Chang et al., 2006). However, there is a problem when imperceptibility and steganographic capacity interact. According to Wang and Wang, this problem is seen when more meta-data are inserted into the cover image and consequently degrade the quality of the stego image (Wang and Wang, 2004; Wang and Chen, 2006). Moreover, simultaneous maximization of a steganographic system's capacity and security is impossible due to the tradeoffs such as the amount of artifacts presented to cover file, the volume of information to be embedded, and the system's immunity against the modification of the stego file (Marvel et al., 1998; Venkatraman et al., 2004). A balance should then be observed between these requirements.

Nevertheless, steganographic systems are not required to always achieve high robustness, though high steganographic capacity as well as imperceptibility of secret data should always be guaranteed. Despite that, watermark imperceptibility and large embedding capacity are not necessary in watermarking schemes. As an alternative, authors such as Marvel et al. and Venkatraman et al. proposed that a high level of robustness is needed to respond to unintentional and malicious attacks (Marvel et al., 1998; Venkatraman et al., 2004). This would show that the capacity seen in spatial domain schemes can be considered to be superior to frequency domain schemes. Yu et al. suggest that better levels of robustness are derived from frequency domain schemes when compared to spatial domain (Yu et al., 2005). The majority of watermarking schemes apply frequency domain schemes because of the

required robustness in watermarking schemes. Furthermore, various embedding techniques that are developed recently strengthen security and boost the capacity of the methods used in steganography (Chu et al., 2004; Lee and Chen, 2003, 2000; Li, Q., Yu and Chu, 2006; Tseng and Chang, 2004). The following section of this Chapter discusses the major techniques applied in steganography.

2.4 Image Steganography Methods

Recently, many techniques for steganography have proliferated. Differences in such techniques are based on the principles or mechanisms that apply when concealing secret messages. Additionally, the difference also lies in the processes and elements of change seen when the whole embedding procedure is carried out. For this reason, three main categories related to the techniques used in steganography are seen in various research publications. Among these are; spatial domain, frequency domain and adaptive steganography techniques (Katzenbeisser and Petitcolas, 2000; Kipper, 2004). Figure 2.5 shows a diagram of steganography techniques based on the research scope.

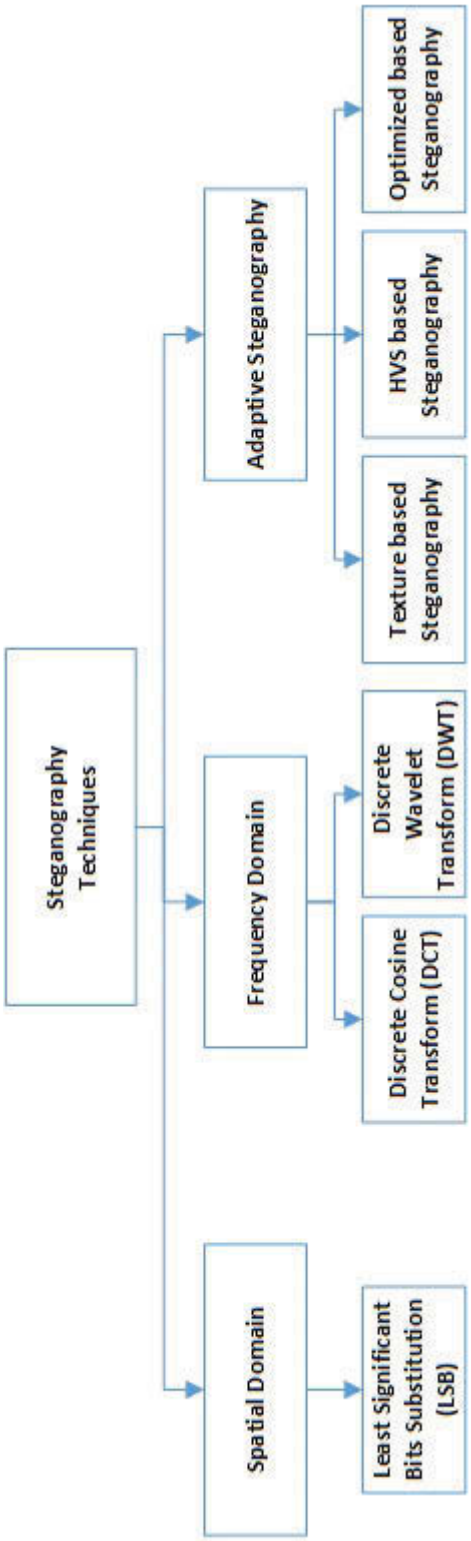

Fig. 2.5: Image steganography techniques

2.4.1 Spatial Domain Technique

For a given cover file, it is important to discover a few zones or subtle elements that might be redone without having any significant impacts to ensure points of interest in the document (Cole and Krutz, 2003). As a consequence, Kipper maintains that integration of key ideas could be done through a process of changing insignificant elements and without losing the key ideas with no critical alarming impact to the ensure that subtle elements are recorded (Kipper, 2004). There are numerous methods based on spatial domain which is include and are not limited to: Least Significant Bit (LSB); Pixel Value Differencing (PVD); Edges based data embedding method (EBE); Random Pixel Embedding method (RPE); Histogram Shifting Methods and Bits Plan Complexity Structure (BPCS). LSB aspect will be explained in the following section as used in current research.

2.4.1.1 Least Significant Bits Substitution (LSB)

Substitution systems as applied in steganography entails the substitution of a key idea, substituting bits through a process known as Least Significant Bits Substitution (LSB). Here, the bytes are seen in the secure points of interest and records are substituted but no remarkable change is seen to ensure the maintenance of the subtle elements within the document. As mentioned by Bracamonte et al., LSB is a spatial domain-based method that has the intention of inserting essential pieces to ensure points of interest are recorded in the simplest way possible (Bracamonte et al., 1997). Due to this straightforward characteristic of the LSB substitution system, it has become a popular method in the field of electronic steganography, especially when working on electronic pictures. While the LSB method has its benefits, Rabah mentions that the points of interest could also easily be destroyed when the output stego picture is applied with minor acclimation such as JPEG squeezes (Rabah, 2004). Nevertheless, LSB substitution is known for its ability to embed confidential data through a process that starts from considering the bits at the rightmost part of the image, resulting in a non-

destructive effect of the embedding in the original pixel value of the image. Therefore, it is important to consider because of the fact that bits at the rightmost side of the image possess least possible weight. The formula for LSB is shown in the equation:

$$x^{'} = x_i - x_i mod 2^k + m_i \tag{2.1}$$

Figure 2.6 shows the general LSB conceptual framework used as a representation when doing a substitution from least significant bits to secret file. The representation of one byte is illustrated in Figure 2.7. The procedures for extraction and embedding used in LSB are described in Algorithm 2.1 and Algorithm 2.2 Here, LSB conducts a straightforward replacement of the cover image's noisy parts or bits that are considered unused through the embedding of secret message bits. Hence, LSB is a preferred technique as far as hiding of data is concerned. This adds to the fact that the process applies a stenographic technique that is easy to understand and is uncomplicated. Similarly, a high hiding capacity is provided by presenting a plain manner of controlling the stego image quality. However, a low robustness in relation to modifications, including low pass filter, compression, and low imperceptibility are cause by using LSB (Goel et al., 2014). The effect of replacing k number of bits through LSB is illustrated in Figure 2.8. With the increase number of bits substitution, the degradation of stego image increase consequently. Therefore, this degradation results in a high rate of error seen in the hidden image that is extracted.

Algorithm 2.1 Embedding Process: LSB method

For $i = 1, \ldots, l(c)$ do
  $s_i \leftarrow c_i$
end for
for $i = 1 \ldots, l(m)$ do
  compute index j_i whereto store i^{th}message bit
  $s_{ji} \leftarrow c_{ji} \rightleftharpoons m_i$
end for

Algorithm 2.2 Extracting Process: LSB method

For $i = 1, \ldots, l(M)$ *do*
  compute index j_i where the i^{th} message bit stored
  $m_i \leftarrow LSB(c_{ij})$
end for

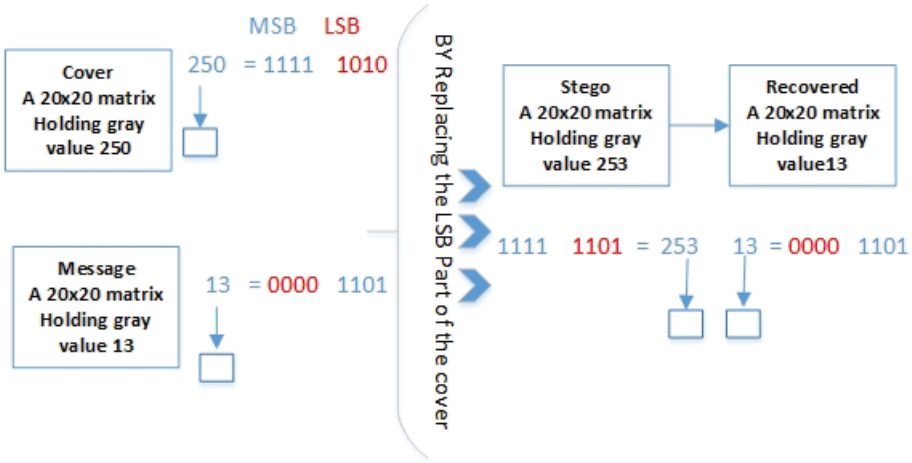

Fig. 2.6: Switching LSBs to fourth bit plane

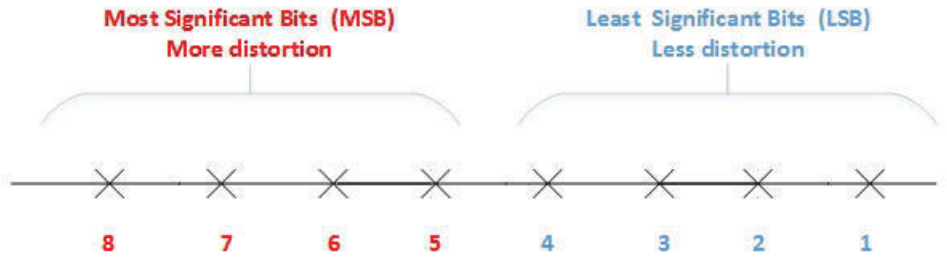

Fig. 2.7: Representation of One Byte

2.4.2 Frequency Domain Technique

The frequency technique assumes that images must be transformed before the message is inserted into it. The approach would allow the concealment of the message in the image's substantial segments. In transform domain,

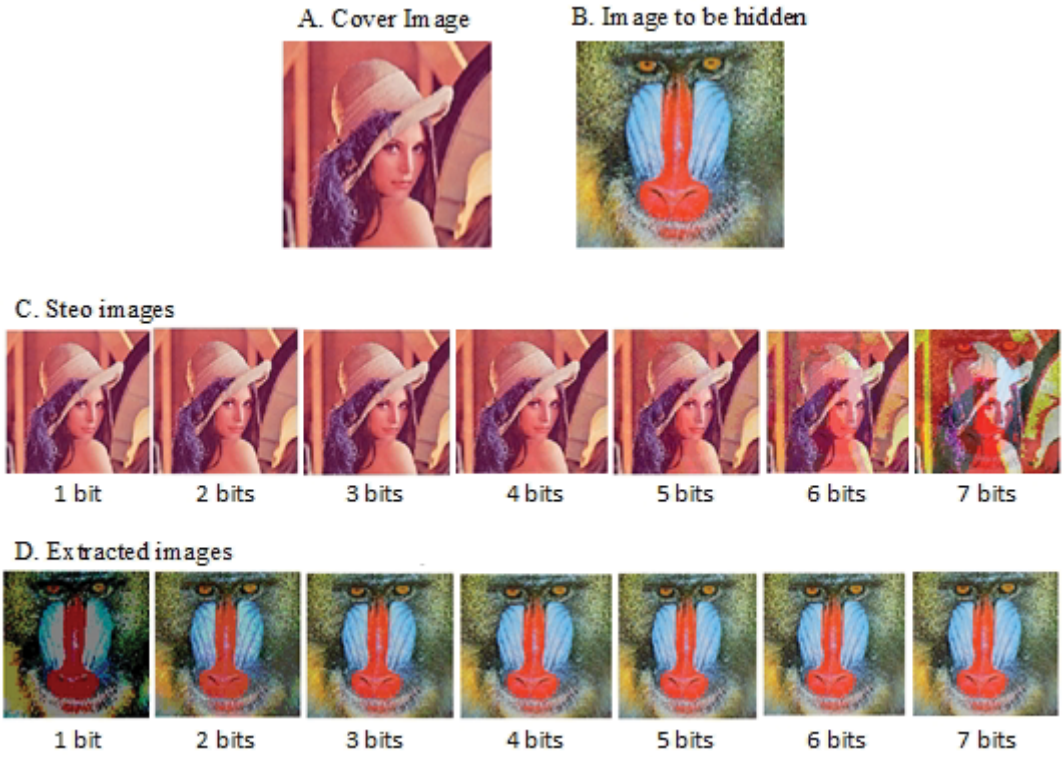

Fig. 2.8: Relation between cover image, stego image and the extracted image for various LSBs

frequencies (low, middle, and high) present in the image should be distinguished, especially when a transform approach is applied. The signal energy's rates are high, as shown in lower frequencies contributing to a result with high quality image visibility. When this dynamic is considered, it would seem that high frequency counters the possibility of image distortion when confidential data or information is embedded. Furthermore, approaches related to transformation domain are considered to be better when compared to other various techniques for the reason that the format of the image is not the basis when embedding the message in the image.

Frequency techniques are not at all like spatial part procedures (for example LSB procedure); change over (recurrence) division strategies conceal key subtle elements in paramount parts of the secure interest record. Accordingly, consistency part procedures are viewed as more successful to strike

than spatial procedures and depend on normality segment methods. There are numerous changes used to guide a sign into the normality part. Unique cosine change over (DCT), Discrete Wavelet change over (DWT), and Discrete Fourier Transform (DFT) are systems utilized as mediums to install key subtle elements in digital images (Cachin, 1998). Nonetheless, when we include a minor aggravation or key points of interest to some normality part segments, it changes the entire picture instead of changing just a piece of the picture. In this manner, key and included subtle elements will be circulated over the whole picture without focusing on one certain range or locale.

2.4.2.1 Discrete Cosine Transform

The transform domain technique aims to transform an image from one domain to another, that is, from spatial to frequency. The Discrete Cosine Transform (DCT) process is conducted through a generation of sub-bands (i.e., low, middle, high transform components) in relation to the visual quality of the image. Normally, the highly significant visual parts are seen in the low frequency sub-band, while the insignificant ones are in high frequency parts. Since the presence of the insignificant parts, they are often removed by using either noise compression or noise attach. In order to address the concern on the effect of frequency to visibility, DCT aims to embed the secret data along the sub-band at the middle frequency, and as a result, the image will not be adversely affected.

Equation 2.2 and Equation 2.3 show the general equation representing 1D and 2D DCT, respectively. In relation, the main process of extracting and embedding seen in DCT are shown in Algorithm 2.3 and Algorithm 2.4, (Barni et al., 2000) and (Jithesh and Kumar, 2010).

$$c(u) = a(u) \sum_{i-0}^{N-1} x_i \cos(\frac{(2i+1)u\pi}{2N}) \tag{2.2}$$

Where N data items and $u = 0, 1, 2, \ldots, N-1$

$$C(u,v) = a(v) \sum_{i=0}^{N-1} [a(u) \sum_{i-0}^{N-1} x_i \cos(\frac{(2i+1)u\pi}{2M})] \times \cos(\frac{(2i+1)v\pi}{2N}) \quad (2.3)$$

Algorithm 2.3 Embedding Process: DCT

For $i = 1, \ldots, l(M)$ do
  Choose one cover block b_i
  $B_i = D\{b_i\}$
  if $m_i = 0$then
    if $B_i(u_1, v_1) > B_i(u_2, v_2)$then
      swap $B_i(u_1, v_1)$ and $B_i(u_2, v_2)$then
    end if
  else
    if $B_i(u_1, v_1) < B_i(u_2, v_2)$then
      swap $B_i(u_1, v_1)$ and $B_i(u_2, v_2)$then
    end if
  end if
  adjust both values so that $\mid B_i(u_1,v_1) \_ B_i(u_2,v_2) \mid > x$
  $b_i^{'} = D^{-1}\{B_i\}$
end for
creat stego-image out of all $b_i^{'}$

Algorithm 2.4 Extracting Process: DCT

For $i = 1, \ldots, l(M)$do
  get cover-block $b_i$associated with bit i
  $B_i = D\{b_i\}$
    if $B_i(u_1, v_1) \leq B_i(u_2, v_2)$then
      $m_i = 0$
  else
      $m_i = 1$
    end if
  end if

Some of the usual applications of DCT can be seen in the compression of image and video media, particularly when considering JPEG loss compression. A quantization of the block DCT coefficients computed based on

Equation 2.3, specifically with the use of a certain Quantization Table (QT). Table 2.2 presents the matrix in relation to the JPEG standard annex. While the matrix presented is specifically used for this research, some manufacturers of cameras impose their own QT, and because of this, they do not really follow the JPEG table shown here. The DCT coefficient is represented in Table 2.2 in bold face as seen in value 16, while the other values shown represent AC coefficients. In here, the trade-offs between quality factors and image compression are balanced, hence, the value representations.

Table 2.2: Quantization table

16	11	10	16	24	40	51	61
12	12	14	19	26	58	60	55
14	13	16	24	40	57	69	56
14	17	22	29	51	87	80	62
18	22	37	56	68	109	103	77
24	35	55	64	81	104	113	92
49	64	78	87	103	121	120	101
72	92	95	98	112	100	103	99

Quantizing is aimed at loosening up precisions that have been produced and tightened through the DCT, and at the same time with the intention of preserving valuable information descriptors in the image. The formula below illustrates the quantization step followed:

$$f'(\omega_x, \omega_y) = \left[\frac{f''(\omega_x, \omega_y)}{\Gamma(\omega_x, \omega_y)} + \frac{1}{2} \right], \omega_x, \omega_y \in 0, 1, 2, \ldots, 7 \tag{2.4}$$

where, x and y represent the two image coordinates, while $f''(\omega_x, \omega_y)$ indicates result function, and $f'(\omega_x, \omega_y)$ is shown in a non-overlapping intensity image block, together with $\lfloor . \rfloor$ representing floor rounding operator. $\Gamma(\omega_x, \omega_y)$ is the quantization step when correlated with JPEG quality. In

particular, it is given through a formula as follows:

$$\Gamma(\omega_x, \omega_y) = \begin{cases} \max\left(\lfloor \frac{200-2Q}{100} QT(\omega_x, \omega_y) + \frac{1}{2} \rfloor, 1\right) & 50 \leq Q \leq 100 \\ \frac{50}{Q} QT(\omega_x, \omega_y) + \frac{1}{2} & 0 \leq Q \leq 50 \end{cases} \tag{2.5}$$

where, $QT(\omega_x, \omega_y)$ represents the table of quantization as seen in Table 2.3 while Q represents quality factor (Ji et al., 2015). Accordingly, entropy coding is applied by JPEG compression, specifically the Huffman algorithm with the aim of compressing the outcome represented by $\Gamma(\omega_x, \omega_y)$. In this particular stage, majority of data are seen to be redundant as well as the noise seen in the image is eliminated. The above mentioned process refers to discrete theory that is independent of the steganography process. This method of steganography is presented by Li and Wang (Li and Wang, 2007) explaining that the aim of this method is to modify the QT and subsequently introduces the concealed bits specifically in the mid frequency coefficients. Table 2.2 presents the QT that is modified as an outcome of this process. This results into a new QT version that provides 36 coefficients as placed in every block where the needed secret data is embedded, and a reasonable payload is then obtained (Chang et al., 2007).

Table 2.3: The modified quantization table

8	1	1	1	1	1	1	1
1	1	1	1	1	1	1	55
1	1	1	1	1	1	69	56
1	1	1	1	1	87	80	62
1	1	1	1	68	109	103	77
1	1	1	64	81	104	113	92
1	1	78	87	103	121	120	101
1	92	95	98	112	100	103	99

The steps followed by steganography are illustrated in Figure 2.9. These steps are mainly based on DCT and JPEG compression. JPEG images are generally used when carrying out these processes or techniques, particularly

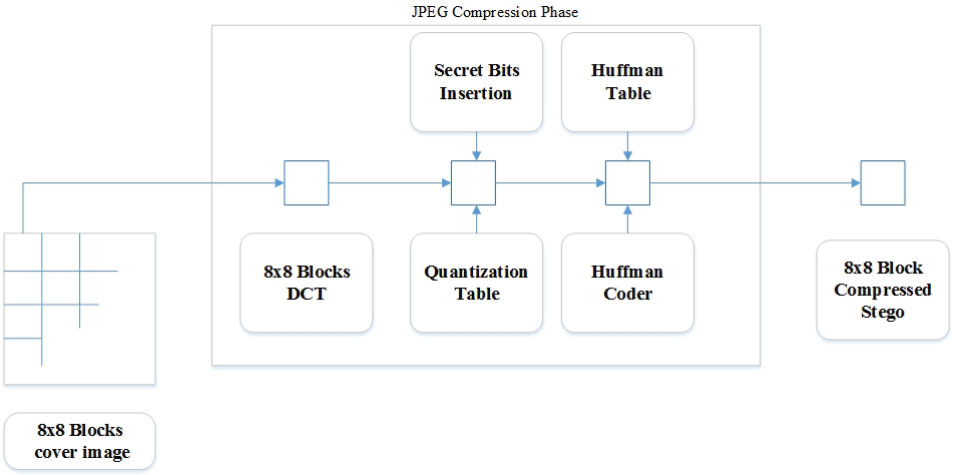

Fig. 2.9: Discrete Cosine Transform Diagram

when embedding the data. DCT involves JPEG compression in order to transform consecutive sub-image blocks. The coefficients are embedded with data despite the insignificant bits. This may, however, alter any sole coefficient that could have an impact to the whole 64 block pixels (Fard et al., 2006a). When the coefficients of the cover image are taken with great care, a lower visibility of change will be seen among them; especially if the change operates along frequency domain rather than spatial domain (Hashad et al., 2015).

2.4.2.2 Discrete Wavelet Transform

Discrete Wavelet Transform (DWT) is based on two operations. These are the horizontal and vertical operations. To illustrate the procedure, scanning of pixels is done by starting from the left hand side to the right and along horizontal axis. The processes of addition and subtraction are therefore performed, particularly on pixels that are considered neighbours. As part of the addition and subtraction, sums are stocked in the left part, while results relating to differences go towards the right side. Figure 2.10 elucidates this process through an illustration. The step is reiterated and is only stopped when every row is done. As a result, pixel sum (L) is generated, which refers to the sections having low frequency as seen in the initially generated image.

On the opposite, high frequency components of the initial image are called pixel differences (H).

Secondly, the scanning of pixels is done from top going to the bottom part of the image through the vertical axis. Neighboring pixels undergo operations such as addition and subtraction. The sums are then cached on the top part while the differences will be at the bottom. Figure 2.11 presents this process. A repetition of the procedure is done as soon as the completion of columns becomes apparent. The four sub-bands are then determined and indicated as: HH, HL, LH, and LL. The initial image will be relatively similar with the LL sub-band, which serves as a representation of the low frequency portion.

Despite the benefits seen in DWT-based steganography, it is still quite young and needs to be further developed. However, it is also known that DWT coefficients possess relatively similar properties with Human Visual Systems (HVS), especially when compared to DCT coefficients. Additionally, the modification that is made through compression and noise is not easily detected by the human naked eye. DWT does a conversion of the secret images by changing it to 1-D vectors and performs an insertion of the messages going to two components that have high frequencies (i.e., HL1 and HH1) seen in the cover image's 1-level DWT. Moreover, this is conducted through a pseudo random number generator as well as the use of a session key.

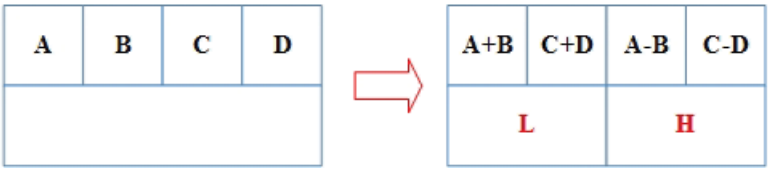

Fig. 2.10: DWT vertical operation

2.4.3 Adaptive Steganography

Adaptive steganography was borne out of the different strategies seen in frequency and spatial methods. The process involves a processing of the image's statistical global features prior to its interaction with the LSB / DCT coefficients. The process and the statistical component of which are aimed at

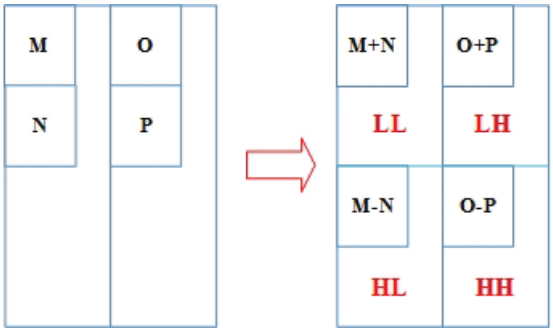

Fig. 2.11: DWT horizontal operation

dictating the direction of the changes to be made in the image (Goel et al., 2014). The pixels are identified through a random adaptive selection with consideration to the present cover image as well as the manner of selecting the pixels based on a certain block. The objective of this process is to prevent the presence of uniform colored areas as well as smooth areas in the image. Adaptive steganography explores the whole image if there are noises having color complexity that have been deliberately added or currently existing in the cover image. To clarify the matter, this section presents three categories of adaptive steganography that are classified through: local texture features; Human Visual System (HSV) characteristics; and Evolutionary Algorithm (EA).

2.4.3.1 Steganography based on Texture Features

In this type of steganography, the cover medium's features are highly considered when concealing secret information. The approach is done by identifying the most appropriate regions where the data should be hidden. Adaptive steganography posits that data should be hidden in a region possessing several textures, high contrast, and with a lot of gray level variations. These features or regions most likely occupy a very noisy part of the image, and as a result, detection of the hidden message will not be an easy job. To complete the process, statistical definition of the image's texture is utilized in identifying heterogeneous local textures in the region, and then a selection of some pixels from that region will be used in embedding the secret message at the

level of gray scale. Table 2.4 shows some useful literature relating to texture based steganography. The table summarises only the main contribution of each study.

Table 2.4: Key literature on texture features steganography approaches

Author	Description
(Lie and Chang, 1999)	The embedding of secret information is based on intensity value obtained from pixel intensity values, either from the edge or other parts of the original image.
Wu and Tsai (2003)	Proposed the method called pixel-value differencing (PVD)
Zhang and Wang (2004)	Developed an improved version of PVD. IPVD exploited the weaknesses of PVD
Ker (2005)	Developed LSB matching revisited (LSBMR) technique.
Yang et al. (2008)	Designed an adaptive edge LBS-technique by deleting uneven pixels differences using readjusting step
Luo et al. (2010)	Judged the poor performance of randomly placed the data
(Wen Jan Chen Chang et al., 2010)	Utilized fuzzy edge detection approach with canny edge to provide hybrid edge based steganography techniques
(Youssef Bassil, 2012)	Used Canny edge detector before inserting the embedded message with the use of k LSBs
(Arora and Anand, 2013)	Designed 3x3 window of the edge detection, including the secret information that has been embedded via human vision component.
(Wazirali et al., 2014)	Developed a new score metric approach to judge the embedding pixels
Wazirali and Chaczko (2016)	Proposed a hyper-edge detector through the application of zero crossing with clustering and gradient features in 9x9 mask of Laplacian of Gaussian (LOG)
(Hussain et al., 2015)	Performed an analysis of PVD methods by considering different evaluating parameters such as payload, resistance of attacks and visual quality

2.4.3.2 Steganography based on Human Visual System

Researchers have developed and used different models of the Human Visual System (HVS) to improve the quality of an image or its capacity for data hiding (Table 2.5). Similarly, identical visual models are also used in image steganography. In applying steganographic techniques, the procedure entails some requirements such as perceptual transparency, capacity and robustness. In spite of the need for such, a conflict between the requirements exists. One way to respond to this conflict is through the integration of HVS in the procedure of steganography. When HVS models incorporate hidden data, perceptually significant components of the image to be embedded and steganography components to be scaled undergo prior embedding to the original data. Here, entropy masking of the HVS model is done. As an outcome, higher level of complexity as well as uncertainty is seen in the image's high entropy regions. On the other hand, weak entropy contributes to the numerous redundancies in the pixel values of the image. Human vision has low sensitivity when looking at the modifications along the areas possessing high entropy. This is for the reason that higher complexity is present in such scenarios. This characteristic aids in the choosing of the image elements having high entropy value suitable for embedding data. The eyes of humans are sensitive to different spatial frequencies. This sensitivity is selected through frequency sensitivity. Computation of luminance sensitivity is performed to determine the effect of noise threshold to the constant background, based on detectability. In connection, frequency sensitivity also undergoes correction, in relation to changes that happen in background luminance. As such, the process of masking happens. This process occurs when a certain signal's visibility is decreased as an effect of interacting with a new signal known as a 'masker'.

2.4.3.3 Steganography based on Evolutionary Algorithm

Evolutionary Algorithm (EA) follows a randomized processes in solving optimization problems (Spector, 1997). A matching of solution and problem

Table 2.5: Key literature on HVS steganography approaches

Author	Description
(Mannos and Sakrison, 1974)	Used Contrast Sensitivity Function to improve the stego image quality
Lie and Chang (1999)	Proposed an adaptive number of LSBs using human visual sensitivity of contrast weaknesses
Lu et al. (2007)	Used noise visibility function with dynamic programming strategy for data hiding in order to partitioned pixels
(Yu et al., 2008)	Proposed approach called 2k Correction. Contrast sensitivity function (CSF) and Just Noticeable Difference (JND) are used in this approach.
Abdul et al. (2010)	Used contrast sensitivity function (CSF) to manage the insertion of the data in a color image
Kumar (2013)	Developed a method that considers Human Vision System f or inserting the secret message in DCT domain
(Farag and El-Khamy, 2014)	Weighted multi-level wavelet transform based on their perceptual significance
(Sajasi and Moghadam, 2015)	Developed a hybrid steganography scheme that integrates Noise Visibility Function (NVF) as well as an optimal chaotic-based encryption scheme.
Sajasi and Moghadam (2015)	Used NVF to select an acceptable payload rate of each area of the image

is done along the genetic algorithm represented by chromosome with many genes. Fitness function is an objective function applied when chromosome quality is measured. The process starts by identifying a starting population. In each of the generations, processes of reproduction, mutation and crossover are observed in the production of off spring. Quality is then determined by applying fitness function to every offspring. Individuals possessing the most superior quality tend to survive and start the next generation population.

GA does an extensive search with the aim of obtaining optimum results based on the selected fitness functions. Particularly, Genetic Algorithm (GA) is used for selecting the best place to allocate the meta-data. Therefore, minimum error and degradation can be achieved. Table 2.6 provides a key of some study for Evolutionary Algorithm steganography approaches.

Table 2.6: Key literature on EA steganography approaches

Author	Description
Mandal (2000)	Explored GA-based colors used in hiding or authentication technique as seen in frequency domain through DFT
Hempstalk (2006)	Optimal pixels are adjusted accordingly to obtain a function that is best for mapping a lower discrepancy error seen when the image and the cover media are compared.
Fard et al. (2006a)	Developed a secure approach that use the concept of GA and JPEG
Li and Wang (2007)	An optimal substitution matrix for transforming the secret messages is first obtained using Particle Swarm Optimization algorithm (PSO) algorithm
Raja et al. (2007)	Proposed Steganography method using DCT and DWT
Yu et al. (2009)	Proposed plus minus 1 (PM1) algorithm using GA which provide an improvement of LSB performance
Wang et al. (2010)	Developed a method that aim to keep the statistic characters of stego image unchanged
Ghasemi et al. (2012)	Used Genetic Algorithm and Optimal Pixel Adjustment Process to search for the best region to insert the secret message and therefore reduced the difference error
Trochim (2014)	Developed an optimal block mapping for LSB method
(Nosrati et al., 2015)	Proposed a method that aims to search for appropriate locations in the carrier image where messages having the least bit changes.
(Roy and Laha, 2015)	Proposed a novel fitness function that is grounded on Peak Signal to Noise Ratio (PSNR). The PSNR is acquired from every pixel's 8-connected neighbors.

2.5 Steganographic System Evaluation

A process of evaluating steganographic systems is necessary to deliver a concrete decision when selecting the appropriate steganographic technique or system. At present, there is no standard measure or test available for the assessment of the technique or system's effectiveness or performance. Nonetheless, some guidelines have been proposed for such purpose, as mentioned by (Cox et al., 2008).

In general, steganographic systems can be assessed based on two factors:

1) the volume of hidden information; and

2) the level of complexity of detecting the stego files.

When these two are evaluated, the steganographic technique's superiority can be determined and measured. As a result, undetectability and capacity of the steganography technique can also be used in evaluating the system's efficiency.

2.5.1 Payload Capacity Evaluation

It is essential to identify and understand the amount of bits that can be embedded in a steganographic system in terms of imperceptibility. This is due to the fact that the primary aim of which is the concealment of information or the secret communication. This is also important in order to compare it with other methods being used for the same purpose. Identifying the capacity of a steganographic technique aims to search for the maximum amount of bits allowed for undetectable concealment.

While tradeoffs exist when imperceptibility and steganographic capacity interact, techniques for steganography are still considered to be worthless systems if messages with large size are embedded in cover files and then the stego file is introduced with more distortion. On the contrary, it becomes a positive contribution if it is aimed to increase steganographic capacity and to maintain a certain level of stego image quality that is acceptable. This is also

true if the quality of the stego image quality is significantly improved while retaining steganographic capacity in the process (Wu and Hwang, 2006).

2.5.2 Imperceptibility Evaluation

There are differences present in various systems, methods and techniques when it comes to the evaluation of imperceptibility in steganographic systems. These differences are mostly based on the cover file type as applied in the concealment of information. For instance, undetectability of the image based steganography can be represented by image quality, while the existence of data that is hidden in a certain text file can be determined based on the file size. These could also be considered as factors to the detection of the secret information or data.

It is essential to ensure that no visual variation is seen between the stego image and the cover image. The imperceptibility of this difference should be perfect as far as HVS is concerned. If the quality of stego image is high, the steganographic system's imperceptibility is also implied to be high. Thus, quality of stego images should be evaluated because it is a vital metric in assessing performance of the steganography techniques (Wazirali et al., 2015).

The aim of image quality metrics is to determine and assess the image quality through various quality indicators. This is conducted to understand similarities between raw input image and processed image, specifically their spatial and spectral properties. When applied in steganography, the raw image is referred to as the host image while the processed image refers to the stego image. A categorization of the image quality metrics is considered to be broad since it is based on the objective quality metrics aimed at providing computational metrics in assessing sameness between the stego image and host. Similarly, metrics for subjective quality is used as a basis for the image quality score through an inspection of the images using Human Visual System (HVS). The following sections present a short introduction of the categories related to image quality metrics.

2.5.2.1 Objective Quality Evaluation

The objective image quality metrics provide a predictive measure of visible differences in two images. Several image quality metrics have been developed to quantitatively measure the similarities between the processed and the raw images including: the pixel-based metrics such as MSE, SNR, PSNR, UIQI; the correlation measures such cross-correlation, and Czekanowski distance; the edge quality measures such as Pratt distance and Edge stability; the spectral distance measures such as Spectral Magnitude Distortion, Spectral Phase Distortion, and variants of the magnitude and phase distortion; information fidelity metrics such as Visual Information Fidelity; and HVS based metrics such as Absolute HVS Error, SSIM, Multi-Scale SSIM, and HVS PSNR (Al-najjar and Soong, 2012; Malhotra and Tahilramani, 2013; Ponomarenko et al., 2008; Uhrina et al., 2013).

The objective quality assessment is performed using most commonly used quality metrics. A brief description of the metrics used in this article is presented.

2.5.2.1.1 Mean Square Error (MSE)

MSE is computed by considering the average of the squared error, and the error is known as the difference between the two images being assessed. The formula below represents this calculation:

$$MSE = \frac{1}{m \times n} \sum_{i-1}^{m} \sum_{j-}^{n} (C_{ij} - S_{ij})^2 \tag{2.6}$$

Where m and n are the number of rows and columns of the images, and C and S are corresponding pixels in each image. It is obvious that the images must be of same size, or scaled to achieve one to one correspondence for each pixel. Here, the MSE is calculated for each channel of the color images and averaged over all three channels to obtain a single value for each pair of images.

2.5.2.1.2 Peak Signal-to-Noise Ratio (PSNR)

A typical image quality metric used in steganography is the peak signal to noise ratio. The basic version of PSNR is generally known and used in evaluating quality because of its simplicity, although many PSNR variants are available today. PSNR is mathematically illustrated as follows:

$$PSNR = 10 \log_{10} \frac{(I_{max})^2}{MSE} \tag{2.7}$$

Where I_{max} refers to the maximum intensity of each pixel's given resolution. For this 8 bit gray scale images, the value is 255. Similar value is also true for the individual color channels.

2.5.2.1.3 Weighted Peak Signal to Noise Ratio ($wPSNR$)

The weighted PSNR (Voloshynovskiy et al., 2000) is known as a stochastic approach. It is designed to assign particular value for weight in relation to the standard PSNR in order to improve the assessment of the image quality through HVS. Noise Visibility Function (NVF) is used as a basis for the computation of the weight and this is expressed as:

$$NVF(i,j) = \frac{1}{1 + \theta\sigma_x^2(i,j)} \tag{2.8}$$

Where $\sigma_x^2(i,j)$ denotes the pixel's standard deviation as well as the normalization function. On the other hand, modification of PSNR is used as a basis in the computation of the weighted PSNR through the following:

$$wPSNR = 10 \log_{10} \frac{MAX^2}{||(C_{ij} - S_{ij})||_{NVF}^2} \tag{2.9}$$

$$wPSNR = 10\log_{10}\frac{MAX^2}{||(C_{ij} - S_{ij}).NVF||^2}$$

2.5.2.1.4 Universal Image Quality Index

Three factors are combined in the derivation of models pertaining to universal image quality index and its relation to image distortion. These include luminance distortion, contrast distortion, and loss of correlation. The following formulas illustrate the quality metric (Wang and Bovik, 2002).

$$UQI(c,s) = L(c,s), C(c,s), S(c,s) \tag{2.10}$$

$$UIQI = \frac{4\mu_c\mu_s\mu_{cs}}{(\mu_c^2 + \mu_s^2)(\sigma_c^2 + \sigma_s^2)} \tag{2.11}$$

where

$L(c,s) = \frac{2\mu_c\mu_s}{\mu_c^2+\mu_s^2}$ (Luminance Distortion)

$C(c,s) = \frac{2\sigma_c\sigma_s}{\sigma_c^2+\sigma_s^2}$ (Contrast Distortion)

$S(c,s) = \frac{2\sigma_{cs}}{\sigma_c+\sigma_s}$(Structural Comparisons)

Where $\mu_{c,}\mu_s$ denotes mean values of both the stego and cover images and $\sigma_c\sigma_s$ denotes standard deviation for the two images. Moreover, σ_{cs} represents covariance for the two images.

The quality index present in the dynamic range is known as [-1, 1] and the value for maximum similarity is 1. A high correlation was seen in various applications of the UIQI in relation to the subjective scores derived when certain experiments have been done.

2.5.2.1.5 Structural Similarity Index

Structural Similarity Index (SSIM) was developed and proposed as an improvement of UIQI (Wang, Simoncelli and Bovik., 2004). SSIM aims to measure the quality of an image based on an original initial image. Nevertheless, this image is deemed compression or distortion-free. In here, an SSIM index is used to estimate perceived errors, wherein image distortion is considered to be a perceived alteration present in the structural information of the image. The basis of which is the estimation of pixels and the process of having interdependencies, specifically when the said pixels are close to each other in a spatial manner. Therefore, significant structure information related to the objects are provided based on the presence of interdependencies. The mathematical representation of SSIM is presented as:

$$SSIM(c,s) = \frac{(2\mu_c\mu_s + C_1)(2\sigma_{cs} + C_2)}{(\mu_c^2 + \mu_s^2 + c_1)(\sigma_c^2 + \sigma_s^2 + C_2)} \tag{2.12}$$

where

$\mu_x$the average of c;

μ_y the average of$s$;

σ_x^2 the variance of c;

σ_y^2 the variance of s;

σ_{xy} the covariance of c and s;

C_1=$(k_1L)^2$,C_2=$(k_2L)^2$ two non consistent variables to stable down the division with weak divisor;

L the dynamic domain of the pixel-values (usually this is $2^{\#bits\ per\ pixel}-1$);

k_1=0.01and k_2=0.03 by default.

SSIM is a decimal value and $SSIM \in [1,-1]$ and the value 1 refers to identical set of data.

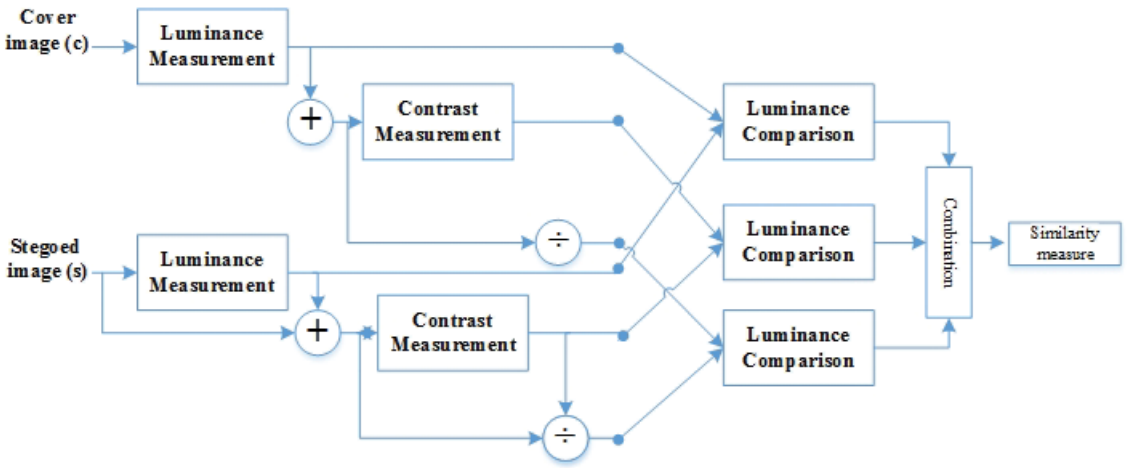

Fig. 2.12: Flowchart diagram of SSIM for steganography

On the other hand, some researchers such as Dosselmann and Yang also argue that SSIM cannot produce a correlation through the use of HVS when compared to MSE values (Dosselmann and Yang, 2011). Nonetheless, SSIM can produce quality measures according to human perception without HVS modeling and is used in its equations. Additionally, the total relay of SSIM on parameters that are non-perceptual is not significant.

2.5.2.1.6 PSNR-HVS

The HVS based peak signal to noise ratio (Egiazarian et al., 2006) measures three HVS based factors for the image evaluation, including: error sensitivity; structural distortion; and edge distortion. It is based on taking away the mean shifting and contrast stretching utilizing a scanning window as shown in Figure 2.13. These three factors are calculated as:

- **Error Sensitivity**

$$E_i = \frac{1}{MN} \sum_{m=1}^{M} \sum_{n=1}^{N} [C(m,n) - S(m,n)]^2; \text{for } i = 1,2,3(\text{color channels}) \quad (2.13)$$

$$PSNR_E = 10\log_{10}\frac{3}{\sum_{i}^{3} E_i} \tag{2.14}$$

Where x(m,n), y(m,n) are the individual pixel values for each color channel i = 1,2,3; M and N are the number of rows and columns of the image.

- **Structural Distortion.**

$$S_i = \frac{1}{N}\sum_{r=1}^{R}[0.5(C_{a_r} - S_{a_r})^2 + 0.25(C_{p_r} - S_{p_r})^2 + 0.25(C_{b_r} - S_{b_r})^2]; \tag{2.15}$$

for $i = 1, 2, 3$ $(colorchannels)$

$$PSNR_S = 10\log_{10}\frac{3}{\sum_{i}^{3} S_i} \tag{2.16}$$

Where $C_{a_r}, C_{p_r}, C_{b_r}$ and $S_{a_r}, S_{p_r}, S_{b_r}$ represent mean, maximum, and minimum pixel values for the reference and distorted image, respectively. The images are divided in regions to calculate the structural distortion

- **Edge Distortion**

$$ED_i = \frac{1}{MN}\sum_{m=1}^{M}\sum_{n=1}^{N}[C'(m,n) - S'(m,n)]^2; \text{ for } i = 1, 2, 3(\text{color channels}) \tag{2.17}$$

$$PSNR_{ED} = 10\log_{10}\frac{3}{\sum_{i}^{3} ED_i} \tag{2.18}$$

Where $C'(m,n) - S'(m,n)$ are the individual pixel values in the edge maps of the reference and distorted images for each color channel $i = 1, 2, 3$; M and N are the number of rows and columns of the image.

The HVS PSNR is obtained by calculating the weighted addition of the three factors:

$$PSNR - HVS = \alpha PSNR_E + \beta PSNR_{ED} + \gamma PSNR_S \tag{2.19}$$

The weights are given as 0.32, 0.38, and 0.3, respectively in Prateek et al. (2012).

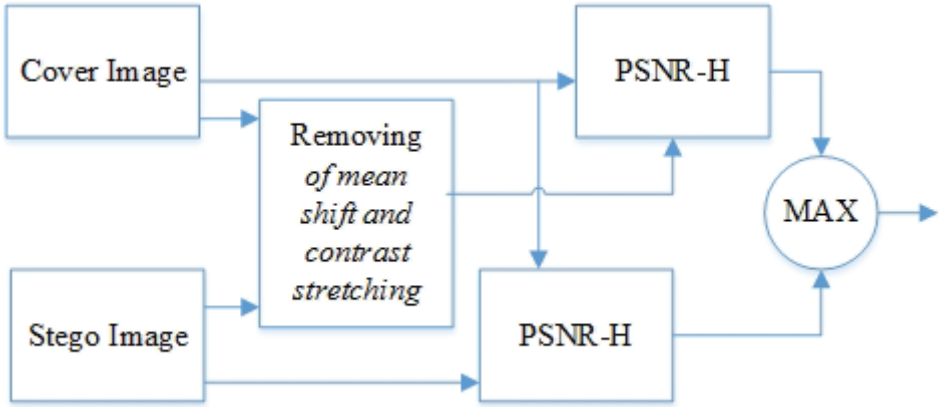

Fig. 2.13: PSNR-HVS flowchart

2.5.2.2 Subjective Quality Evaluation

To undertake Subjective Quality Evaluation (SQE), observation of certain images is done. This is then followed by an evaluation or assessment of the images' visual quality. The problem lies in the different levels of visual sensitivity held by observers and the underlying changes seen in it as time goes by over time. Despite subjective experiences, it is known that every objective image quality measure could not really show a perfect impression as perceived by humans. It is therefore proposed by Stoica et al. that subjective

quality measures be used in depicting a genuine performance benchmark, particularly for various image processing tools (Stoica et al., 2003). Subjective measures will pose a higher reliability in identifying actual image quality for the reason that humans are still seen to be the definitive receivers of the message being subjected in almost all applications. Moreover, Marini et al. mentioned that subjective test offers the best method for the evaluation of image quality in terms of certainty and reliability (Marini et al., 2007).

Furthermore, structured experimental designs are used in subjective measures. According to some authors, this positions the human end user as an evaluator of image quality as they are the best party to do so (Tan et al., 1998; Wu and Rao, 2006). Subjective measures are also highly recognized methods because of the manner of quantifying the concrete quality perceived. Problems seen by Wu and Rao in such methods, however, are complexity, non-reliability, expensive nature, and a time consuming process (Wu and Rao, 2006). During the process, the image quality is rated by the observers based on a reference image or a given quality scale or impairment scale (Table 2.7).

The images are rated-based on an average score known as Mean Opinion Scores (MOS). This is considered as a measure for subjective quality expressed as a strong measurement of quality. The MOS is computed by subjecting a variety of test condition k (i.e. steganography method) and using the formula:

$$MOS_k = \frac{\sum_{n=1}^{N} m_{nk}}{N} \tag{2.20}$$

where m_{nk} reflects the score garnered by subject n when subjected to test condition k , while N denotes the total number of subjects (Su et al., 2015).

Table 2.7: Mean opinion scores rating

MOS	Quality	Impairment
5	Excellent	Unnoticeable
4	Good	Noticeable but not irritating
3	Fair	Slightly irritating
2	Poor	Irritating
1	Bad	Very irritating

2.6 Summary

This chapter presented the major issues related to the process of digital steganography. Similarly, core components of the steganographic approach and fundamental techniques used in steganography were also discussed. The chapter discussed the background of major steganography algorithms as they are applied in digital imaging. The trade-off between the various steganographic criteria became apparent. It also presented the process and concepts considered in evaluating efficiency and effectiveness of steganographic techniques and systems.

A steganographic system is robust if a certain way of detecting or recovering some of the signal processing operations is known. Cox et al. posit that the main objective of steganography is to design the algorithms used in hiding information with the intent of making the data statistically undetectable while retaining large volumes of data in the image (Cox et al., 2008). Therefore, steganographic systems do not necessarily concern themselves with robustness in relation to modifications or they possess limited level of robustness when technical modifications are put into the scenario. These modifications include: compression; digital-to-analogue conversion; and format conversion. However, watermarking systems require the presence of robustness and resistance to any sort of transformations and manipulations done to get rid of the watermark.

Two techniques are commonly used in hiding data; spatial domain; and transform domain. Spatial domain hides data in a time frame to conceal the data into the pixel value directly. Transform domain is a mathematical function

that transformed cover image's into frequency coefficients. Although spatial domain provides high embedding rate, it results in high error rate to the output. Transform domain is seen as more robust, however the capacity of the meta-data to be hidden is very limited. Finally, adaptive steganography in terms of embedding information in regards to the cover image content can assist in improving the performance of steganography. Embedding meta-data based on the texture of digital images could reduce the resulting degradation. The exploitation of human vision perception weaknesses to assist in providing better stego images was also considered. Moreover, for better trade-offs between the conflict requirement, there should be an optimum embedding level of the cover image. In order to achieve this optimum embedding level one should consider steganography as an optimization problem. Therefore, the use of Evolutionary Algorithm (EA) enhances the overall performance through searching for the best location to insert the meta-data with minimum degradation.

Finally, it is necessary to select an accurate evaluation aspect to asses any steganography method. The chapter provides a key concept for evaluating steganography capacity and imperceptibility. The most accurate and reliable way to determine the visual quality of such stegoe file would be by human visual evaluation (subjective evaluation), (Yan et al., 2013; Zhang et al., 2014). However, subjective evaluation is time consuming, expensive, and is not an automatic. Thus, researchers have used objective evaluation for assessing the quality of the image as it based on mathematical equations and provide faster results.

Chapter 3

Methodological Perspectives of Steganography

The process of designing a candidate system aims to solve the defined gap and is proposed as a plan for the research solution. The design of the candidate system involves taking the output of the literature review which identifies the purpose and the specification of the research approach. The design includes low-level components and approaches, implementation encounters and designing an architectural model. The research involves a mixed set of different methods.

Mainly the research consists of quantitative method, qualitative method and one case study. Quantitative studies include discovering 'data analytics' and various other tools, databases, studying distributions and assessing hypotheses. This will also involve simulations using Matlab and .Net framework. In addition, the research involves qualitative data collected from web pages, textual documents, negotiations with other researchers, application developers and own experience on the process and practices; these are combined with results from quantitative studies. In this chapter, section 3.1, section 3.2 and section 3.3 provide the mathematical prospective of the tools used to achieve the research hypothesis and aim.

The use of Human Visual System (HVS) in detecting concealed information will assist in providing high payload capacity with minimum degradation. This model manifests a certain independence from the cover image and

this is primarily done to map certain information based on the cover image contents, thereby achieving high steganographic imperceptibility. Nevertheless, such models show high complexity along with a suboptimal nature. To achieve the most out of the perceptual model, some global and adaptive search techniques such as Evolutionary Algorithm include Genetic Programming (GP), Genetic Algorithm (GA), Ant Colony Optimization (ACO), or Particle Swarm Organization (PSO) are recommended.

3.1 Human Visual System

The Human Visual System (HVS) is capable of supporting the optimal design of steganographic algorithm. However, it is necessary to carefully select an appropriate model for visual information processing, as well as representation in order to define the different effects like contrast sensitivity and masking. Significant improvement in the performance of steganographic techniques can be achieved, if these considerations are taken into account. Human beings have perfected their communicative abilities by utilizing their hearing and vision abilities (Van Nes et al., 1967). This section discusses the HVS, as applied in image steganography.

The process starts with the division of a visual signal by the retina which is then separated into different components. The key characteristics are frequency, spatial location and the signal's orientation (i.e. horizontal, vertical, or diagonal). Every component brings about stimulation to the cortex through different channels (Watson, 1987; Martin and Cochran, 1994). This is followed by a process called 'masking'. In this process, an enhancement of the detection threshold happens through interaction with a powerful signal having similar properties with the existing signal. In this chapter, the concepts of the HVS in steganography will be covered as following:

- Contrast Sensitivity
- Contrast Sensitivity Function
- Just Noticeable Distortion

- Noise Visibility Function
- Region of Interest
- Watson's Perceptual Model

3.1.1 Contrast Sensitivity

A point's perceptible brightness is based on background luminance and the point's total luminance. Figure 3.1 shows this dynamic. The central square intensity as seen in Figure 3.1.(a) as well as the target central square as seen in Figure 3.1.(b) appear as similar. However, target (b) has a darker appearance than target (a). The illustration clearly reflects the idea that apparent brightness is dependent on two things: luminance of the surrounding regions; and the absolute luminance. As a result of this interaction, a comparative change of luminance is encountered as a result of the background. This change is known as "contrast". On the other hand, when the contrast threshold is seen in spatial frequency, it is known as "contrast sensitivity".

Fig. 3.1: Demonstration of the apparent brightness

In particular, contrast masking has two definitions. The first, based on Weber contrast, is defined as the measurement expressed in relation to an object's

local contrast as seen on a uniform background. Figure 3.1 shows and example and its definition as illustrated by the equation:

$$C = \frac{\triangle L}{L} \tag{3.1}$$

where $\triangle L$ represents the difference derived from the target luminance and the background luminance L.

The second definition is the Michelson contrast, defining contrast masking. This is the measurement applied to a periodic pattern contrast (e.g., sinusoidal waves). Figure 3.2 illustrates the example and Equation 3.2 shows its definition.

$$C = \frac{L_{\max} - L_{\min}}{L_{\max} + L_{\min}} \tag{3.2}$$

where $L_{\max}$ is the maximum luminance, while $L_{\min}$ denotes minimum luminance.

3.1.2 Contrast Sensitivity Function

Human Visual System (HVS) provides mathematical models relating to the way humans perceive their surroundings. An example of a model that was developed through the HVS is a way of distinguishing sensitivity of humans to color and brightness (Wandell, 1995). In relation to this, a function called contrast sensitivity function (CSF) is known to describe the spatial frequency sensitivity. Originally, Mannos and Sakrison proposed a CSF model for luminance or gray-scale images (Mannos and Sakrison, 1974) based on the following formula

$$H(f) = 2.6(0.192 + 0.114f)e^{[-0.114f)^{1.1}]} \tag{3.3}$$

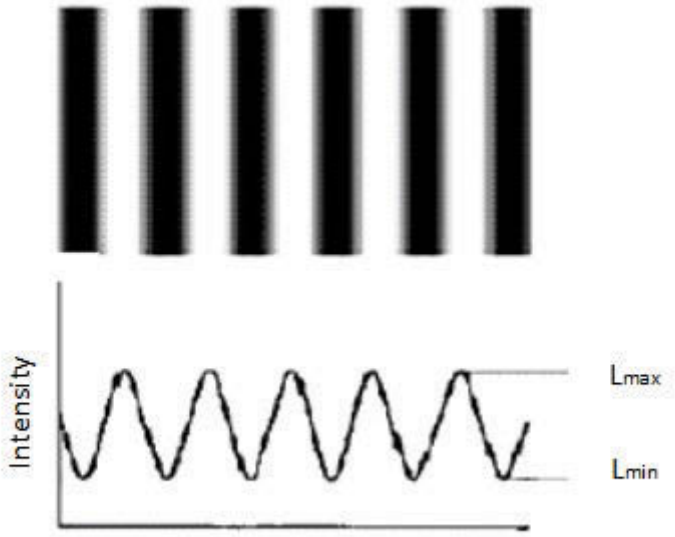

Fig. 3.2: Example of Michelson contrast with sinusoidal waves

where, the spatial frequency is denoted by $f = (f_x^2 + f_y^2)0.5$ having the units cycles / degree. It is to be noted here that f_x and f_y represent spatial frequencies along horizontal and vertical directions, respectively. Spatial frequency is normalized then through the formula:

$$f(cycles/degree) = fn(cycles/pixel) \cdot fs(pixels/degree) \tag{3.4}$$

where f_n represents the normalized spatial frequency having cycles / pixel as units. In here, f_s is at 64 $pixels/degree$, based on the observers' placing, at about a 2 feet viewing distance. This particular value representing f_s is about four times the height of the image, which is roughly 6 inches. fn bears a range value between 0 and 0.5 because f is ranged between 0 and $f_s/2$, f_n as seen in Equation 3.4.

The CSF curve is shown in Figure 3.3. It indicates the HVS luminance sensitivity based on the normalized spatial frequency function. CSF is considered

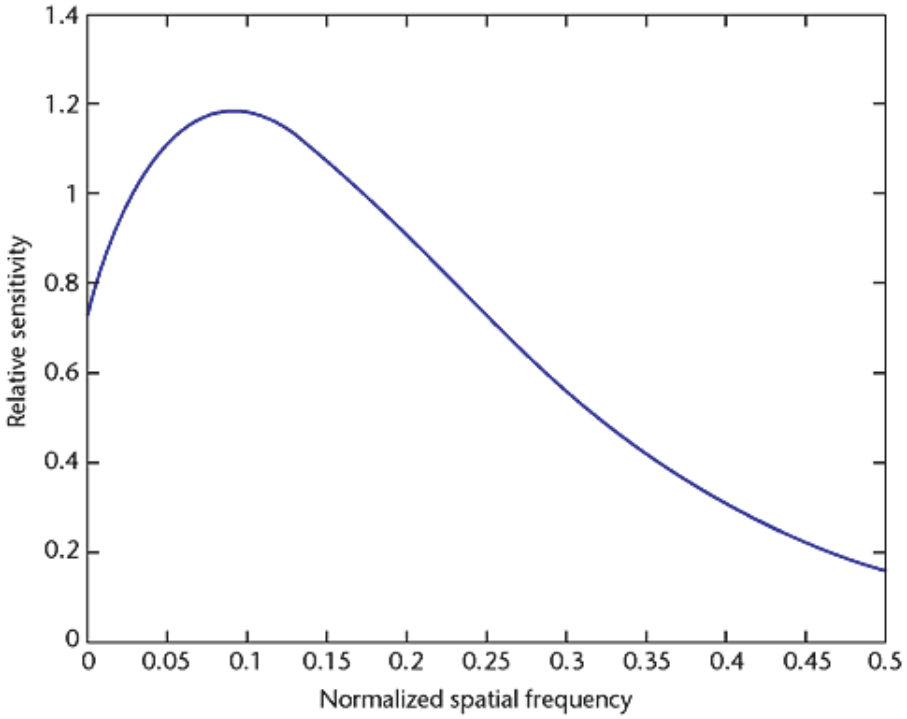

Fig. 3.3: CSF curve

as a band pass filter. For this reason, high sensitivity to spatial frequencies ranging from 0.03 to 0.23 is seen using HVS, and it has low sensitivity when frequencies are very high and very low. Similarly, CSF curves remain when chrominance stimuli are present. The sensitivity of humans to chrominance stimuli is nearly uniform when seen across spatial frequency as compared to luminance stimuli (Wandell, 1995).

3.1.3 Just Noticeable Distortion

Just Noticeable Distortion (JND) refers to quantification for characterizing luminance transformation perceived through the HVS. JND provides the luminance values, particularly the maximum difference perceived by the eyes. The JND model's visibility threshold is evaluated through the use of percep-

tual function, which is illustrated through the equation

$$JND(k) = \begin{cases} T_0[1 - (k/127)^{0.5}] + 3 & k \leq 127 \\ \gamma(k - 127) + 3 & otherwise \end{cases} \tag{3.5}$$

Where, k denotes luminance value between the range 0 and 255 while parameters T_0 and γ are based on viewing distance seen between the monitor and the tester. T_0 represents visibility threshold at 0 background gray level, and γ is the line slope modeling JND visibility threshold function when subjected at a luminance with a higher background. T_0 and γ are at 17 and 3 / 128, respectively for this particular study. The basis for which is Chou and Li subjective experiment (Chou and Li, 1995). The gray value visibility threshold for this research is calculated and shown in Equation 3.5 and illustrated in Figure 3.4. HVS is known to have a relative sensitivity to luminance change when the medium related to luminance range is considered. On the other hand, HVS is known to have lower sensitivity to change of luminance (Barten, 1999; Lee et al., 1994) particularly for regions having bright or dark characteristics. Figure 3.4 show the smallest visibility threshold, calculated as 3 if k is at 127.

3.1.4 Noise Visibility Function (NVF)

The foundation of Noise Visibility Function (NVF) is a non-stationary Gaussian model. The primary function of NVF is the estimation of regional complexity through the analysis of local image properties in every region. The following formula illustrates NVF at every position of the pixel when C denotes cover image:

$$NVF(m, n) = \frac{1}{1 + \mu\sigma_x^2(m, n)} \tag{3.6}$$

where $\mu = \frac{D}{\max[\sigma_x^2]}$

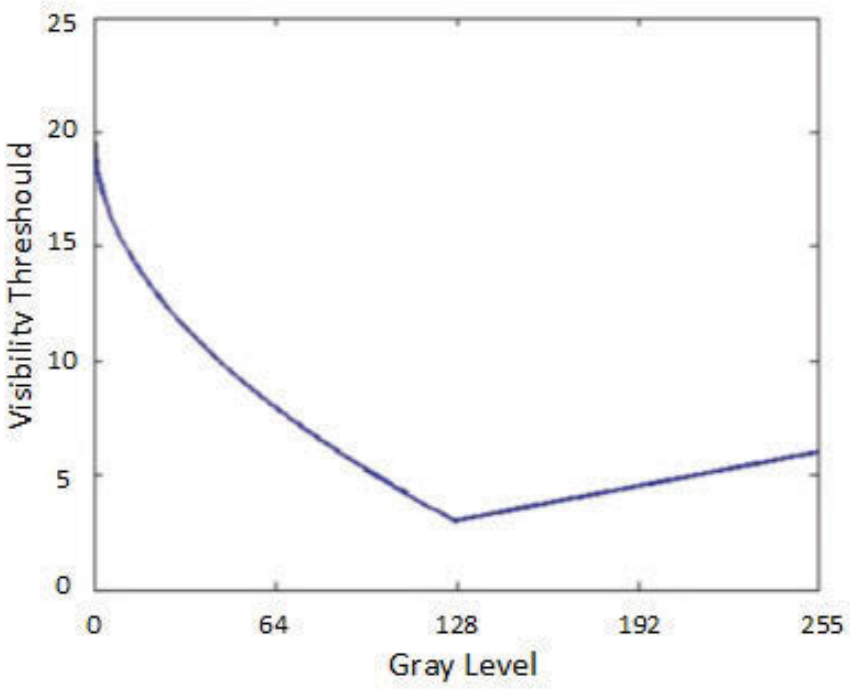

Fig. 3.4: Visibility threshold $JND(k)$ applied in varied gray levels

$$\sigma_x^2(m,n) = \frac{1}{(2L+1)^2} \sum_{k=-1}^{L} \sum_{l=-1}^{L} (x(m+k, j+l) - \bar{x}(m,n))^2$$

$$\text{with } \bar{x}(m,n) = \frac{1}{(2L+1)^2} \sum_{k=-1}^{L} \sum_{l=-1}^{L} (x(m+k, j+l)$$

where the region size $(2L+1)^2$

where $\sigma_x^2(m,n)$ is the image's local variance when a centering of the window on the pixel having coordinates (m,n) is seen. On the other hand, μ denotes the function of the contrast adjustment in each specific image. Also, $\max\lfloor\sigma_x^2\rfloor$ denotes maximum local variance, while $D \in [50,100]$. Usually, D is set at 75. Moreover, NVF could be '1' when it is in flat areas while it is '0' in areas that are complex. NVF images built from the aforementioned strategy is shown in Figure 3.5. In Figure 3.5, the cover images and the NVF images outcome are shown. Particularly, NVF is able to distinguish complex areas from the given smooth areas through a clear and precise way. Darker regions in NVF-images imply the presence of higher amount of edge pixels meaning

that higher complexity is seen. These regions are used to expand embedding capacity while eliminating the possibility of any artifacts that can be easily identified as anything other than their primary meaning.

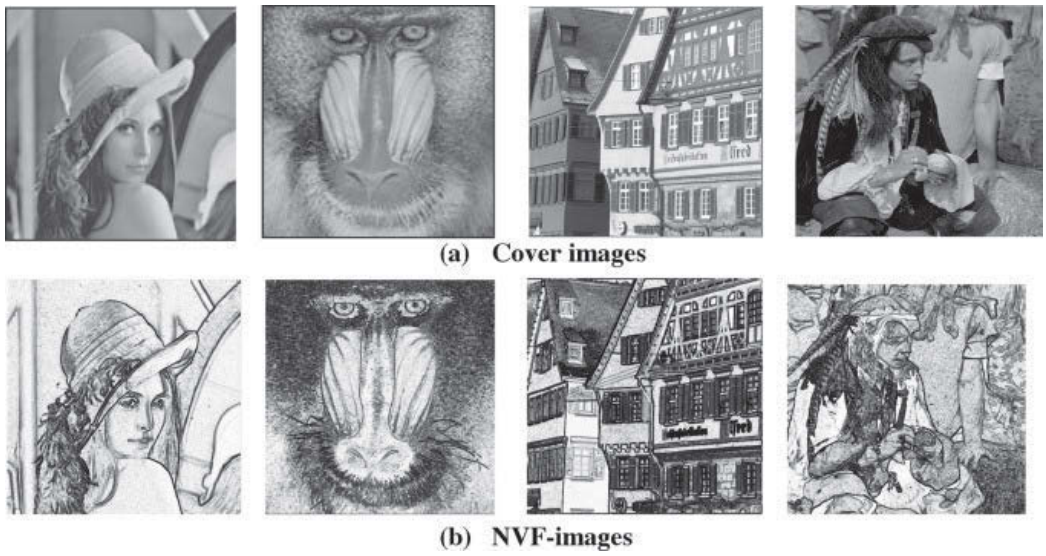

Fig. 3.5: Comparison of cover images (a) and resulted NVF images (b)

3.1.5 Region of Interest

One significant subject in the field of image processing is the process of searching the image regions that potentially attract the attention of humans. When this region illustrates a heightened interest for the human eye, this is called Region of Interest (ROI) and this is used to emphasize image detection. The process starts with the division of the image into blocks with the same sizes, wherein each block is known as 'a region'. The division is followed by the computation of ROI score for every block that represents the human eye interest that could be attributed to the region.

The amount for the block capacity is based on the identification of block scores and ROI measure, followed by the estimation of image complexity. The ROI score in the image blocks is derived from Osberger's idea (Osberger and Maeder, 1998). To summarize, the score for the ROI of sub-images can be derived through the application of influencing parameters with the objective

of estimating block scores that correspond to needed ROI attractiveness. These parameters are also called ROI score parameters. These parameters include the concept of intensity, contrast, location, edginess, and texture.

The concept of intensity is characterized by the location of the blocks. In particular, the intensity is known if image blocks are seen to be closer to the mid-intensity frequency of the image, illustrating the regions that possess the highest sensitivity to human vision. Contrast is associated with the high level of attraction to human attention and perceptual importance depending on the surrounding blocks. On the other hand, location is concerned with the perceptual importance of the image's central-quarter as compared to other areas of the image. Edginess is seen when the human eye becomes attracted to a block that include edges that are perceived as prominent.

Lastly, when texture is discussed, the attractiveness to the human eye is most often based on regions that are not flat or those that are known as textured. The ROI is derived by dividing the value of host image by having the formula N_1 by N_2 representing sub-images (blocks). This is followed by the calculation of quantitative measure (M) for all the five score parameters for ROI at every block. With this process, the following mathematical equation is proposed to obtain parameter quantitative measure:

3.1.5.1 Intensity Metric

The equation below is used to derive a sub-image's Si mid intensity importance $M_{intensity}$

$$M_{intensity} = |\text{AvgInt}(S_i) - \text{MedInt } (I)| \tag{3.7}$$

where $\text{AvgInt}(S_i)$ denotes the sub-image S_i average luminance while $\text{MedInt } (I)$ represents the average luminance characterizing the entire image I.

3.1.5.2 Contrast Metric

If a sub-image has the ability to attract human vision and attention, it his seen to have a high contrast level which results in a perceptually impor-

tant character. The constant measure is known when average sub-image S_i luminanceAvgInt(S_i) and average luminance of surrounding sub-images AvgInt($S_{surrounding-i}$) are known as:

$$M_{contrast} = \text{AvgInt}(S_i) - \text{AvgInt}(S_{surrounding-i}) \tag{3.8}$$

3.1.5.3 Location Metric

The measurement of location importance $M_{Location}$ seen in every sub-image is calculated by considering the ratio of the total number of sub-image pixels seen in the image's center-quarter and the total pixel number present within the certain sub-image. It happens when experiments related to eye tracking show that visions are focused at center 25 seen are the screen with the purpose of perceiving the materials. The equation below represents this process:

$$M_{Location} = \frac{\text{center } (S_i)}{\text{Total } (S_i)} \tag{3.9}$$

In here, the center (S_i) denotes the amount of pixels seen within the sub-image i in the central quarter. On the other hand, the total S_i represents the overall pixel number present in the sub-image. This represents the total sub-image area. There is an essential role being played by this certain parameter especially in the detection of ROI. However, comparing this against other parameters may not be worthwhile between two different images because blocks of some pixels in the quarter center is equal with the parameter as seen in the two images. Furthermore, this parameter is considered when consistency is distinguished, particularly for ROI detection.

3.1.5.4 Edginess Metric

Edginess $M_{Edginess}$ represents the overall number of sub-image edge pixels. In here, Laplacian edge detection was used having a threshold of 0.7. This

threshold represents minor edges ordinarily occurring and also those presented in the background; however, no effects are seen on the edginess metric.

3.1.5.5 Texture Metric

Texture parameter can be obtained through a calculation of the variance of pixel values which are present in every sub-image. There are also other methods that are more advanced, aimed at analyzing textures, including the Tamura measures (Bae and Jung, 1997). However, such methods require more time for the computation process. In this research, the aim is to estimate the textured area and differentiate these from other regions that are flat. This is to say that texture metric does not aim to categorize textures (Mohanty et al., 2013). Because of this, a suitable measure is presented with the purpose of indicating a high value for a variance to illustrate a sub-image that has a texture or not flat. The calculation of which is shown in Equation 3.10:

$$M_{Texture} = \text{var } ((\text{pixel\_graylevels(i)}) \tag{3.10}$$

where pixe_graylevels(i)) denotes pixel gray level values present in the sub image i.

In order to generate a general output for Importance Measure (IM) corresponding to every particular sub-image, the exact weight for the various factors and their corresponding relationships has not been studied extensively. While several factors influencing visual attention were already noted by some researchers (Basu et al., 2015; Osberger and Maeder, 1998; Wazirali and Chaczko, 2015b,c), little quantitative data about the topic exists. Furthermore, this dynamic has a possibility of undergoing a transformation from one particular image to another. Hence, each factor is treated and considered to have identical significance. An appropriate weight is yet to be simply integrated if a specific factor is seen to have higher importance than the other.

Equation 3.11 emphasizes the significance of the regions that possess higher

ranks based on the score parameters of ROI known as IM equation. Every parameter here undergoes the computation of its square before being applied to the equation. This is due to the fact that the value of the regions with high ranks is not in accordance with just a simple ROI score averaging. Every sub-image Si for the final IM is then illustrated as follows:

$$IM(S_i) = M_{intensity}(S_i)^2 + M_{contrast}(S_i)^2 + M_{Location}(S_i)^2 \tag{3.11}$$

$$+M_{Edginess}(S_i)^2 + M_{Texture}(S_i)^2$$

After IM values have been computed for the entire spectrum of sub-images, these are sorted leading to the identification and selection of IM with the maximum value, and this is identified as the region that is perceptually most important. Next, the input image is divided into 16 sub-images with equal sizes with the aim of running the blocks. Consequently, the IM is also computed for every block. Figure 3.6 illustrates the ranking for the two images, specifically the Lena and Couple. It should be noted here that the 8 highest score blocks initially presented were just the ones given through the numbers 1 to 8 as seen on the blocks at the upper left corner.

3.1.6 Watson's Perceptual Model

When the block of the image is considered in relation to the estimation of perceptibility to changes, the Watson perceptual model can be used for this purpose. The model is ideal in this situation as it offers a way of measuring the amount of distortions present in relation to the number of resistances by the DCT coefficient. A cover media's kth block is denoted as C, and $C[i; j; k]; 0 \leq i; j \leq 7$. $C[0; 0; k]$ represents DC term (i.e., mean pixel intensity present in the certain block). This model is made up of a function related

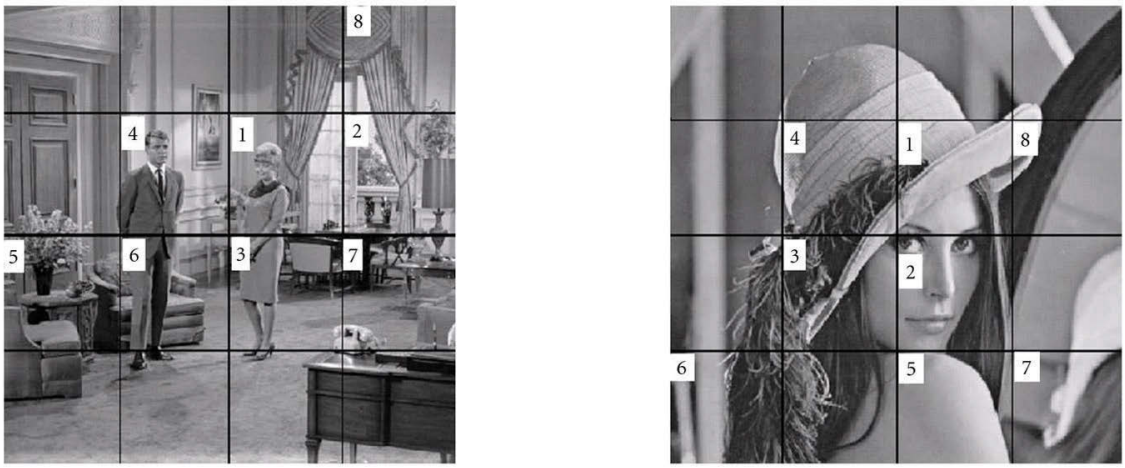

Fig. 3.6: Ranking of subimages (blocks) based on ROI score calculation

to sensitivity, two components for masking that use contrast masking and luminance as bases, and a specific component for pooling.

3.1.6.1 Frequency Sensitivity

To illustrate frequency sensitivity, the table t below shows the entry table $t[i; j]$ representing a definition illustrating the approximated smallest magnitude attributed to corresponding DCT coefficient present in a certain block perceptible despite the lack of any kind of masking noise applied in the image. Cox sets the value table as a constant (Cox et al., 2008) as shown in Table 3.1.

1.40	1.01	1.16	1.66	2.40	3.43	4.79	6.56
1.01	1.45	1.32	1.52	2.00	2.71	3.64	4.60
1.16	1.32	2.24	2.59	2.98	3.64	4.60	5.88
1.66	1.52	2.59	3.77	4.55	5.30	6.28	7.60
2.40	2.00	2.98	4.55	6.15	7.46	8.71	10.17
3.43	2.71	3.64	5.30	7.64	9.62	11.58	13.51
4.79	3.67	4.60	6.28	8.71	11.58	14.50	17.29
6.56	4.93	5.88	7.60	10.17	13.51	17.29	21.15

Table 3.1: Table for frequency sensitivity

3.1.6.2 Luminance Masking

The threshold for a luminance pattern is usually detected based on the image

region's mean luminance. In here, it is said that luminance threshold is higher if the background is brighter (Van Nes et al., 1967). This change is generally referred to as "light adaptation" and it is presented as "luminance masking" in this research to highlight its parallel to the idea of contrast masking. The computation of luminance-masked threshold matrix applied for every block is based on the following formula as also used by Ahumada and Peterson (Ahumada Jr and Peterson, 1992):

$$t_{i,j,k} = t[i,j](\frac{L_0 C_0[0,0,k]}{C_{0,0}})^{\alpha\tau} \tag{3.12}$$

In here, $\alpha\tau$ denotes a constant but possessing a recommended value amounting to 0.649, while mean display luminance is known as L_0. DC coefficient of k^{th} block, as seen from the source image is shown as $C_0[0,0,k]$. $C_{0,0}$ denotes DC coefficient average. Lastly, $C_{0,0}$ can be placed as a part that has a constant value showing expected image intensity.

To initially compute for the $t_{i,j,k}$, a display luminance, $L0$ should be assumed. The name of the parameter $\alpha\tau$ was based on the formula proposed by Ahumada and Peterson (Ahumada Jr and Peterson, 1992). In here, the authors proposed 0.649 as its value. Luminance masking has the possibility of being suppressed by making the parameter $\alpha\tau$ equal to 0. Also, $\alpha\tau$ is known as the extent of the possibility of the occurrence of masking. It should also be noted here that incorporation of non-unity display Gamma will be easier because of the power function and through the multiplication of $\alpha\tau$ using Gamma exponents.

3.1.6.3 Contrast Masking

If the visibility of an image element by another image is reduced, this is known as contrast masking. The masking process becomes very strong when the components have similar elements such as spatial frequency, location, and orientation. Only masking that occurs within a particular block and DCT coefficient were considered (i.e., masking across DCT blocks and between DCT coefficients. If the DCT coefficient as well as a matching absolute thresh-

old for the masking rule are present, masked threshold is then illustrated as follows:

$$s[i,j,k] = \max(t_L[i,j,k], |C_0[i;j;k]|^{w_{ij}} t_L[i,j,k]^{0.3}) \tag{3.13}$$

where, exponent w_{ij} is situated between the range 0 and 1. However, this exponent has the possibility to be different for every frequency. For this reason, a matrix of exponents having equal size with the DCT is present. It should be noted that masking does not happen if this is equivalent to 0 and threshold is considered constant. On the other hand, Weber's Law is evident if w_{ij} is equal to 1and the threshold occurs as constant either in log form or in percentage terms (i.e., $C_{ijk} > t_{ijk}$). An empirical value that is usually at 0.7 is known for this function (Figure 3.7).

The DC terms are then excluded for the reason that the DC coefficient's effect on the thresholds were already expressed through the application of luminance masking. Specifically, this is done by making 0 as w_{00} value. Luminance masking here presents that DC frequency is strongly correlated to each of the frequencies despite the assumption that contrast masking has an independent characteristic from coefficient to another coefficient or frequency to frequency.

3.2 Edge Detector Techniques

Edge detection is a tool utilized in image processing for feature recognition and abstraction, the purpose being to classify points in an image where the intensity of image deviates suddenly. In a gray scale image the edge is a ingenious feature that, within a neighborhood, splits areas where the gray level changes more or less abruptly on the two sides of the edge or texture representations.

The main idea behind edge detection embedding is to identify areas of tone change or object boundaries of the original image in order to find carrier

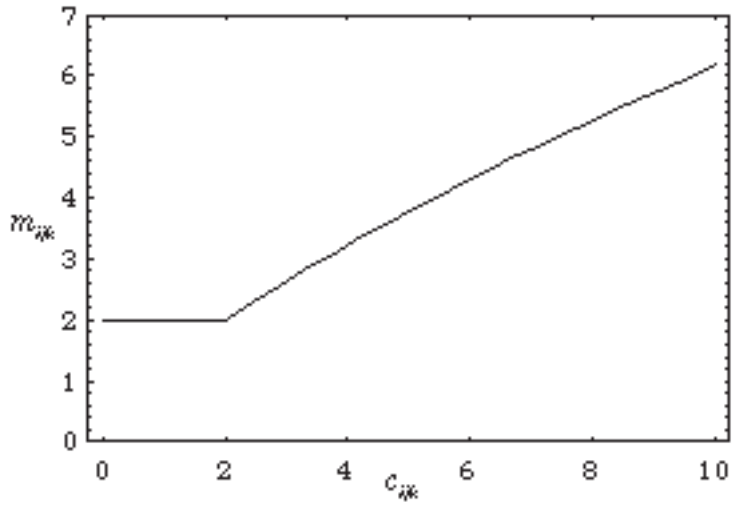

Fig. 3.7: Contrast masking function with the description of masked threshold

pixels best suitable for data insertion. Most of the existing edge-based embedding use Laplacian, Canny or Fuzzy edge detection operators separate useable edge pixels from uniform tone areas ensuring minimum changes to the cover image and are therefore hardly detected with any alteration by the HSV. However, most of the existing approaches are used in gray-scale images while there is limited edge detection in color images; this reflects the lower embedding capacity of gray-scale images compared to color images. Therefore, effective techniques to extract the edge region in color images are needed for the embedding process. Figure 3.8 shows the performance of various edge detector techniques.

3.2.1 Sobel method

The Sobel operator is one of the most commonly used edge detectors. It is a separate variation operator used to calculate an estimation of the gradient of image concentration function for edge detection. At every pixel of an image, Sobel operator provides either the matching gradient vector or standard to the vector. It convolves the host image with the kernel and calculates the slope scale and direction. It utilizes a 3x3 kernel matrix as given in

Fig. 3.8: Various edge detector approaches

Equation 3.14 emphasizing pixels that are near to the center of the mask.

$$S_x = \begin{matrix} -1 & 0 & +1 \\ -2 & 0 & +2 \\ -1 & 0 & +1 \end{matrix} \quad \text{and} \quad S_{y=} \begin{matrix} -1 & 0 & +1 \\ -2 & 0 & +2 \\ -1 & 0 & +1 \end{matrix} \tag{3.14}$$

The Sobel edge operator is the degree of the gradient calculated by: $M\sqrt{s_x^2 + s_y^2}$ where the partial derivatives are calculated by:

$$s_x = (a_2 + ca_{3+}a_4) - (a_0 + ca_1 + a_6) \tag{3.15}$$

$$s_y = (a_0 + ca_{1+}a_2) - (a_6 + ca_5 + a_4) \tag{3.16}$$

with the constant c=2

3.2.2 Prewitt method

The procedure of the Prewitt detector is almost similar to that of the Sobel detector but with different mask values it provides better performance as shown in Equation 3.17. It uses the same equation as given in Equation 3.15 and Equation 3.16 with constant $c = 1$.

$$D_i = \begin{matrix} -1 & 0 & +1 \\ -1 & 0 & +1 \\ -1 & 0 & +1 \end{matrix} \quad \text{and} \quad D_{j=} \begin{matrix} +1 & +1 & +1 \\ 0 & 0 & 0 \\ -1 & -1 & -1 \end{matrix} \tag{3.17}$$

The main advantages of both Sobel and Prewitt detection are: simplicity, which provides simple estimation to the gradient magnitude; easy detection of edges and their orientations due to approximation of the gradient magnitude.

3.2.3 Canny Edge Detector

Canny Edge Detection is considered to be the most optimal solution in terms of computing power expenses and produces clearly defined edges, preventing possible data corruption. This algorithm was developed by John F. Canny in 1986 evolved from his work, *A Computational Theory of Edge Detection* (Canny, 1986) It is widely used in various image and video processing applications, such as object detection, feature extraction and many raster image filters. It offers optimal edge detection, that is efficient, strong and showsdecent localization. Good detection can be achieved by selecting as many edges as possible; good localization selects close edges in the real image with

minimal response, rejecting noise, and ensuring that a given edge has been marked only once.

In the Canny method, a pixel can be classified as an edge pixel if the gradient magnitude of that specific pixel is greater than other pixels on either side and in the direction of greatest intensity alteration. The work starts with removing the noise using Gaussian filter with fixed standard deviation. Then the work continues to calculate the gradient magnitude $g_x^2 + g_y^2$ and edge direction $\tan^{-1}(\frac{g_x}{g_y})$ at each point. Points are considered as an edge point when their strength is maximum in the gradient direction.

The Canny Edge Detection algorithm consists of several stages:

1. Gaussian Blur is applied to reduce the amount of noise in the image
2. Gradient detection algorithm is applied to determine gradient magnitude and direction
3. Each pixel is compared to its neighbors in gradient direction. Strongest values are marked as the edge, while weakest are eliminated into background
4. Weakest edges are removed by hysteresis threshold

3.2.4 Laplacian of Gaussian method

Laplacian of Gaussian (LOG) is mainly based on smoothing the host image before it detects the edges. The noise removes through complication between LOG operator and Gaussian shaped kernel as given in Equation 3.18 followed by Laplacian Operator is shown in Equation 3.19.

$$G(x, y) = e^{\frac{-x^2+y^2}{2\sigma^2}} \tag{3.18}$$

Where σ represent the standard deviation. If coiled with an image, this will make it unclear. The amount of blurring is computed by the value of σ.

$$\nabla^2 G(x,y) = \frac{\partial^2 G(x,y)}{\partial x^2} + \frac{\partial^2 G(x,y)}{\partial y^2} = \left[\frac{x^2+y^2-2\sigma^2}{\sigma^4}\right] e^{\frac{-x^2+y^2}{2\sigma^2}} \tag{3.19}$$

The laplacian $L(x,y)$ with intensity of $I(x,y)$ of a specific image can be calculated as follows:

$$L(x,y) = \frac{\partial^2 I}{\partial x^2} + \frac{\partial^2 I}{\partial y^2} \tag{3.20}$$

The standard 5 by 5 LOG mask is giving in equation Equation 3.21

$$\begin{matrix} 0 & 0 & -1 & 0 & 0 \\ 0 & -1 & -2 & -1 & 0 \\ -1 & -2 & 16 & -2 & -1 \\ 0 & -1 & -2 & -1 & 0 \\ 0 & 0 & -1 & 0 & 0 \end{matrix} \tag{3.21}$$

The resulting capacity of the stego image depends on the amount of edge pixels detected by the Canny operator. While this technique allows us to embed more data in carrier areas, the total payload capacity is much smaller in comparison to standard LSB algorithm.

3.3 Evolutionary Algorithm

3.3.1 Overview

Evolutionary Algorithm (EA), when applied in the field of computational intelligence, refers to a certain evolutionary computation subset. It is also

considered as a meta-heuristic optimization process that is known as generic and population-based. These are also known as search methods based on biological evolution as a result of natural selection and natural genetics. EAs are done through the process of searching solutions from a certain population. This makes it distinct from other optimization techniques traditionally used because other techniques only process from one point. EAs also apply an objective function as well as stochastic/genetic operators. EA then discards those individuals that have poor characteristics and selects candidate solutions that are considered to possess high fitness. This process happens after each generation. There are four Evolutionary Algorithms types generally known: Genetic Programming; Genetic Algorithms; Evolutionary Strategies; and Evolutionary Programming. EA can do both exploration and exploitation processes. For this reason, EAs are classified as a robust optimization technique.

EAs have better security and capacity characteristics when compared to other techniques (Fard et al., 2006b). EA is used with the objective of capturing areas that have been embedded with consideration on the message size and the improvement of the image region's threshold position.

During the process of data embedding, the process starts with the initialization of specific parameters (Spector, 1997). These parameters are applied to the succeeding data process as well as the capturing of the region that assists in optimizing threshold values. Concealment of data commences when captured regions seem to be enough for the message. This process is done in a repetitive manner with the use of EA and adjustment of the regions. It is repeatedly done until the embedding of the hidden message is complete.

3.3.2 Genetic Algorithm (GA)

This algorithm is known as a heuristic search function, mimicking the natural selection process. It is usually applied for optimizing and achieving solutions to problems. GAs are part of a larger EA class aimed at generating solutions for problems relating to optimization through techniques that have been as-

sociated with natural evolution, for example inheritance, selection, crossover and mutation.

This algorithm involves the population in the evolution through itemized selection rubrics showing the principle popularly known as "survival of the fittest". It minimizes costs and was originally proposed in 1992 by Holland (Holland, 1992). If there is no knowledge regarding the correct solution, then the algorithm starts and this is completely based on the responses coming from the environment as well as the given evolution operators. These operators include reproduction, crossover and mutation and their objective is the attainment of the correct and best possible solution (Chan C. K. and Chan L. M., 2004).

The different but independent positions, as well as ways of finding parallel dimensions, are based on an algorithm that circumvents the local minima. This is followed by a congregation of the sub-optimal elucidations. Through this process, GAs to be considered are based on their ability to search for high-performance expanses along the complex domains while maintaining an easier way to determine concomitants related to high dimensionality. As a result, a difficulty could occur with techniques or methods that are based on the information that will be derived, particularly through a descent ascent method (Chang C. C. et al., 2003). Genetic algorithm refers to a scheme aimed at mimicking genetic evolutions to explain and address current problems (Zollner, J. et al., 1998). The input is based on a given problem, and it is followed by the coding of the result through a specified pattern. Subsequently, evaluation of all possible solutions is done through fitness functions. In particular, evolution begins from random entity sets then a reiteration of the process is made for the other generations (Zollner, J. et al., 1998). The suitable ones are considered, and they are combined with each the generations. The basic procedure for this specific Genetic Algorithm is presented in Figure 3.9.

3.3.2.1 Initialization

The basis for the determination of population size is the problem's nature. As a result, it usually involves thousands or hundreds of probable solutions. Furthermore, the preliminary population is usually generated in a random manner. This process allows the generation of many possible solutions as seen in the entire search space. However, the solutions are rarely "seeded" especially in areas possessing optimal solutions.

3.3.2.2 Selection

A selection of the current population is done for every subsequent generation with the aim of breeding another original generation. This is followed by selecting single solutions based on a fitness-based process. Here, the fitter solutions are selected through a measure related to the fitness function. Selection methods are also used to rate fitness characteristic for every solution and the selection of preferred and best solutions. Other methods may only measure a certain sample that has been randomized to avoid a time-consuming process.

The definition of fitness function depends on genetic representation as well as the aim of measuring the quality of solution being represented. In addition, this also depends on the problem. This is also shown to maximize the object's total value by putting it in a pocket having fixed capacity. A solution will be represented with an array of bits. Every bit represents a corresponding object while their value is represented as 0 or 1, implying the presence of the object in the knapsack. However, not all of these representations are valid. This is for the reason that the object size could go beyond the knapsack capacity. The solution fitness then is known as the sum of all the object values inside the knapsack when the validity of the representation is known. This is known as 0 if it is not inside.

A difficulty in defining fitness expression is seen to be persistent in some of the problems presented. In such circumstances, the identification of fitness function value is derived through a simulation of the phenotype. For

instance, computational fluid dynamics can be applied to identify air resistance encoded as phenotype or when the application of interactive genetic algorithms becomes evident.

3.3.2.3 Genetic operators: crossover and mutation

The process is followed by a creation of a second generation population to be applied for solutions from the selection. This step is done by combining genetic operators such as “crossover” and “mutation” (Vose, 1999).

Every new solution generated through this process is based on two "parent" solutions. These solutions are selected for the purpose of breeding based on the pool which has been previously selected. New solutions are made by generating "child" solution through mutation and crossover methods. This typically shows the same characteristics as its "parents". Furthermore, the selection of new parents is done for every one of the new children. This procedure is continued and only ends when new sets of solutions with a suitable fitting size have been produced (Vose, 1999). While these methods for reproduction depend on a biological perspective, other studies propose other ways to generate high-quality chromosomes that have more than two "parents".

As a result, the next-generation population becomes distinct from the original generation. In general, an increase in the average fitness is seen through this process due to the fact that the best organisms are chosen from first generation population. These are the ones considered in the process of breeding together with the smaller proportion of solutions that are considered unfit. The unfit solutions are then guaranteed genetic diversity in the parent’s pool and genetic diversity in the following generation.

Other operators can also be used including colonization/extinction, genetic algorithm migration, and regrouping. Sometimes, it is also good to tune or combine different parameters with crossover probability, mutation probability, and the size of the population to search for the most reasonable settings in relation to the solutions for the certain problem class sought. However, even

if the mutation rate is only tiny, a genetic drift may occur. This is seen to be naturally non-ergodic. On the other hand, if the recombination rate is very high, the genetic algorithm convergence could occur prematurely. Lastly, if the mutation rate is very high, good solutions may be elusive. Nonetheless, this can be addressed if we apply an elitist selection process.

3.3.2.4 Termination

A repetition of the generational process continues until a certain condition required for termination is attained. Some of the conditions for the termination process include:

1. when a solution that responds to the minimum level criteria has been sought;
2. when a fixed amount of generations has been attained;
3. when a certain budget allocation has been reached through computation time and money;
4. when the fitness of highest ranking solution has been reached, and this can be attained when subsequent repetitive processes being done does not generate better results anymore;
5. through manual inspection; and
6. any combination of the above mentioned conditions.

3.3.3 Genetic Programming

Genetic Programming (GP) is an optimization of search algorithm proposed by (de Garis, 1993). It is a part of the probabilistic optimized search algorithms, which is based from ideas related to genetics, natural selection and biological evolution. The process of GP includes a development of candidate

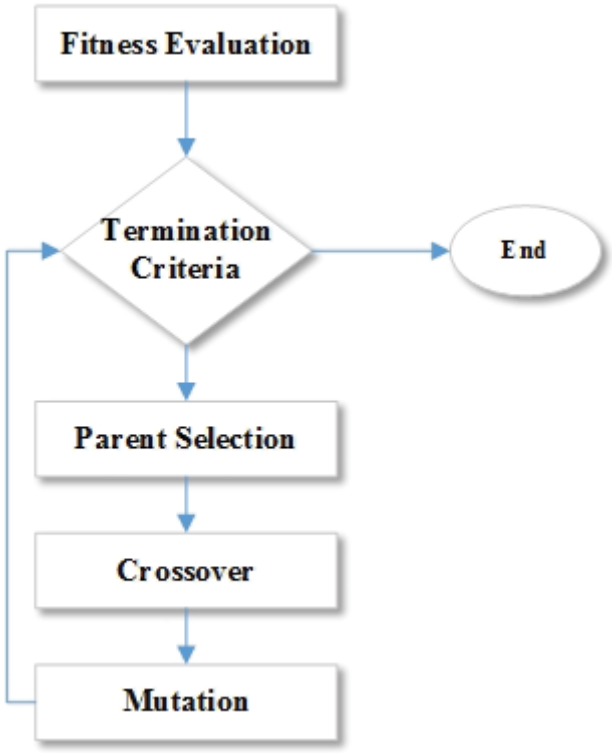

Fig. 3.9: General Flowchart for Genetic Algorithm

solutions aimed at a given specific problem and subsequently follows a repeated evolution through stochastic operators. Every candidate solution is then assessed in terms of fitness function designed for the specific purpose. To indicate a high probability of offspring generation, fitter solutions are included after the assessment. A continuous iteration and its cycle only end when an optimal solution has been obtained or a completion of predefined iteration sets are achieved.

When GA and GP are compared, the difference lies in the chromosome element. In GA, value is the element while a tree is the element in GP chromosome. Much has been been written about GP (Banzhaf et al., 1998) and GA (Holland, 1992).

3.3.3.1 Typical Representation

To create a GP program, both the function and terminal sets are needed. Function sets or Non-terminal sets work by processing a certain value by passing as parameter, which is typically composed of cos, log, sin, abs, exp, not, or, floor, ceil, max, min, gt, le, eq, etc., as well as operators (e.g., +, -,%, *) among others. On the other hand, the terminal does not include any arguments. However, it involves variables as well as constants where the application of the various operations is evident. The GP tree is then created through the identified functions and terminals. The GP tree (Figure 3.10) is also known as an individual candidate solution.

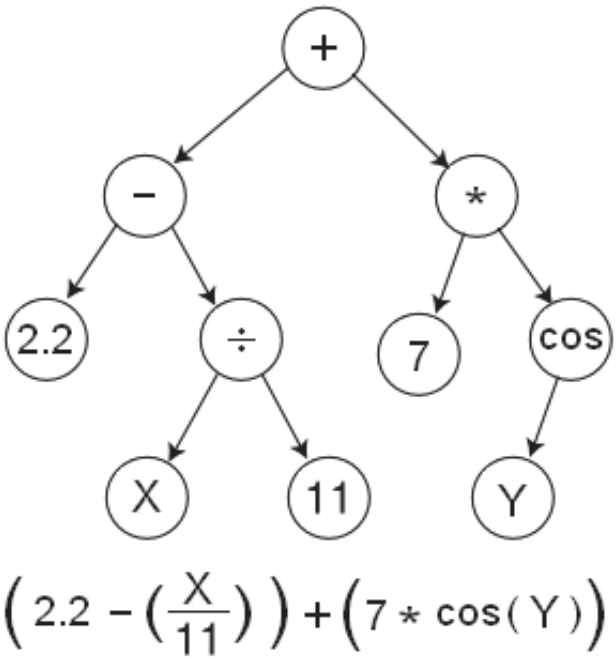

Fig. 3.10: GP Tree

3.3.3.2 GP Generation

Every individual sample of the GP population, also known as candidate solution, is denoted by a certain data structure, known as a tree. The tree is created through a combination of non-terminals and terminal. GP simulation

starts by setting a maximum size for the program that corresponds to the tree's maximum depth. The generation of offspring for chosen parents is done through the use of specific operators. Different methods can be used to generate different programs. Some of the methods can be used to generate different programs. Some of the methods include: 1) The Full Method; 2) The Grow Method; and 3) The Ramped Half-and-Half Method.

3.3.3.3 GP Operators

A low fitness value is possessed by the initial population and it is for this reason that various genetic operators can be used for the generation of offspring. Operations used in this process include reproduction, mutation, and crossover. During the reproduction process, selection of one generation present in a program happens and this is transferred to the succeeding generation with the same characteristics or no change in its trait becomes apparent. On the other hand, crossover process involves selection of best attributes from various programs present in a certain population with the purpose of creating offspring and moving this offspring to the subsequent generation. As a result, sub-trees involving two trees are swapped, which will become two different programs to be transmitted to the subsequent generation. The purpose of which is to aid in converting them to an optimum solution. The last process known as mutation involves the flipping of a candidate solution based only on a certain small part of this solution. As an effect, diversity is seen in the solution based on this tiny random change. This also aids when things get stuck in the local optima.

3.3.3.4 Fitness Criteria

Each of the single candidate solutions in every population undergoes evaluation with the use of fitness function. Fitness refers to how well the program generates and output from a given input set. So a solution's fitness can be derived by considering the fitness function. Nonetheless, there is a variation of fitness function within a variation of fitness function within a given

problem set.

3.3.3.5 Termination Criterion

GP simulation is ended after defining the termination condition. It generally occurs when a pre-identified generation number has been obtained, and this number should be processed. Similarly, this also happens when a certain level of threshold fitness has been obtained. The single most optimal individual is generally considered as the solution. Choosing terminals and functions is crucial in this process for the reason that not having good selection could lead to a very slow convergence or the possibility of futile generation of solutions.

3.4 Conclusion

This chapter discussed the different perspectives related to the methodologies used in steganography. In particular, visual system characteristics which will be used in this research as well as the methodology of the optimum effect on the steganographic technique have been discussed. The Human Visual System (HVS) was discussed by stating that this has three important channels including: the frequency; spatial location; and signal orientation. In here, the process of masking happens where enhancement of the detection threshold occurs. Similarly, the chapter also focused on Contrast Sensitivity, which is based on background luminance and intensity. Contrast Sensitivity Function using spatial frequency is based on the sensitivity of human perception. Just Noticeable Distortion (JND) which provides luminance values particularly the maximum difference perceived by the eyes. Likewise, Noise Visibility Function (NVF) is based on the estimation of regional complexity through the analysis of local image properties in every region. This section also presented some metrics or parameters for Region of Interest (ROI). These parameters include contrast, location, edginess and texture. To summarize, the score for the ROI of sub-images can be derived through the application of influencing parameters with the objective of estimating block scores that

correspond to needed ROI attractiveness. These parameters are also called ROI score parameters. These parameters include: the concept of intensity; contrast; location; edginess; and texture. The Watson Perceptual model and edge detection tools have been also discussed. In addition. edge detectors approaches have been presented.

The second part of this chapter presented the concept of Evolutionary Algorithm (EA) which is a meta-heuristic optimization process in the field of computational intelligence, generally applied to a certain evolutionary computation subset. The process includes different sub-processes including initialization, selection and generation. In all of the processes, consideration should also be present when simulating the genetic program and operators as well as fitness criteria since we want to have the best possible solution to the problem, as far as steganography process or methodology is concerned.

Chapter 4

Optimized Embedding Rate in Edge based Steganography [1]

4.1 The Problem

Considering that digital artifacts have become an important facet of daily life, the need to preserve meta-data in digital media has grown remarkably. As stated in Chapter 1, steganography is considered a potential solution through embedding the meta-data of digital artifacts. Therefore, effective steganographic techniques are required that hide large size meta-data while avoiding any visible or statical distortions. Spatial domain and frequency domain are the main common and effective techniques for inserting data into a carrier as mentioned in Chapter 2. Although spatial domain provides a high embedding rate, it results in a high error rate to the output.

Most of the spatial domain approaches assume that the least significant bits of the cover image are insignificant. Thus, the Pseudo Random Number Generator (PRNG) is mostly utilized for selecting pixels targeted to embed data. The use of PRNG is not always accurate particularly for the kind of images that have higher proportion of smooth areas than sharp areas.

[1] Some of this chapter contents have been published on Journal of Networks, Vol 10, No. 8 (2015) entitled "Data Hiding Based on Intelligent Optimized Edges for Secure Multimedia Communication". Another related works have been published on Journal of Information Hiding and Multimedia Signal Processing Vol. 7 No. 1 (2016) entitled "Hyper Edge Detection with Clustering for Data Hiding"

As human eyes are more sensitive to changes in smooth regions, current researchers attempt to use edge based steganography (Chen et al., 2010; Hempstalk, 2006; Luo et al., 2010; Nitin, Jain et al., 2012; Simra Pal Kaur and Singh, 2012; Youssef Bassil, 2012; Yu et al., 2008). These jagged edge areas have extra complex features, in turn making it difficult to notice alterations in the areas of an image. Although edge-based steganographic approaches provide high stego image imperceptibility, they have a limited capacity as the message will be hidden in edge pixels only.

To acquire the best embedding level with minimum alteration, there should be optimization of the steganographic problem. The best likely optimized search processes is Genetic Algorithm (GA) linking natural collection and genetics to the process. Therefore, GA is taken as a concept from the evolution of biological practice. The process of GA develops a group of possible answers for the required problem, then develops these repeatedly via use of stochastic operators. A fitness function is crafted to evaluate each pupil's answer. The fitted answers have high supposition to produce offspring. The number of cycles would execute till the time best resolution/answer or predefined set is evaluated.

In this chapter, a novel edge-based steganographic approach is proposed to expand the capacity of steganography, relying upon the edge with least modification in a stego file. Contrast Sensitivity Function (CSF) and Genetic Algorithm (GA) feature prominently in the work. This uses Differences of Gaussian (DoG) detectors which just replicates the performance of human visual system (HVS). DoG provides close judgement to the human perception compared to Marr's Laplacian of Gaussians (LoG) (Wandell, 1995; Marr and Hildreth., 1980; Enroth-Cugell, Christina and Robson, 1966). This strengthens the framework achieved by utilizing the perceptible edge from the DoG which directs the consolidated framework. Supplementary usage of both CSF and GA facilitate the optimization of the embedding capacity by developing the irregular edge visibility; this depends upon the size of the secret data.

4.2 Proposed Model

The proposed technique is to hide data at the intelligent edge visibility level using Human Visual System (HVS) with characteristics of Contrast Sensitivity Function (CSF) supported by Genetic Algorithm (GA). The work combines Edge Detection and Vision Science Research. Firstly, it is uses differences of Gaussian detectors instead of Laplacian of Gaussian because it is closer to human visual behavior. Secondly, the edge profusion indicates threshold visibility with the help of Genetic Algorithm.

For a cover image C, GA produces a candidate solution to hide the meta-data. A candidate expression optimizes options for each selected coefficient. A fitness function is used to measure the performance of each candidate expression. It is based on measuring imperceptibility and providing optimized high payload capacity with the lowest distortion.

During GA training, the best individuals are maintained to engage in the operation of materialization. However, the weak individuals are excluded. Materialization is generated by prospectively employing GA's processes which are a selection of the individuals, mutation and crossover. The operation moves ahead repeatedly until the stopping criteria is achieved. The best individual of the last generation is protected which will consequently be used for embedding secret data in the images. GA operations essentially precedes the threshold of edge visibility Th which indicates the embedding rate for each region of the cover image based on the size of the meta-data. Figure 4.1 shows the embedding process of the proposed method. The cover image C is split into non-overlapping sub-blocks and then the model detects the edges of the object using DoG filters in order to inaugurate the vision of CSF utilizing GA operators to produce the best edges. The GA determines the proper embedding rate threshold using the visibility of $SDoG(C)$ for each block based on the fitness function. The following sections will describe the theoretical concept of the proposed scheme.

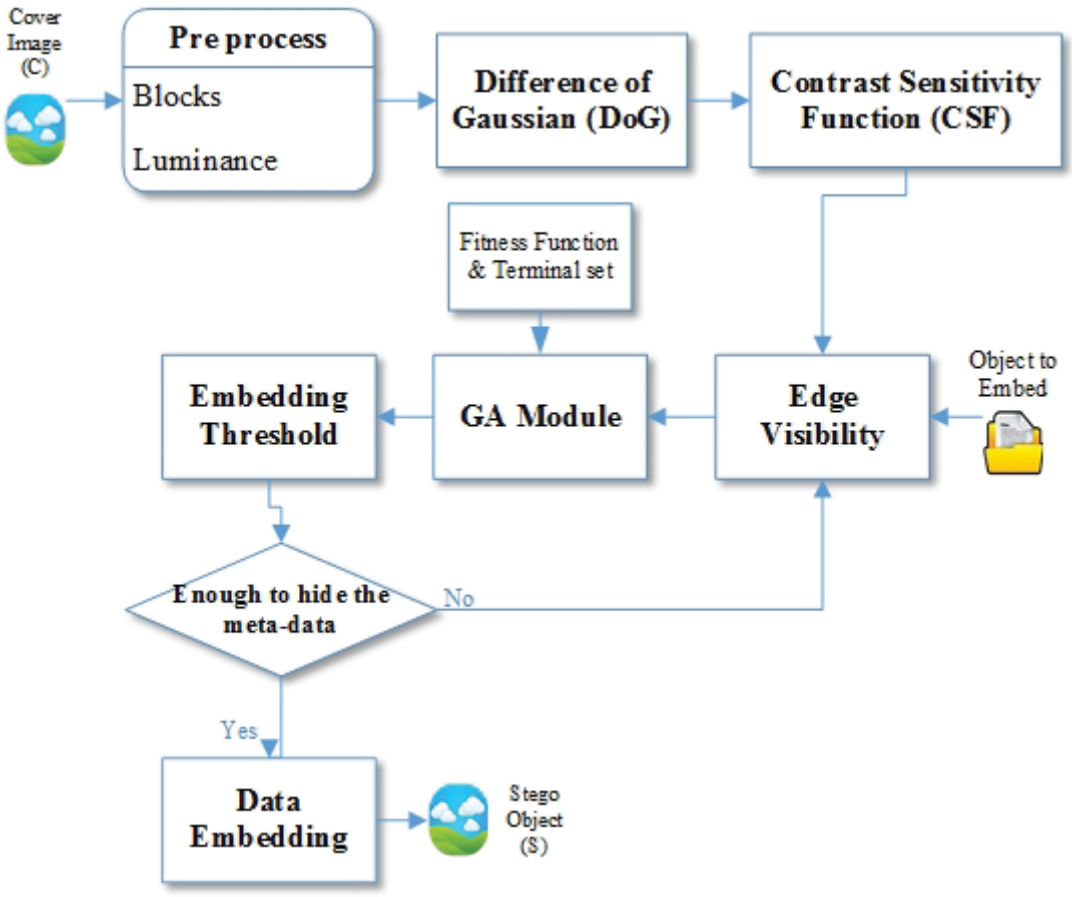

Fig. 4.1: General architecture of the proposed model

4.2.1 The Detection of Edges

Difference of Gaussians (DoG) is one of the logical models which was anticipated in vision science in the receptive fields of X-cells in the Lateral Geniculate Nucleus (LGN) in the thalamus (Enroth-Cugell, Christina and Robson, 1966; Wandell, 1995). DoG, provides close judgment to the human perception compared to Marr's Laplacian of Gaussians (LoG) as described in Chapter 3 (Enroth-Cugell, Christina and Robson, 1966; Wandell, 1995; Marr and Hildreth., 1980). The model deployed the CSF in band-pass filters within frequency domain, called weighted sum of DoG (or SDoG). This made DoG the creator of bandwidth of the CSF taking the visual system as a multi-scale analyzer and ON/OFF cells, along with receptive fields of

a required size (Enroth-Cugell, Christina and Robson, 1966). The equation referring weighted sum of DoG is :

$$SDoG(C) = \sum_{k} Th_k \lfloor G^{+}_{\sigma k} - G^{-}_{\sigma k} \rfloor (C) \tag{4.1}$$

Here C is taken as the cover image (in luminance units), G_σ as the normalized Gaussian operator, Standard Deviation (SD) σ, σ^+ and σ^- are the SD of the positive and negative parts of a DoG ($\sigma^- = \lambda\sigma^+$), and Th is taken as embedding threshold wherein the illustration is in the next part.

A DoG is not viewed as a second derivative but it achieves the edge detection with the same superiority as with $\nabla^2 G$ expressed in the forms of localization and coefficients. The positive and negative weights are to be same as per equation (as in Eq. Equation 4.1).

4.2.2 Embedding Threshold Using CSF

The CSF describes the observing trend of humans to the visibility of sine gratings as mentioned in Chapter 3. (Mannos and Sakrison, 1974) had anticipated a logical and eminent form of the CSF to the field of computer. Subsequently, it was the turn of (Barten, 1999) who united accessible psycho-visual information to carry out the absolute model of CSF which is most up-to-date. Below is the employed Barten's CSF:

$$CSF(f) = afe^{-bf}\sqrt{1 + ee^{bf}} \tag{4.2}$$

where f denotes frequency in cycle per degree, $c = 0.06$,$b = 0.3(1+100/L)^{0.15}$, furthermore

$$a = \frac{540(1 + 0.7/L)^{-0.2}}{1 + \frac{12}{\omega}(1 + f/3)^{-2}} \tag{4.3}$$

Many researchers have been taking in the gradient modulus, the form of index of the edge amplitude. When selection of true edge from over-segmented edge detector is done, the index is calculated on the carrier image C perhaps to assist with fine consequences. Other troubles might exist when it is utilized for edge visibility estimation, so a logical scheme is used. Let us take a 1D sine wave grating along with spatial frequency f:

$$C_f(x) = A\sin(2\pi f x) \tag{4.4}$$

The gradient modulus is taken at zero-crossing which is $2\pi f A$, whereas the visibility of the gratings is:

$$V = A \rangle CSF(f) \tag{4.5}$$

Here, it is evident that the gradient modulus forms a massive assumption. CSF is extreme from linear with Marr and Hildreth planned for a concept where the strength of edge needs to be proportional to the slope s having output signal $\nabla^2 G$ (C) divided by f. The work here has taken this planning into account; SDoG has yielded better results and exhibits the finishing computational framework. The DoG contributes both to edge localization and edge-visibility computation.

Taking a look into the measurement of a set of DoG which suggests a given CSF, using similar 1D example, the difficulty of C given by a Gaussian function G_σ is:

$$G_\sigma \star C_f e^{-f^2\sigma^2/2} \tag{4.6}$$

Hence, the convolution with a DoG is:

$$[G_\sigma - G_{\lambda\sigma}] \star C_f = C_f[e^{-f^2\sigma^2/2} - e^{-f^2\lambda^2\sigma^2/2}] \tag{4.7}$$

The modulus of the gradient on the zero-crossings possibly calculated from:

$$\frac{\partial}{\partial x}([G_\sigma - G_{\lambda\sigma}] \star C_f) = 2\pi K C_f \tag{4.8}$$

with $k = e^{-f^2\sigma^2/2} - e^{-f^2\lambda^2\sigma^2/2} - e^{-f^2\lambda^2\sigma^2/2}$, that is, $s = 2\pi A f K$. Now take gradient modulus as a function of f. It is highest when $\frac{\partial s}{\partial f} = 0$, which directs to:

$$\sigma = \frac{2}{f}\sqrt{\frac{\lambda^2 - 1}{\ln \lambda}} \tag{4.9}$$

There is a relation linked to f and σ which helps to measure the SDoG from the CSF. Here, the earliest DoG is adjusted to the approach of the CSF, as σ 1 is computed from Equation 4.9 and f is taken as communicated to the maximum of the CSF. Afterwords, the embedding threshold is maintained to:

$$Th = \frac{CSF(f)}{e^{-f^2\sigma^2/2} - e^{-f^2\lambda^2\sigma^2/2}} \tag{4.10}$$

So the summation of DoG is calculated based on the quantity of edges:

$$SDoG(C) = \sum_k Th_k \lfloor G^+_{\sigma k} - G^-_{\sigma k} \rfloor (C) \tag{4.11}$$

Figure 4.2 illustrates different edge visibility based on different threshold

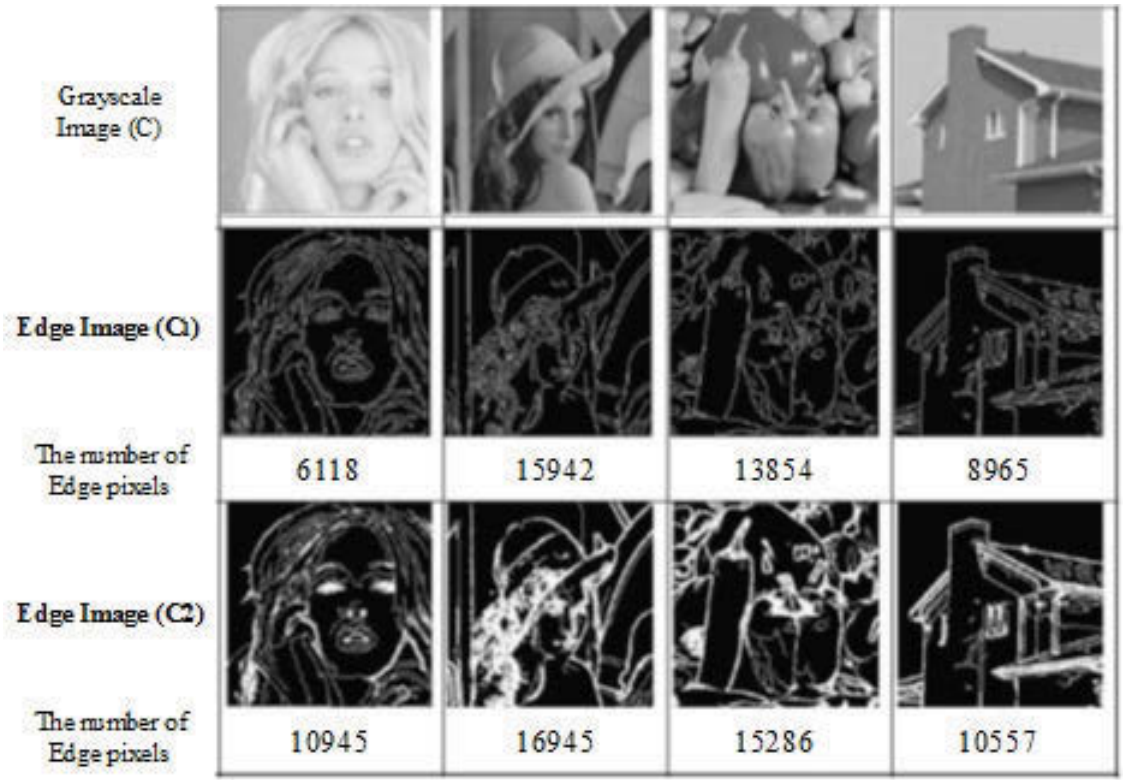

Fig. 4.2: Edges visibility for 2 different threshold value

value. The higher threshold provides higher and thicker edges. Therefore, for small size meta-data, only few edges are needed. However, the larger meta-data requires higher and a thicker number of edges.

4.2.3 Optimized Edges Using Genetic Algorithm

After obtaining the image with edges from the previous subsection, evolutionary training will begin to optimize the edges based on the size of embedding data. Figure 4.3 is an edge training flowchart.

In the GA training system, a chromosome is performed by a list of 64 X 64 bit string. The initial chromosomes are generated randomly from the previous step (SDoG). The chromosome value can be either zero or one where zero

expresses non-edge pixel and one indicates an edge pixel. The chromosome of pixel $P(x, y)$ can be generated as follow:

$$Chromosome(x, y) = E1 \times Integer(P(x, y) + E) \tag{4.12}$$

where $E1$ is a random integer to be either 0 or 1 and $E2$ is a random number range between 0 to 0.99.

Many factors should be considered during GA training for optimum data embedding, which includes maximum fitness function $wPSNR$, diversity of edges C_d, thickness of edges C_t, fragmentation of edge C_f and the total number of edge pixels C_e as explained in Equation 4.17, Equation 4.18, Equation 4.19 and Equation 4.20.

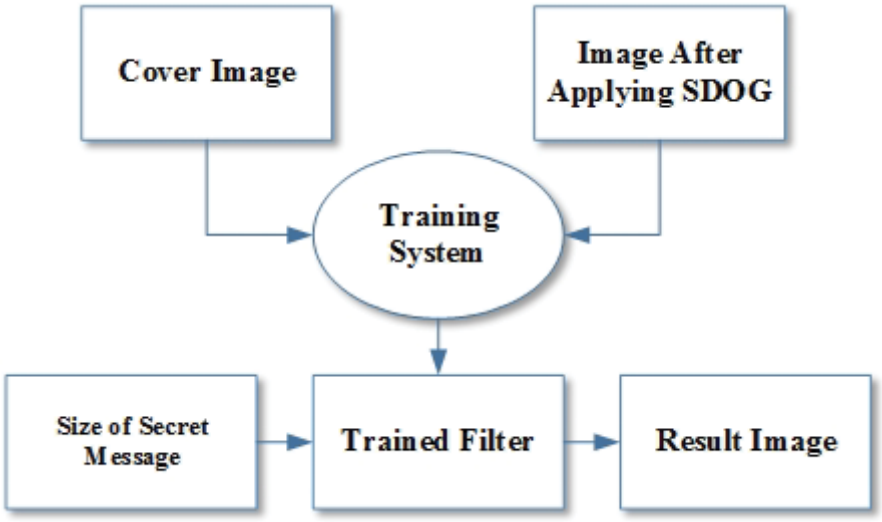

Fig. 4.3: Edge GA edge training flowchart

Function of Fitness: here, we take the weighted Peak Signal to Noise Ratio (wPSNR) as a function of fitness and wPSNR considers entire HVS properties. This is done in view of the theory that the decreased sensitivity of the human eye modifies the texture areas more effectively than the smooth areas. wPSNR is taken as an alternative quality metric, and it is relies upon the calculation of Noise Visibility Function (NVF) as a correction factor

(Voloshynovskiy et al., 2000). It is constituted as the picture property found on textured as well as edge areas since embedding information of this area could conceal extra information efficiently and will have less distortion. NVF is approximately 1 whereas for the edge areas, it is approximately 0, which reflects that for the smooth area. wPSNR takes out extra positive and reliable results more so than PSNR methods that are edge detection schemes.

$$wPSNR = 10\log_{10}\frac{MAX^2}{||(C_{ij} - S_{ij})||^2_{NVF}} \tag{4.13}$$

$$wPSNR = 10\log_{10}\frac{MAX^2}{||(C_{ij} - S_{ij}).NVF||^2}$$

$$NVF(i,j) = \frac{1}{1 + \theta\sigma_x^2(i,j)} \tag{4.14}$$

Where $\sigma_x^2(i,j)$represents the limited alteration of the picture in a window-pane dashed on the pixel with parameters (i,j) and θ is a variation factor dependable to the precise image which can be computed in Equation 4.15 and Equation 4.16.

$$\overline{x}(i,j) = \frac{1}{(2L+1)^2}\sum_{k=-L}^{L}\sum_{l=-L}^{L} x(i+k, j+L) \tag{4.15}$$

$$\sigma_x^2(i,j) = \frac{1}{(2L+1)^2}\sum_{k=-L}^{L}\sum_{l=-L}^{L} (x(i+k, j+L))^2 \tag{4.16}$$

The image based on alteration factors is specified as$\theta = \frac{D}{\sigma^2_{x(max)}}$ Where σ_x^2 is the highest local variance for a fastidious image and $D \in [50, 100]$ is a

calculated value.

Diversity of region C_d,

$$C_d = \begin{cases} 0 & p \text{ is an edge pixel} \\ D(p) & \text{otherwise} \end{cases} \tag{4.17}$$

Thickness of edges C_t,

$$C_t = \begin{cases} 0 & p \text{ is a thin edge pixel} \\ 1 & \text{otherwise} \end{cases} \tag{4.18}$$

Fragmentation of edge C_f

$$C_f = \begin{cases} 1 & \text{more than one neightboring edge pixel} \\ 0.5 & \text{only one neightboring edge pixel} \\ 0 & \text{no neightboring edge pixel} \end{cases} \tag{4.19}$$

Total number of edge pixels

$$C_e = \begin{cases} 1 & \text{more than 2 edge pixels} \\ 0.5 & \text{only one edge pixel} \\ 0 & \text{no edge pixel} \end{cases} \tag{4.20}$$

4.2.4 Data Embedding

Based on the complexity of the selected region, different rates will be applied to embed the secret data. Therefore, the sharp edge region will hide higher percentage, while the smoother will hide less. Moreover, as the green color has more visual perception intensity in the Human Visual System (HVS), blue has the lowest perception contribution to the color image. Therefore, the last bite of each pixel is the most appropriate bite in which to hide more data.

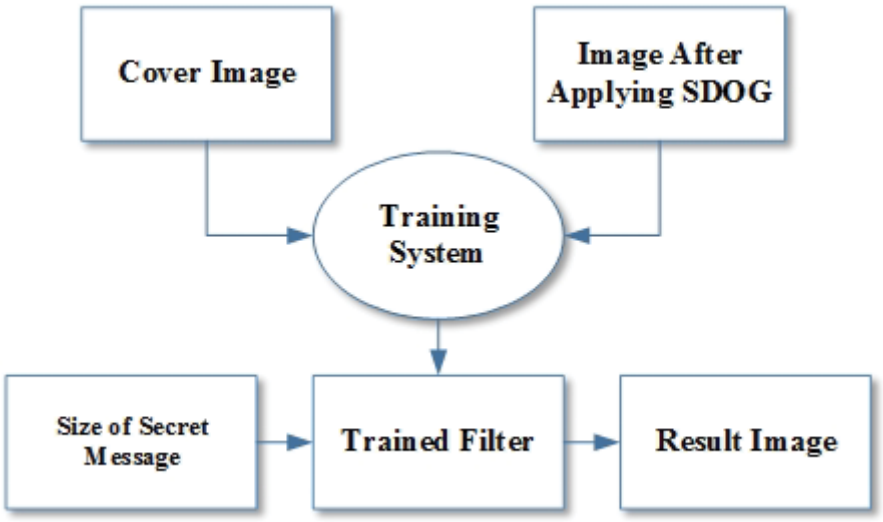

Fig. 4.4: Edge GA edge training flowchart

Figure 4.5 illustrates the decision tree for embedding evaluation which mainly examine the pixel whether it place in edge and non-edge region. This is followed by an evaluation of the neighbor pixel, the number of the edge pixels and the thickness of the edge. Various amounts of data will be embedded based on the feature of the pixel.

Non-edge pixel will hide smaller amounts of bits while edge pixels will hide more numerous bits. Figure 4.6 indicates the bit replacement rate of pixels based on the position of the pixel.

4.3 Results and Discussions

For demonstration purposes, a graphical user interface simulation was built using Matlab R2014a. The algorithm was implemented with help of Genetic Programing Toolbox (GALAB). Comprehensive experiments have been conducted on a 400 data-set of RGB images, however, six images such as Lenna, Pepper, Baboon, House, Tiffany and, Airplane are referred to in this chapter for imperceptibility, capacity and detectability evaluation. They are all RGB images with size 512X512. All the meta-data files were hidden successfully in cover images and produced stego files using the best evolved expression. In

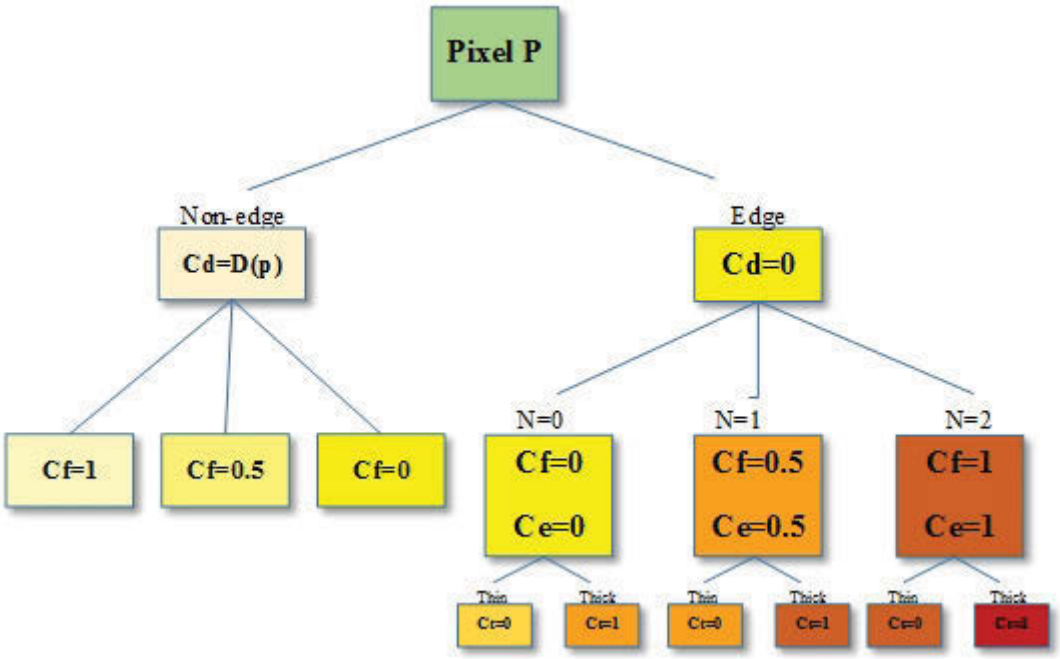

Fig. 4.5: Decision tree for embedding evaluation

order to get best evolved expression, several GA simulations were generated, which is standard practice. The best expression was generated based on achieving the fitness function. Imperceptibility, capacity, detectability and performance of GA will be evaluated in the next sub-sections.

4.3.1 Imperceptibility Evaluation

In order to evaluate the imperceptibility of the stego image, subjective and objective tests were performed. The output of subjective test showed that the proposed method provide high quality stego images with minimum distortion along with low and high embedding capacity. Figure 4.7 shows the cover image with five different stego images at various embedding rates. Obviously, the resulted stego images are very close to the cover image which indicate high visual quality. Moreover, PSNR, wPSNR, SSIM and UQI have been used to objectively measure the quality of stego images. Table 4.1, Table 4.2, Table 4.3 and Table 4.4 show the result of the objective measurements for the proposed method. In addition, to prove the efficiency of the

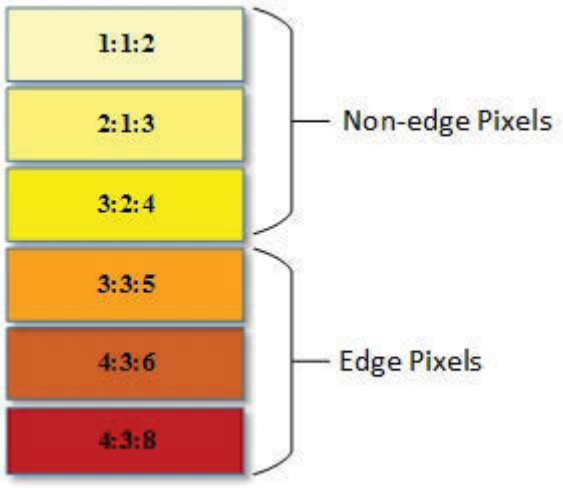

Fig. 4.6: Embedding rate for edge and non-edge pixels

proposed method, results were compared with other methods. LSB, PVD, Hyper Edge detection developed here was used for the comparison. It is clear from Table 4.1, Table 4.2, Table 4.3 and Table 4.4 that the proposed method provided better imperceptibility even with high embedding capacity.

4.3.2 Detectability Evaluation

Bit plane is used to evaluate the detectability of the stego images. Bit plane is the range of bits related to a specific bit position in each of the binary bits. The first bit plane represents the roughest but the most important for statical evaluation. In order to be robust against statical detectability, this work used bit plane to evaluate the detectability of the stego image. Figure 4.8 shows four different cover image images in the first row follow by four bit planes for the cover images; and then the third row shows the stego images with 50% embedding rate followed by the related bit planes of the stego images. Figure 4.9 shows 3 different stego images for embedding 10%, 30%, and 50% with its corresponding bit plane. It can be understood from the figures that no visible differences can be observed. The bit planes of the cover and stego images are very similar, which indicates good reliability. Figure 4.10 shows the bit planes for the cover image, from our previous work

Table 4.1: The performance in Lenna image of various quality metrics for different embedding rates

	Quality Metric	10%	20%	30%	40%	50%
Proposed	PSNR	59.451	57.785	56.252	55.371	54.883
	wPSNR	75.598	72.083	70.455	69.547	68.354
	SSIM	0.99985	0.99964	0.99932	0.99893	0.99875
	UIQI	0.99965	0.99935	0.99910	0.99857	0.99853
(Wazirali and Chaczko, 2016)	PSNR	58.357	55.365	54.487	52.158	51.184
	wPSNR	71.863	70.472	69.458	68.365	66.555
	SSIM	0.99954	0.99925	0.99853	0.99773	0.99751
	UIQI	0.99952	0.99912	0.99855	0.99738	099742
(Youssef Bassil, 2012)	PSNR	51.454	48.458	46.354	52.025	44.457
	wPSNR	56.587	43.358	51.987	50.587	49.678
	SSIM	0.99725	0.99254	0.98542	0.96541	0.93594
	UIQI	0.99712	099233	0.98248	0.96247	0.93585
Pixel Value Differences	PSNR	49.358	47.546	45.253	42.155	38.258
	wPSNR	52.898	49.987	45.158	43.487	40.897
	SSIM	0.96585	0.90574	0.85641	0.80100	0.75653
	UIQI	0.96325	0.90037	0.84595	0.80014	0.75783

which are "Hyper Edge Detection" Wazirali and Chaczko (2016) and Youssef Bassil (2012), PVD and the proposed model. The figure clearly proves the high statistical performance of the proposed method as the bit planes is very close to the cover image. This make it difficult to detect hidden information.

4.3.3 Payload Capacity Evaluation

Steganographic limit is present in the vast majority of pieces that could be incorporated in a given secure information document with negligible plausibility distinguishing an aggressor. Then again, inserting a limit occurs in the majority of pieces that might be incorporated in a given secure information document. As such, the inserting limit is prone to be greater than the

Table 4.2: The performance in Baboon image of various quality metrics for different embedding rates

	Quality Metric	10%	20%	30%	40%	50%
Proposed	PSNR	59.356	57.658	56.155	55.254	54.654
	wPSNR	75.585	72.554	70.355	69.254	68.125
	SSIM	0.99974	0.99945	0.99918	0.99854	0.99865
	UIQI	0.99955	0.99952	0.99903	0.99842	0.99851
(Wazirali and Chaczko, 2016)	PSNR	58.254	55.255	54.425	52.114	51.157
	wPSNR	71.7441	70.485	69.425	68.314	66.125
	SSIM	0.99951	0.99913	0.99854	0.99785	0.99766
	UIQI	0.99965	0.99914	0.99845	0.99725	099725
(Youssef Bassil, 2012)	PSNR	51.256	48.554	46.752	52.255	44.454
	wPSNR	56.622	43.548	51.755	50.425	49.545
	SSIM	0.99777	0.99355	0.98452	0.96524	0.93545
	UIQI	0.99654	099454	0.98454	0.96155	0.93475
Pixel Value Differences	PSNR	49.254	47.654	45.354	42.256	38.351
	wPSNR	52.954	49.992	45.244	43.541	40.985
	SSIM	0.96654	0.9354	0.84574	0.84527	0.74558
	UIQI	0.96454	0.91547	0.83547	0.81567	0.75445

steganographic limit (Cox et al., 2008).

Table 4.5 shows the embedding capacity with various threshold values. With the increase of the threshold value, the embedding capacity increases. Therefore, the model will choose the proper threshold based on the size of the meta-data. In addition, Table 4.5 shows the maximum embedding capacity for different images of the proposed method and other steganographic techniques. Table 4.6 shows a compression of the embedding rate on the proposed method and others. The total capacity of the proposed method provides higher rate of embedding size.

Table 4.3: The performance in Peppers image of various quality metric for different embedding rates

	Quality Metric	10%	20%	30%	40%	50%
Proposed	PSNR	59.406	57.864	56.454	55.464	54.464
	wPSNR	75.321	72.971	70.755	69.512	68.454
	SSIM	0.99983	0.99947	0.99921	0.99879	0.99855
	UIQI	0.99961	0.99924	0.99917	0.99838	0.99866
(Wazirali and Chaczko, 2016)	PSNR	58.255	55.254	54.541	52.753	51.954
	wPSNR	71.844	70.423	69.455	68.687	66.786
	SSIM	0.99965	0.99915	0.99825	0.99777	0.99789
	UIQI	0.99945	0.99975	0.99895	0.99758	099772
(Youssef Bassil, 2012)	PSNR	51.542	48.235	46.258	52.453	44.452
	wPSNR	56.145	43.824	51.854	50.425	49.589
	SSIM	0.99736	0.99283	0.98516	0.96527	0.93584
	UIQI	0.99727	0.99254	0.98244	0.96272	0.93596
Pixel Value Differences	PSNR	49.245	47.875	45.752	42.429	38.431
	wPSNR	52.424	49.744	45.144	43.487	40.458
	SSIM	0.96595	0.90458	0.85754	0.80255	0.75742
	UIQI	0.96458	0.90148	0.84585	0.80045	0.75652

4.3.4 GA Performance Evaluation

To increase the imperceptibility in non-GA techniques, each possible solution must be tested and therefore the overall computation time will be huge and unacceptable. In GA, the parameters are denoted by encrypted binary elements named “chromosome” or “genes”, which will be adjusted to maximize the imperceptibility by ensuring best mapping function between the cover image and the metadata with acceptable number of iterations. In this work, a good balance is sought between the cost of GA for best mapping function selection and the overall completion time.

In the GA preparation procedure, the process selects ten entities for each iteration, through the crossover proportion of 0.25 and mutation proportion

Table 4.4: The performance in Airplane image of various quality metric for different embedding rates

	Quality Metric	10%	20%	30%	40%	50%
Proposed	PSNR	59.354	57.645	56.242	55.458	54.244
	wPSNR	75.457	72.257	70.575	69.854	68.245
	SSIM	0.99933	0.99925	0.99911	0.99885	0.99876
	UIQI	0.99954	0.99942	0.99915	0.99887	0.99865
(Wazirali and Chaczko, 2016)	PSNR	58.254	55.454	54.545	52.245	51.454
	wPSNR	71.754	70.757	69.475	68.377	66.475
	SSIM	0.99965	0.99945	0.99845	0.99773	0.99744
	UIQI	0.99935	0.99911	0.99855	0.99745	099745
(Youssef Bassil, 2012)	PSNR	51.425	48.254	46.454	52.125	44.454
	wPSNR	56.457	43.757	51.757	50.457	49.454
	SSIM	0.99735	0.99257	0.98557	0.96552	0.93575
	UIQI	0.99723	099254	0.98275	0.96275	0.93525
Pixel Value Differences	PSNR	49.254	47.456	45.245	42.453	38.447
	wPSNR	52.755	49.4587	45.454	43.458	42.521
	SSIM	0.96582	0.90545	0.85624	0.80121	0.75642
	UIQI	0.96344	0.90025	0.84575	0.80024	0.75745

of 0.05. The preparation iterations are set to 200. The top twenty individuals with larger PSNR and wPSNR are kept for the new individuals in the next generation.

For RGB image, the process required less than half a minute and all of the test images intersected to optimal fitness almost within 50 iterations of the generation. Table 4.7 indicates the set of parameter values for the implementation. Table 4.8 shows the improvement of PSNR and wPSNR with the increased number of iterations.

Fig. 4.7: The cover image and the resulted stego image of the proposed method with different embedding rate

Table 4.8: Iteration vs PSNR and wPSNR

No. Iteration	PSNR	wPSNR
50	41.258	53.557
100	49.255	56.544
150	51.554	60.554
200	54.844	68.358

4.3.5 Computation Time Evaluation

For any optimal steganographic system, it is significant to observe the total computation time to acquire embedding and extraction. Since the evolutionary algorithm based on testing every possible solution to achieve better result may require a huge computation time, making a balance between acceptable imperceptibility and acceptable computation time should be considered. Table 4.9 shows the processing time of the original LSB substitution and the proposed method. The proposed method consumes almost twice the time of that by the original LSB method. However, the results are still in an

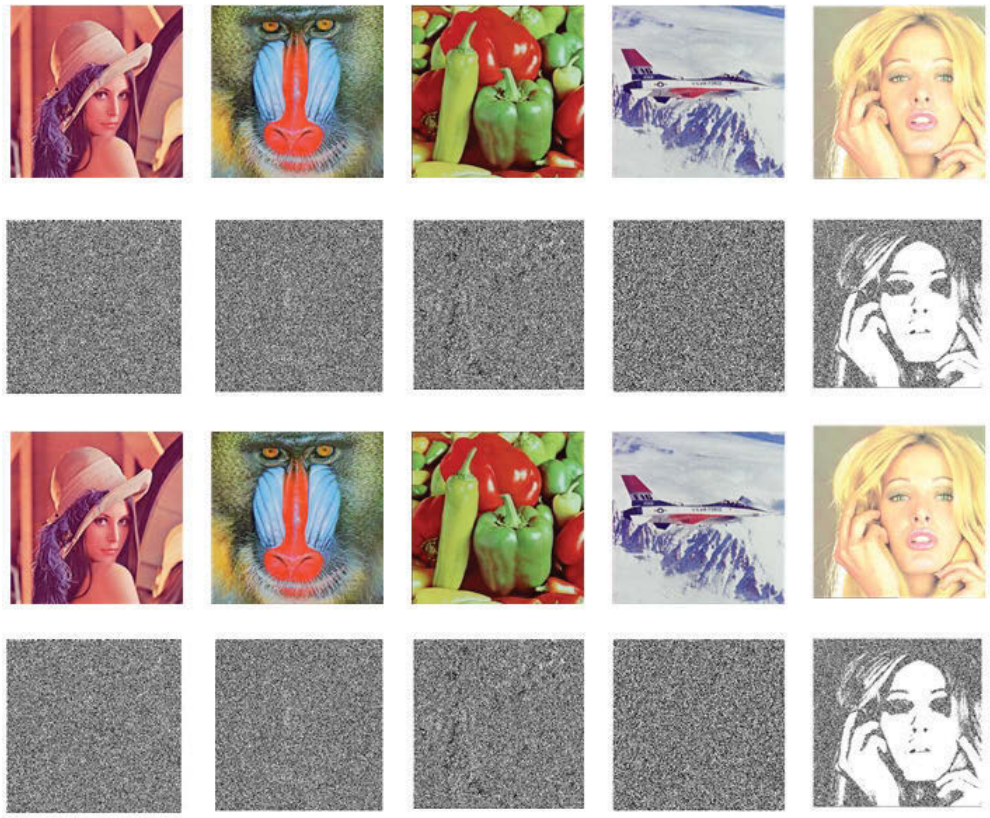

Fig. 4.8: Cover Images with its bit planes and the correspondence stego image with its bit plane

acceptable range of time. The computation time can be further improved by using a faster computer such as a Pentium III PC.

Table 4.9: The computation time for LSB substitution and the proposed method

Cover Image	LSB computation time	Proposed method computation time
Lenna	0.28	0.49
Pepper	0.26	0.48
Baboon	0.28	0.50
Airplane	0.33	0.50
Tiffany	0.31	0.51

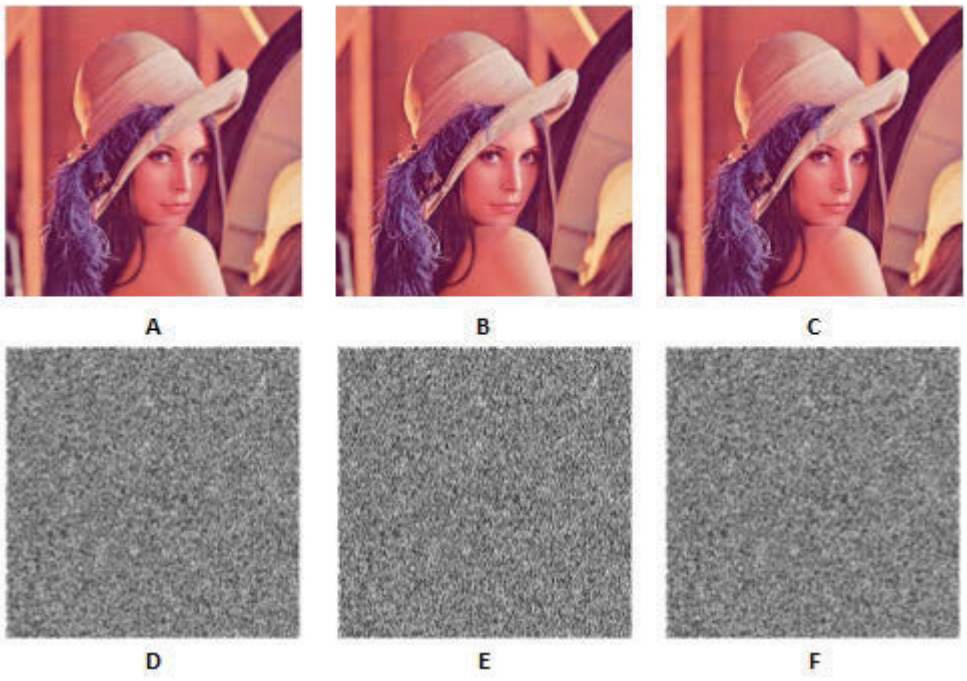

Fig. 4.9: Stego images with 10%, 30% and 50% embedding rate with its correspondence bit plane

4.4 The Effectiveness of the proposed approach in a Multimedia Sharing App (Case Study)

Taking a photo and uploading it has become easy with the introduction of smart phones. Basic meta-data is available in the image file of almost all smart phones. Camera information is restricted but the content of the photo is always available. The meta-data of an image could be considered unsuitable for the purpose of personal information due to its easy access through websites and other applications that can extract meta-data from an image.

A feasible solution to this problem is provided by Steganography. To be able to keep image information safe, it is necessary to embed information directly into the image when it is not separated from the original source. Exchange of information and personalized information is allowed through an image sharing app which does not provide access to keys; meta-data use is

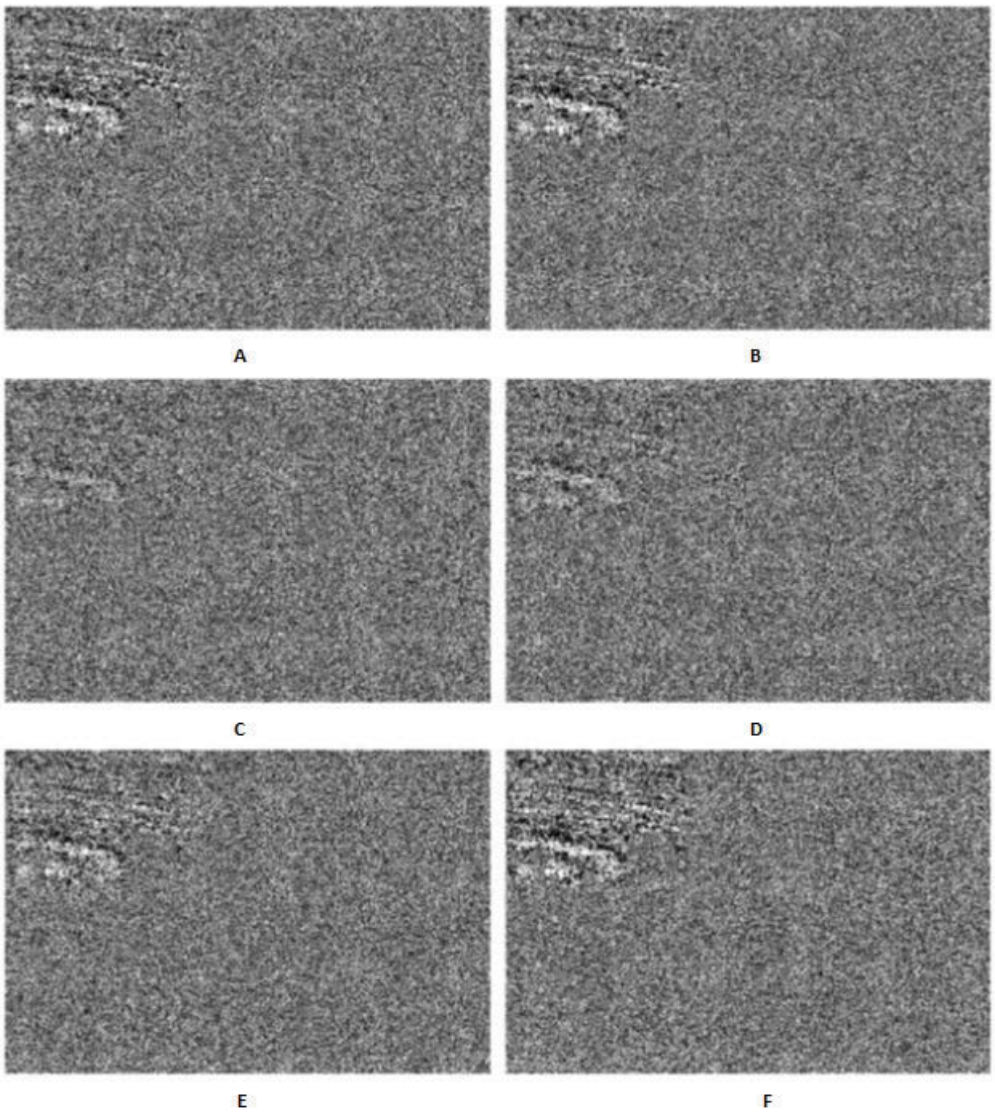

A. First bit plan of cover **B.** First bit plan of our Hyper Edge Detection stego Wazirali and Chaczko (2016)**C.** First bit plan of Wazirali and Chaczko (2015c) **D.** First bit plan of Youssef Bassil (2012) **E.** First bit plan of PVD stego. **F.** First bit plan of the proposed method Wazirali and Chaczko (2015b).

Fig. 4.10: Bit plan comparison

Table 4.5: Various Threshold vs Embedding Capacity

	Threshold	Embedding Capacity
Lenna	2	573,587
	5	758,954
	9	985,587
	13	1,089,587
	Threshold	Embedding Capacity
Pepper	2	515,658
	5	698,744
	9	805,587
	13	987,254
	Threshold	Embedding Capacity
Baboon	2	577,548
	5	748,584
	9	975,587
	13	1,087,954
	Threshold	Embedding Capacity
Tiffany	2	548,255
	5	715,845
	9	948,598
	13	1,025,753
	Threshold	Embedding Capacity
Airplane	2	547,652
	5	753,691
	9	982,364
	13	1,057,286

a possible using search engines to separate the image and its contents. A platform is provided for users to set up an account, share images and to search other uploaded images using this application.

Critical Features:

- A smart phone and website are made possible; users login to their accounts
- Pictures can be taken with the help of smart phones

Table 4.6: The capacity (bits) of the proposed and other methods

Method/Image	Lenna	Peppers	Baboon	Tiffany	Airplane
LSB	786,432	786,432	786,432	786,432	786,432
PVD Wu and Tsai (2003)	548,545	432,258	525,589	402,558	325,587
Hyper Edge Detection Wazirali and Chaczko (2016)	824,658	815,875	812,598	806,594	815,579
Proposed Method	854,589	842,593	832,197	822,156	835,549

Table 4.7: Parameter Settings for Genetic Algorithm

Parameter	Value
Population Size	100
Mutation Probability	0.05
Crossover Propability	0.25
Number of Generation	200
Fitness Function (wPSNR)	50 and above

- Comments could be added to pictures by users
- Search by comments is possible, a search feature of website and the app
- Pictures can easily be found by other users with the help of search tags added onto photos by users
- Steganography is made possible to embed comments into the image
- Photo can be uploaded to a central database by user
- Sharing of photos among users is possible
- Comments become readable to users by viewing photos

Less Critical Features:

- By adjusting the brightness, contrast, colour with filter addition to the photo, the phone application can edit the photos from original
- Several messages, intended for different people, can be fixed into a single image

4.4.1 Steganographic Multimedia Sharing App

The photo app and the gallery will run off of a user's device, which will then communicate via the internet to the central server. The server will store images and other related data in a database. Figure 4.11 shows the diagram of high level design. Additionally, the low level is made up of a number of vital parts as shown in Figure 4.12. Users interact with the Photo App and the Gallery via a web browser. These two parts don't directly interact, but exchange information via the databases Uploads and Search function on the web server. Figure 4.13, Figure 4.14, Figure 4.16 and Figure 4.15 show the class diagram, photo app sequence diagram part 1 and 2, and Gallery sequence diagram respectively. Moreover, the functionality of the user interface, and how it relates to the Software Requirements Specifications are available in **Annex A.**

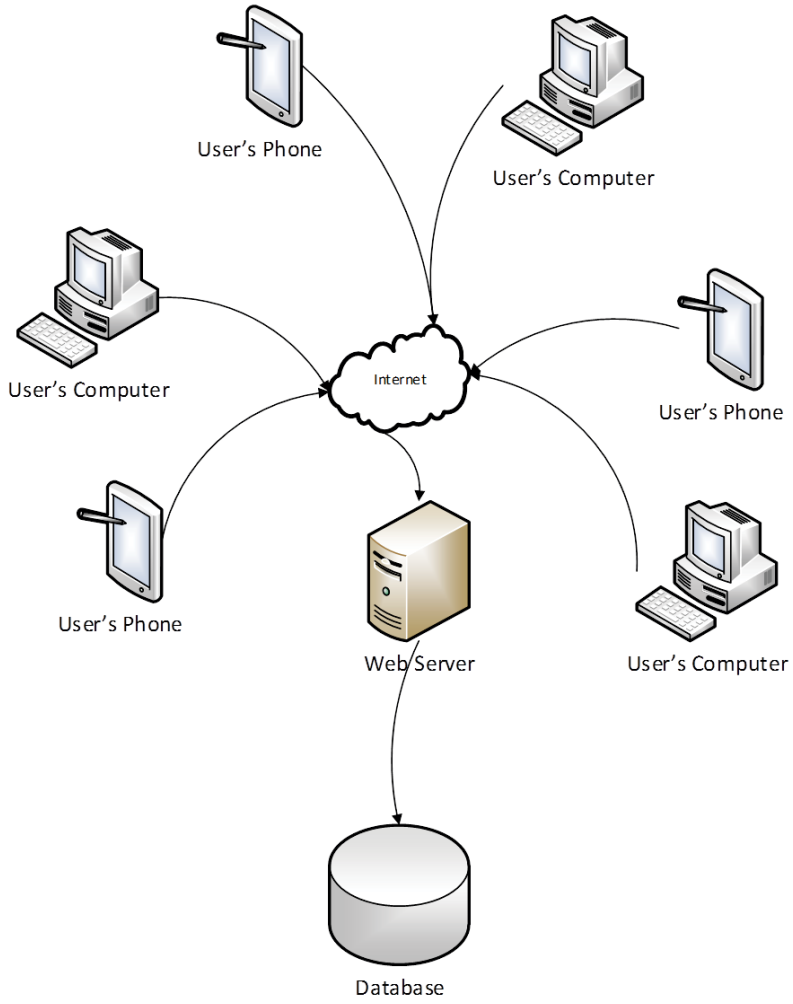

Fig. 4.11: High level design of multimedia sharing app

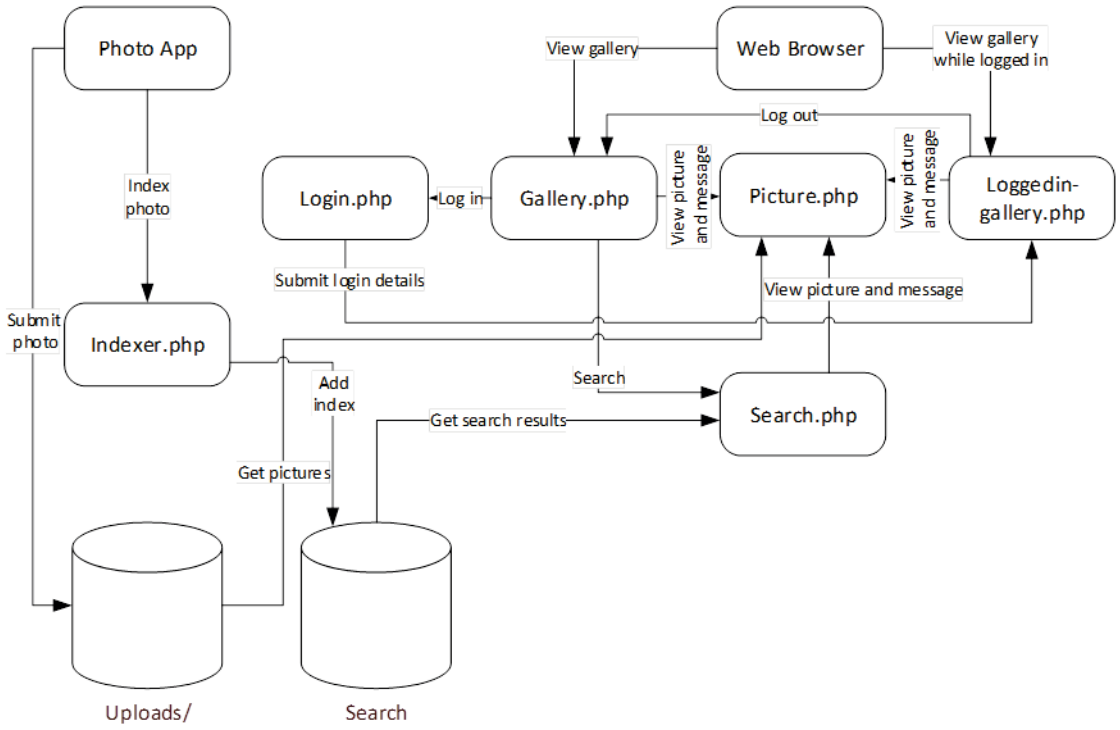

Fig. 4.12: Low level design of multimedia sharing app

Fig. 4.13: Class diagram of multimedia sharing app

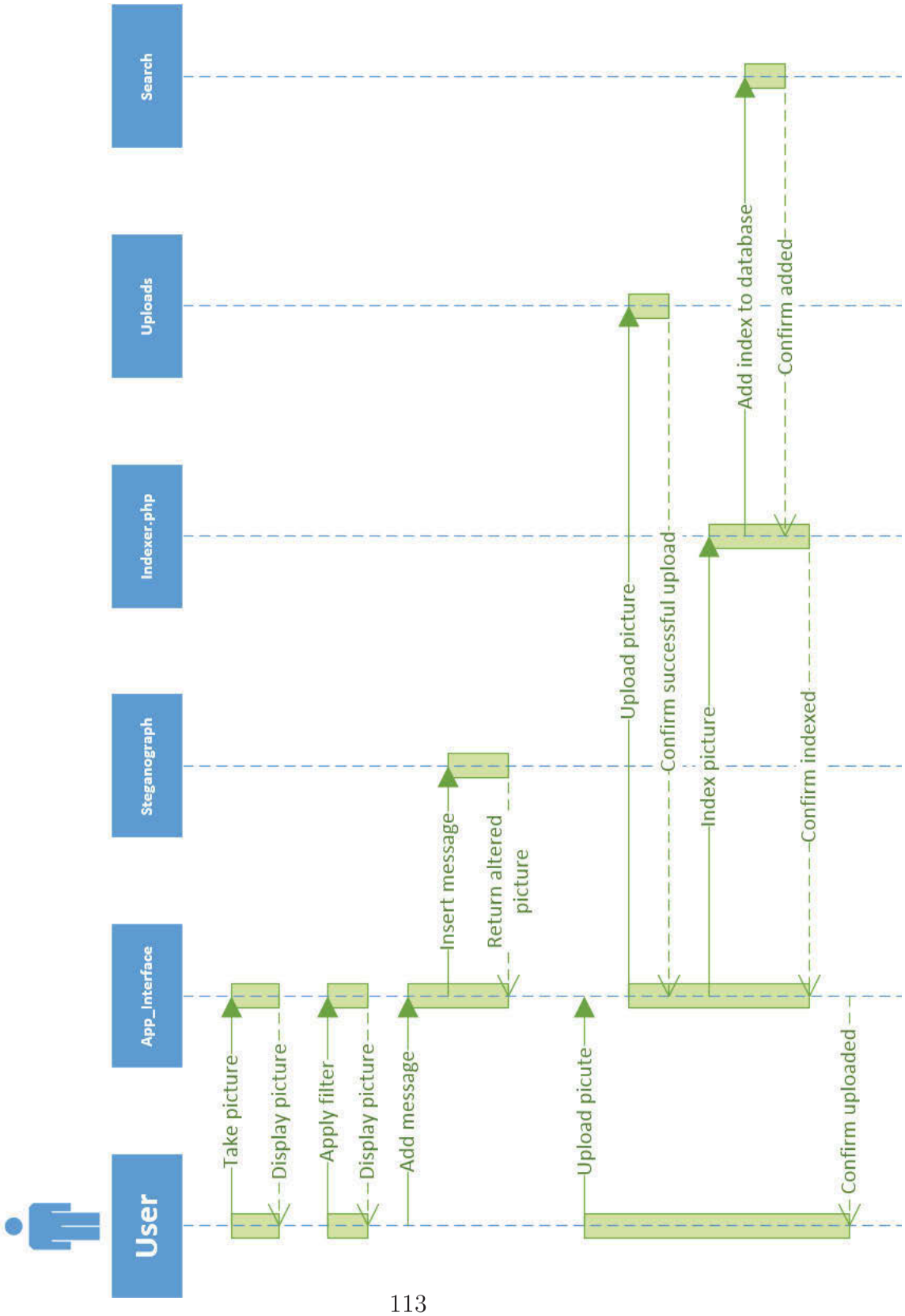

Fig. 4.14: Photo App sequence diagram of multimedia sharing app

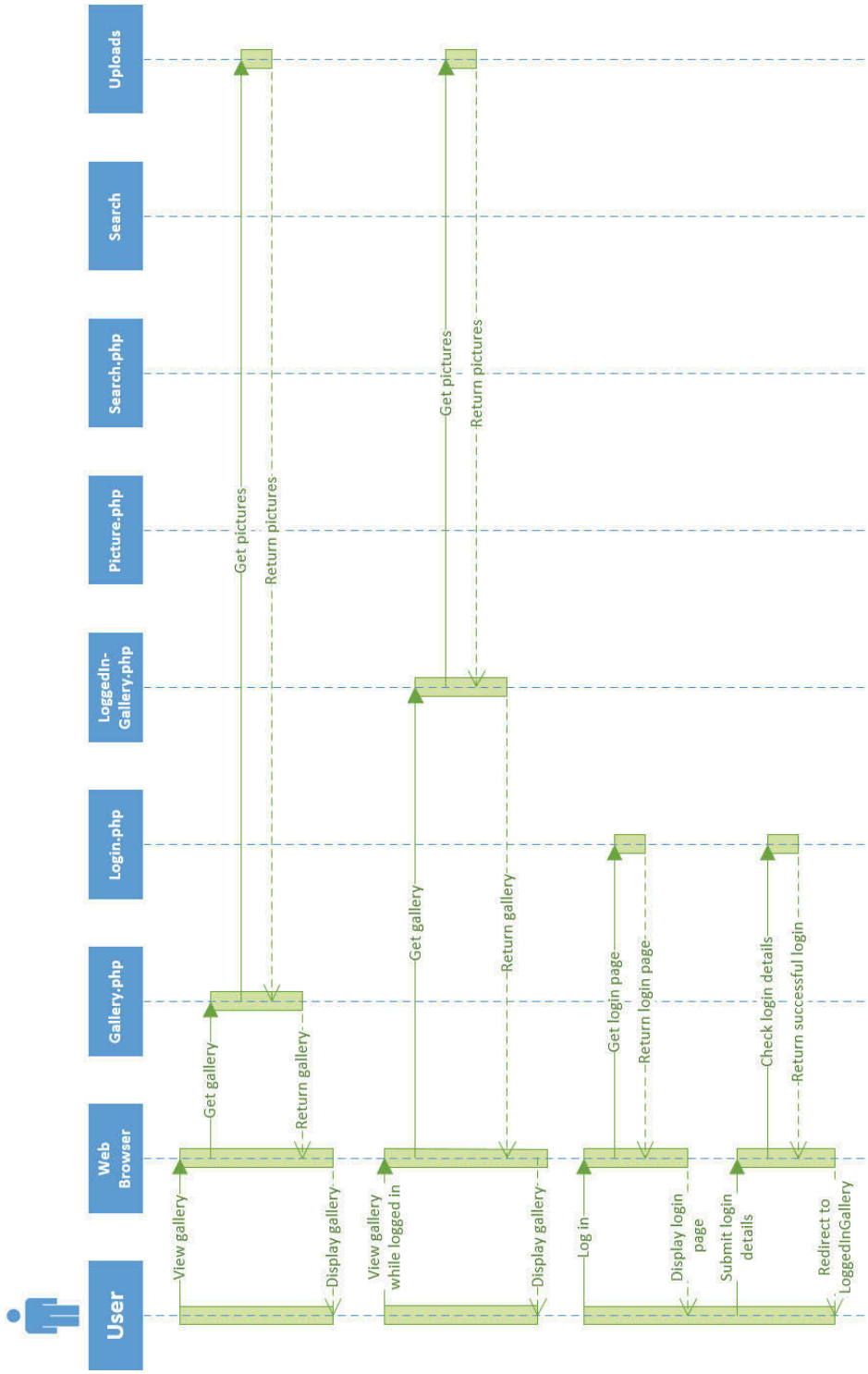

Fig. 4.15: Gallery Sequence Diagram part 1 of multimedia sharing app

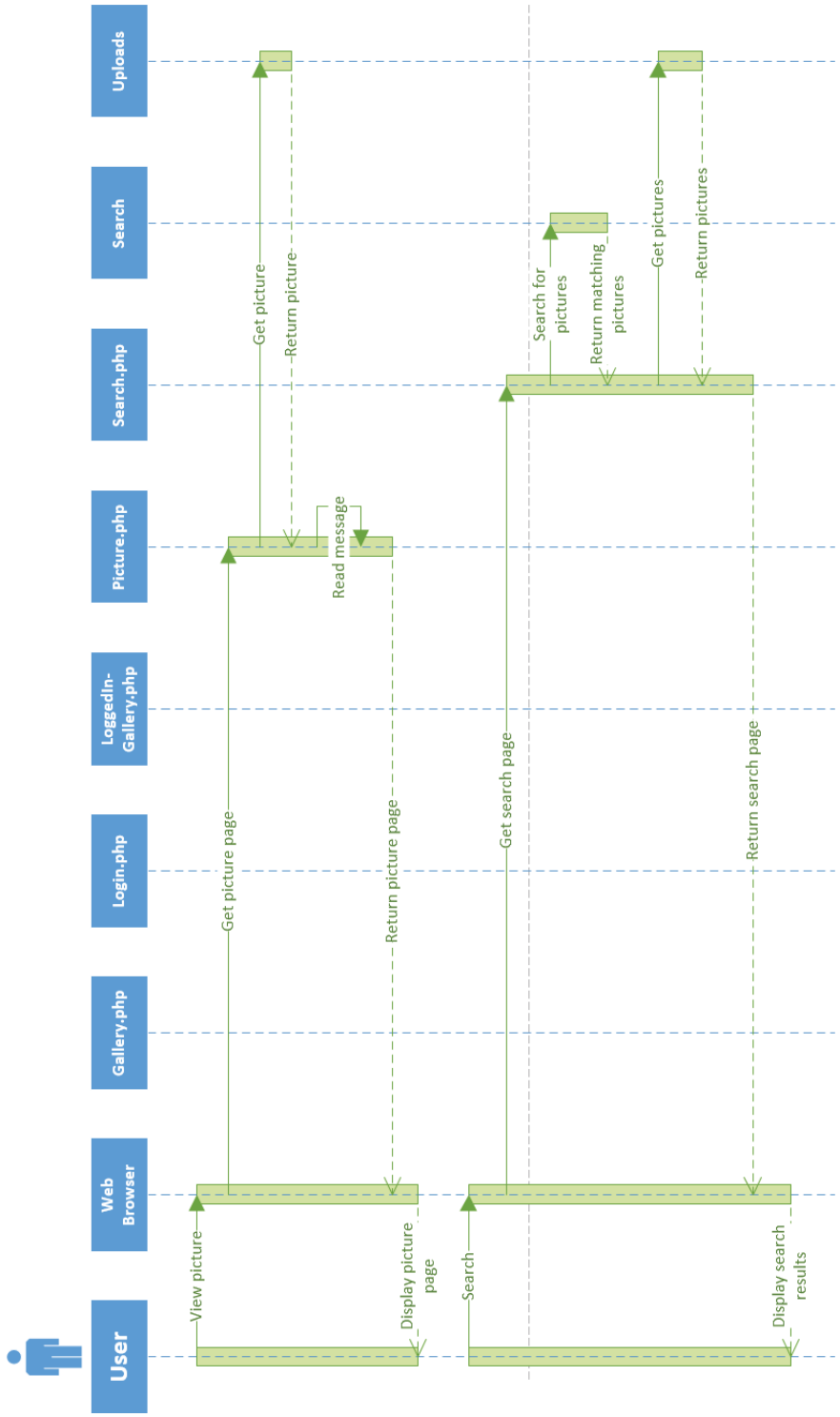

Fig. 4.16: Gallery sequence diagram part 2 of multimedia sharing app

4.5 Conclusion

For secure multimedia communication, effective techniques are required. Image steganography has become increasingly complex and the trade off between high imperceptibility and large capacity faces significant challenges. Many researchers attempt to use edge regions to embed the meta-data as the Human Visual System (HVS) is less sensitive to modification in edge regions. However, the payload capacity of edge-based steganography is very limited. In this chapter, we developed a new idea of optimizing the embedding region in edge areas using the characteristics of the HVS and Genetic Algorithm. The work relies upon a background of edge detection and vision science research. A balanced substitute between security of edge detection is based on embedding and payload capacity of standard LSB and can be achieved in a non-uniform data distribution algorithm with small computational requirements and improved data carrying surface. It is also worth adding non-linear data distribution to secure and provide reasonable resistance to statistical detection of hidden data. The experimental results indicate that not only high imperceptibility could be achieved by this proposed method also but it could ensure a high embedding rate. Finally, the case study was fairly successful in implementing its goals. The effectiveness of the steganography as a multimedia tool is clearly shown in this case study a successful implementation of the goal of this project.

Chapter 5

Perceptual Threshold in Discrete Wavelet Transform [1]

5.1 The Problem

The process of steganography is focused on being a concealed object within another object, which makes it different to cryptography. One way to conduct this process is through a computer-based image steganography, which is also useful to hide meta-data inside a multimedia object that aims to reduce the storage space. The process by which concealment can occur is the main topic of discussion in this Chapter.

As stated in Chapter 2, two techniques are commonly used in hiding data: spatial domain; and transform domain. Spatial domain hides data in a time frame by concealing data into the pixel value directly. Transform domain is a mathematical function that transforms the cover image into frequency coefficients. When compared to the other methods, transform domain is seen as more robust, however the capacity of the meta-data to be hidden is very limited. Some transforms that are usually used in steganography include Discrete Cosine Transform (DCT), Discrete Fourier Transform (DFT) and Discrete Wavelet Transform (DWT). However, the most important thing to

[1] Some of this chapter contents have been published in the 30th International Conference on Image and Vision Computing New Zealand (IVCNZ 2015) entitled "The Use of HVS to Estimate Perceptual Threshold for Imperceptible Steganography"

be considered in any domain technique is where to embed the meta-data and how to do it.

Scholars are always concerned as to the most proper coefficient that can be used to insert the meta-data (Gu and Gao, 2009; Martin and Cochran, 1994; Martin, 1999; Ohnishi and Matsui, 1996; Raja et al., 2007; Shi, 2005). A range of low, middle and high coefficients are applied. Low frequency transform contains the most important visual part while high frequency contains the insignificant visual part such as noise. Low-transform embedding effect the image and it is therefore essential to have the cover image for meta-data extraction and stego image imperceptibility. Nonetheless, the low-transform attractiveness of the data hiding does not upsurge the disarray of the image and enhances the image alterations that have low pass character. Low-coefficient data hiding also has concerns regards less sensitivity to small linear alterations. On the other hand, inserting data into middle and high frequencies is usually less powerful for small pass purifying and small linear distortions of the image, but are exceedingly robust with regards to noise reduction and non-linear distortions, histogram manipulations, brightness correction and contrast modification.

To overcome the confusion regards the best transform coefficient, the model analyzed each coefficient and chose a proper perceptual threshold for each coefficient based on the content of the cover image. This allowed high embedding rate and ensured less distortion of the cover image. To achieve a proper perceptual threshold, Human Visual System (HVS) characteristics and Evolutionary Algorithm (EA) were used. The aforementioned characteristics can be attained through a method involving embedding data imperceptibly as part of the steganographic system. This process allowed the immediate extraction of data, promotion of a high rate of information or the payload, and incorporated resistance to be removed. In short, imperceptibility directly related to how the HVS worked in terms of its perception of the image. This implies that HVS should be considered when undertaking techniques related to the concealment of data. This will result in perceptually plotting the secret data based on the cover image's contents (Gu and Gao, 2009).

The main purpose of the HSV model was to measure the sensitivity of the cover image to human perception. A distance is calculated which was used to restrict changes related to the coefficients as well as in the improvement of imperceptibility (Zhu and Sang, 2008; Ahmidi, 2008). Furthermore, these models are used in the assessment for the identification of suitable regions present in a particular image where more data will be embedded (Zhang and Wang, 2005; Jung and Ko., 2011). It is also considered to be a way of identifying a standard of distortion (Jung and Ko., 2011) as well as simplifying or reducing the data insertion computation (Li et al., 2008). This process includes Contrast Sensitivity Function Masking (CSFM) optimization and Just Noticeable Differences (JND), the aim of being to perceptually shape meta-data in the data base on the present cover image. JND facilitates the gathering of the coefficients' perceptual threshold. Here, the Contrast Sensitivity Function (CSF) is used as a basis for determining wavelet coefficients in CSFM weights. CSF is a human sensitivity model that is directly related with spatial frequency. The aim of the process is to obtain the most perceptible information through the mask and to allocate highest priority present in the particular quantizer.

Genetic Algorithm (GA) is also used to optimize the stego image quality. GA is conducted with the aim of mapping the data based on the cover image's contents whilst considering a minimum error rate. In order to reduce the differences between the stego image and the cover image, a particular fitness function called PSNR-HVS was applied. In this chapter, the distortion was minimized through the conduct of the right-most region in order to map the hidden messages which commenced after obtaining the threshold from the HVS models. The process also included the perceptual mapping of contrast sensitivity optimization and the texture masking selected coefficients, as well as the luminance and contrast masking of selected coefficients and their neighbors. This was done based on the cover image contents through genetic algorithm. The process results in gathering the best result possible data. The objective is to point out the development of Discrete Wavelet Transform (DWT) perceptual threshold and the maintenance of a balance relating to high embedding capacity. The process also includes the percep-

tual mapping of contrast sensitivity optimization and the texture masking selected coefficients, as well as the luminance and contrast masking of selected coefficients and their neighbors. This was done based on the cover image contents through the Genetic Algorithm.

5.2 Proposed Model

The research here presents a new model referring to a data hiding scheme. The process includes a technique related to Genetic Algorithm (GA) with the use of Contrast Sensitivity Masking (CSFM) with an aim of perceptually shaping the meta-data. The data hiding is based on the cover image composition present in the domain of the Discrete Wavelet Transformation (DWT). Moreover, the use of DWT in this proposed model is based on the threshold's multi-resolution hierarchical characteristics as well as its lower resolution embedding and low cost detection (Wazirali and Chaczko, 2015a).

By optimizing CSF Masking and combining it with Noise Visibility Function (NVF) to perceptually shape secret data through GA, excellent results are obtained and established. This chapter proposes a technique where the mapping process of the meta-data, particularly in Discrete Wavelet Transform through Human Visual System is performed. Here, CSF masking is used as well as Just Noticeable Differences (JND) using GA. Furthermore, the luminance of the CSF's non-uniform behavior in an image steganography is wavelet-based and is done to aid the proper classification of the coefficient according to human perception. To accurately determine perceptual threshold for every coefficient, JND is calculated, specifically, the Noise Visibility Function (NVF). The obtained coefficients, including their luminance masking and contrast are transmitted to the module related to the GA. Identification of coefficient embedding threshold β is then carried out through the GA. Furthermore, multiplication of the embedding threshold β follows together with the generation of perceptual mask and the pseudo-random. Subsequently, addition of perceptual mask to the cover image is done, specifically selected coefficients. To obtain the stego image, masking of the inverse CSF wavelet

then proceeds. The model is shown in Figure 5.1 through a flowchart.

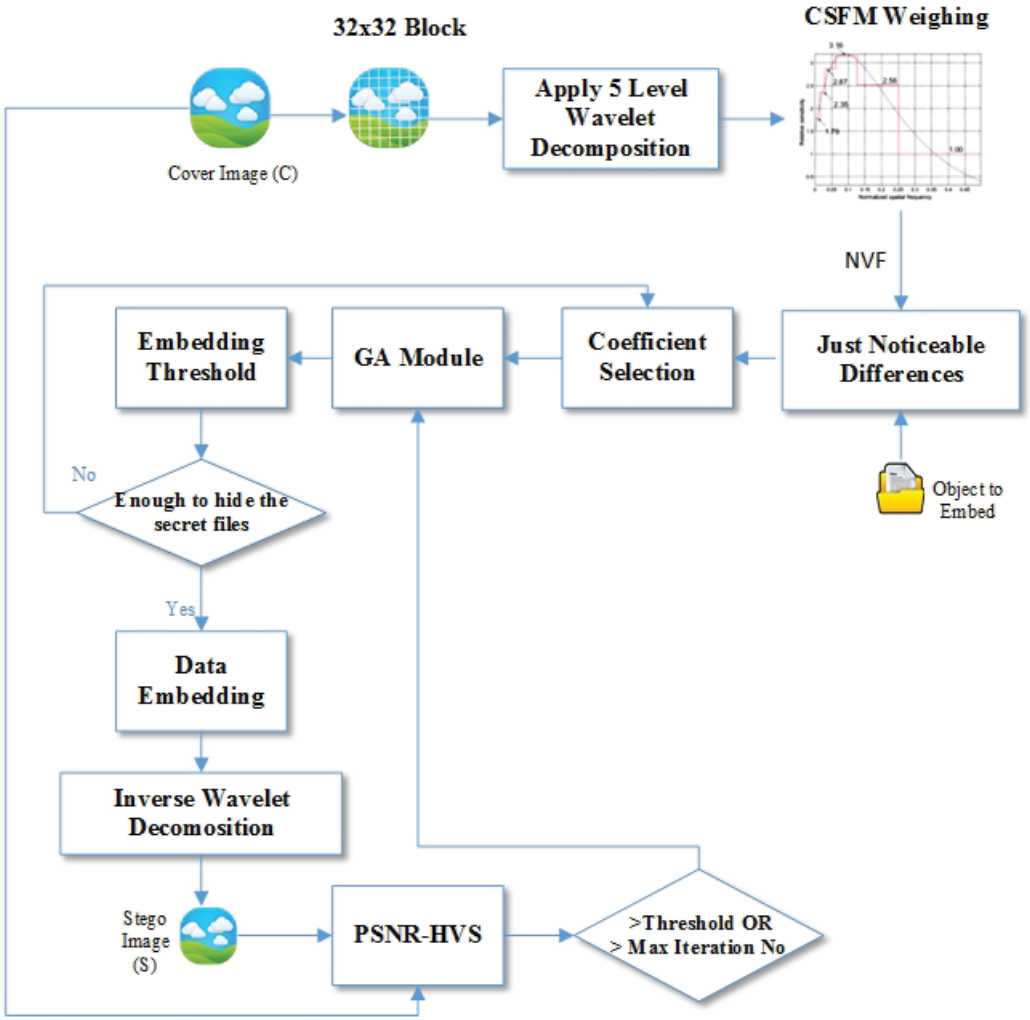

Fig. 5.1: DWT HVS Architecture diagram

5.2.1 CSF Masking

CSF masking is usually applied in the domains of the discrete wavelet. This masking method is performed to weigh wavelet coefficients in relation to the coefficients' perceptual importance. The application of the CSF mask and the inversion of the compression system are illustrated in Figure 5.2. During the design, the transformation of CSF curve poses a problem when included

into the mask of weights, which subsequently leads to a multiplication of the coefficients of the wavelets (Figure 5.6). Specifically, a design and evaluation of the DWT CSF mask is done in this research.

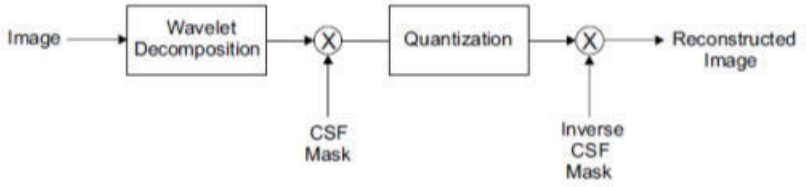

Fig. 5.2: CSF masking diagram

5.2.2 DWT CSF Masks

The process of DWT CSF masking involves a utilization of the information present in every sub-band approximation. Likewise, sub-band details in relation to the yielding of 6 unique weights present in the given mask are included in the process. Weight normalization is then conducted to equalize the lowest weight to one. In the creation of DWT CSF mask, the initial step involves CSF curve wavelet decomposition. This is followed by the identification of mask weights as a result of the decomposition. Two methods are used to determine the weights, which results in the obtaining of two DWT CSF masks known as the '6-weight DWT CSF mask'. When looking at the distortion subjected in regions along the mid-frequency (level 3), a higher sensitivity is seen in HVS. On the other hand, the drifting of frequency value on both sides of the spectrum leads to the decline in sensitivity (level 1, 2, 4 and 5). An application of the square function is combined in the process of approximation in relation to the CSF masking's effects. To determine adequate modulation rate $\beta\lambda$ as seen in every sub-band, the following formula is considered:

$$\beta^{\lambda} = 0.01 + \frac{(7.20 - r^{\lambda})^2}{7.20^2} \tag{5.1}$$

where r^{λ} indicates the sub-bands' wavelet coefficient CSF in relation to perceptual importance weight, while λ is designated as the level of decomposition.

The process of the 6-weight DWT CSF mask formation follows the process:

1. Apply 5 levels of DWT as seen in Figure 5.3.
2. The second step includes the identification of the CSF curve's DWT (Figure 5.4, Figure 5.5 and Figure 5.6). In here, a 5-level Bi9/7 wavelet decomposition of CSF curve is considered and labeled in an explicit manner together with the subspaces (W5, . . .W1, V1).
3. Next, the W5 subspace's peak is labeled as p5. Also, the W4 subspace's peak is labeled as p4. On the other hand, the V1 subspace's peak is designated as q1.
4. In this first level of the decomposition, The weights of sub-bands, specifically, LH, HL, and HH are known as p5, particularly at the beginning of the decomposition.
5. When the decomposition process is at second phase, the various weights of the sub-bands, specifically, LHLL, HLLL, and HHLL are known as p4. The weighting of the bandpass sub-bands is then continued for every consecutive decomposition levels.
6. The next level involves the obtaining of the lowest frequency sub-band's weight (LL LL LL LL LL), which is denoted as q1. 6 distinct weights are then produced in the mask through this method.
7. The final step involves a normalization of each peak in order to derive a lowest peak that is equivalent to one.

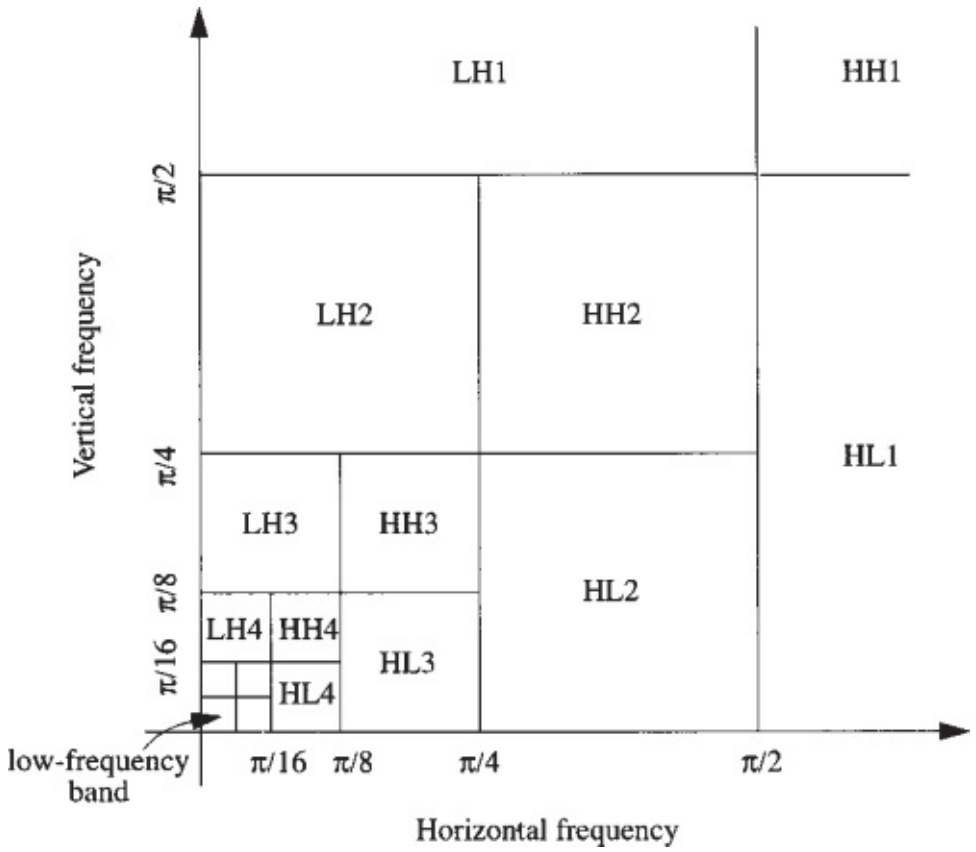

Fig. 5.3: A five level wavelet decomposion

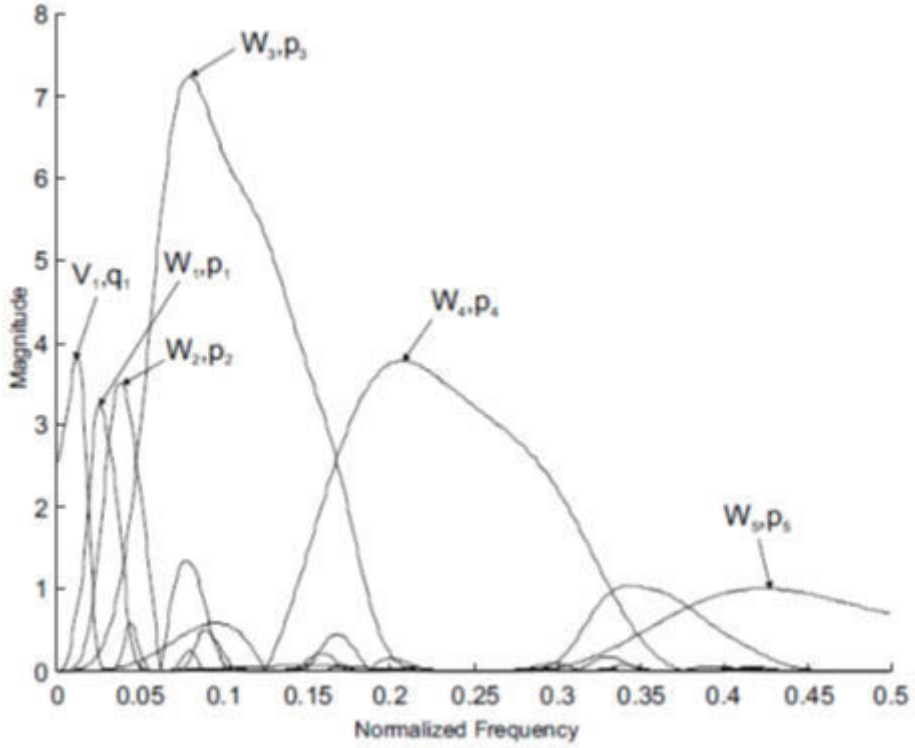

Fig. 5.4: 5-level Bi9/7 wavelet decomposition of CSF for 6-weight mask

Fig. 5.5: Band-average CSF mask with 6 unique weights

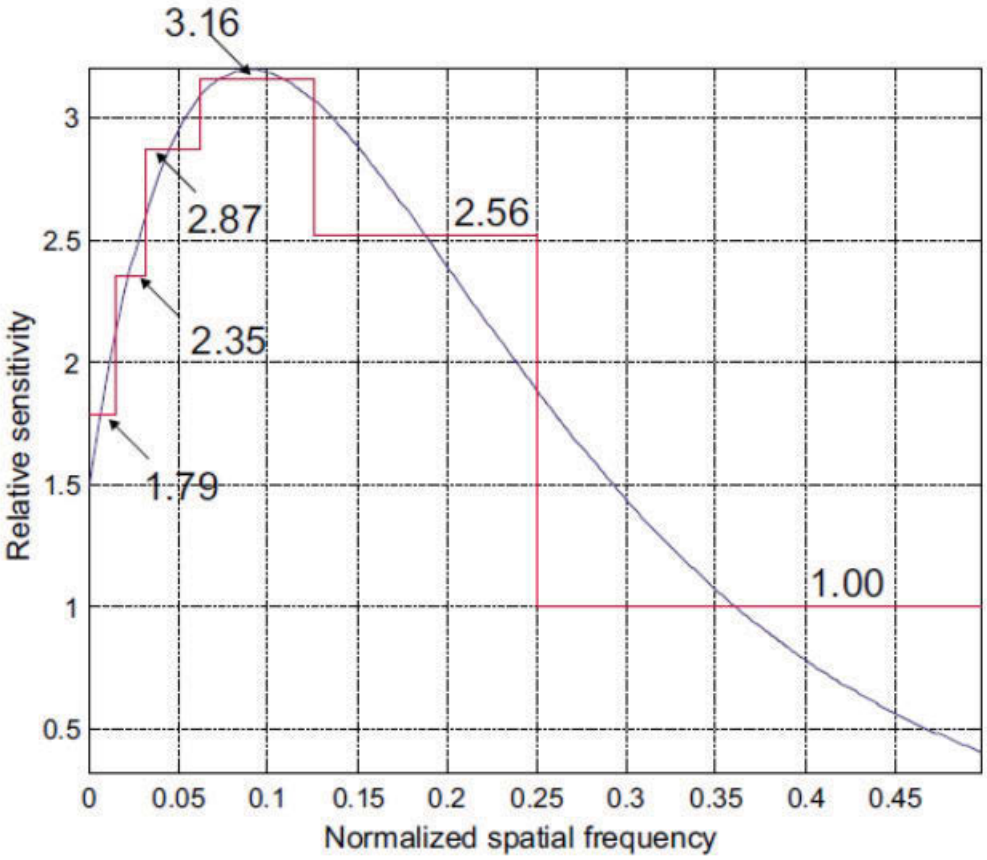

Fig. 5.6: CSF curve shown with the 6-weight band-average CSF mask

5.2.3 Selection of Coefficients

Upon the gathering of DWT CSF weighting mask, another process of obtaining the threshold in every coefficient is done using JND. The process of selecting coefficients is with the objective of classifying these into both important and non-important coefficients wherein the JND threshold is used as a basis. Calculation of JND threshold follows the Equation 5.2.

$$T_{JND} = JND_{\lambda,\theta} a_l(\lambda, \theta, i, ij).a_c(\lambda, \theta, i, ij) \tag{5.2}$$

where,$JND_{\lambda,\theta}$ represents the sub-band's base detection threshold λ; and on the other hand, orientation θ, $a_l(\lambda,\theta,i,ij)$ denotes luminance, while $a_c(\lambda,\theta,i,ij)$ is the contrast masking. Furthermore, the formula below shows the luminance masking (Equation 5.3):

$$a_l(\lambda,\theta,i,ij) = (\nu_{\lambda maxLL,i',j'}/\nu_{mean})\alpha_T \tag{5.3}$$

Where, λmax represents highest level of DWT decomposition. Specifically, λmax is positioned to one in relation to the proposed scheme. ν_{mean} represents mean luminance shown in the sub-band LL. α_T represents the luminance masking degree. The value of this degree is specified at 0.649 similar to other authors' value. Moreover, $\nu_{\lambda maxLL,i',j'}$ represents the DWT coefficient value in LL sub-band. This corresponds to the location (λ,θ,i,ij) seen in spatial domain as shown in Equation 5.4.

$$a_c(\lambda,\theta,i,ij) = a_{c_{self}}(\lambda,\theta,i,ij).ac_{neig}(\lambda,\theta,i,ij) \tag{5.4}$$

Where, $a_{c_{self}}(\lambda,\theta,i,ij)$ represents the contrast masking adjustment factor, while $a_{c_{neig}}(\lambda,\theta,i,ij)$ is known as neighborhood contrast. This is composed of three different coefficients surrounding the chosen coefficient along the similar sub-band as seen in the neighborhood. Furthermore, selection of the coefficients in the HL sub-band with a value that is higher than their corresponding JND threshold follows. On the other hand, coefficients in the LH sub-band having higher value than JND threshold obtained upon the multiplication of the value by 1.6, subsequently are chosen. Lastly, coefficients in HH sub-band are selected when a larger value than the JND is obtained after multiplying it by value 1.8.

To alter data hiding strength in relation to embedding, GA is applied. The

strength is selected by considering the following characteristics in Equation 5.5.

$$\alpha_i[p1.p2] = f(NVF(i,j), X(i,j)) \tag{5.5}$$

where $NVF(i,j)$) is seen to perform contrast sensitivity as well as texture masking. While $X(i,j)$ represents the current block's selected DWT coefficient.

$$NVF(i,j) = 1/(1 + \theta\sigma^2 X(i,j)) \tag{5.6}$$

The image's local variance of pixel (i,j) is denoted by$\sigma^2 X(i,j)$.

To measure the fundamental spatio-chromatic of HVS, CSF is considered in the process. This would indicate the high sensitivity of humans in the regions of mid-frequency. Thus, an embedding of data having low intensity in regions with high sensitivity is needed. The reverse is also required to complete the process.

In order to say that the process of data hiding is effective, low energy present in mid-frequency regions should be embedded from the CSF inverse plot in order to prevent obtrusiveness and in order to see its effect to the visual quality. In here, certain thresholds are needed to be set to refrain from the addition of very high volume of energy when applied in the domains with low DWT frequency. This problem can then be solved by conducting an interpolation method to be able to construct an Adaptive CSF masking and further improve this HVS model in relation to the generation of a higher quality image. In addition, this process will also lead to attainment of higher quality HVS stego image that is more robust and translucent. With this, an Adaptive CSF masking is proposed and shown in Equation 5.7. The corresponding coefficients that are attributed to the sub-bands are also tabulated

and presented (Table 5.1)

$$\beta = (1 - NVF_{i,j}) \times (1 - H(f)) \times f \tag{5.7}$$

In particular, a parameter value that is small enough is obtained to retain the stego image quality. This is done in order to support the LL band which is critical when image reconstruction is being conducted.

Table 5.1: Adaptive CSF masking for a five-level DWT

Orientation	Level				
	1	2	3	4	5
LL					0.000001
HL/LH	0.599316	0.211279	0.031660	0.032198	0.031905
HH	1.000000	0.341371	0.005418	0.031905	0.030574

5.2.4 Embedding Level

High level of imperceptibility could be seen and obtained for the stego object when each coefficient is given different embedding rates. As a consequence, the cover image's statistical features are maintained and provided. In here, the application of the specific mapping technique of Genetic Algorithm (GA) is done, particularly in the selection of the best place where the meta-data is located. This is done to guarantee that identification of error existing between the cover and the stego image. After the cover image analysis is carried out through HVS characteristics is performed for both models, placing the message's entire elements in their corresponding places. This will lead to the definition of the frequency domain position that is the most reasonable, followed by the obtaining of the minimum static feature disturbances that are evident in the selected coefficient.

Maintaining the stego image imperceptibility in an optimized level and simultaneously being consistent of the high payload capacity may be done

through PSNR-HVS testing. This is done to determine if the concealment of meta-data in every possible region is done while having the highest possible embedding rate. As a consequence, this also leads to a larger number of possible substitutions, particularly when a high payload capacity occurs. So, when there is high consumption of time during the PSNR-HVS value computation for every substitution, the process becomes unacceptable. Nonetheless, this can be solved through a carefully selected genetic algorithm.

Here, a particular problem is referred to as the "input" while a codification of the solutions based on a particular pattern is done as a "process". Each candidate solution is evaluated through the concept called fitness function. These candidate solutions are randomly selected, and this is the beginning of the evolution process. Entities having a random nature are repeatedly identified throughout successive generations. As a result, each generation yields those that are most suitable, but not necessarily the best ones. For this research, the GA is focused on improving the quality of the image. Accordingly, one appropriate test that can be used to undertake this process is the PSNR-HVS. In here, three HVS-based factors relating to the evaluation of image is measured through HVS-based peak signal in relation to noise ratio (Egiazarian et al., 2006). These include error sensitivity, edge distortion, and structural distortion. This process is done through the elimination of mean shifting as well as contrast stretching that utilize the scanning window. The fitness function is defined as:

$$PSNR\_HVS = \alpha PSNR_E + \beta PSNR_{ED} + \gamma PSNR_S \tag{5.8}$$

In here, error sensitivity is obtained by the formula measuring E_i as seen below:

$$E_i = \frac{1}{MN} \sum_{m=1}^{M} \sum_{n=1}^{N} [C(m,n) - S(m,n)]^2; \tag{5.9}$$

for $i = 1, 2, 3$(color channels)

Therefore:

$$PSNR_E = 10 \log_{10} \frac{3}{\sum_{i}^{3} E_i} \tag{5.10}$$

Where $C(m, n)$ and $S(m, n)$ are the individual pixel values for each color channel $i = 1, 2, 3$; M and N are the number of rows and columns of the image. Moreover, structural distortion can be calculated by the following equations:

$$S_i = \frac{1}{N} \sum_{r=1}^{R} [0.5(C_{a_r} - S_{a_r})^2 + 0.25(C_{p_r} - S_{p_r})^2 + 0.25(C_{b_r} - S_{b_r})^2]; \tag{5.11}$$

for $i = 1, 2, 3(colorchannels)$

$$PSNR_S = 10 \log_{10} \frac{3}{\sum_{i}^{3} S_i} \tag{5.12}$$

Where $C_{a_r}, C_{p_r}, C_{b_r}$ and $S_{a_r}, S_{p_r}, S_{b_r}$ represent mean, maximum, and minimum pixel values for the cover and stego image, respectively. Furthermore, edge distortion can be measured as follows:

$$ED_i = \frac{1}{MN} \sum_{m=1}^{M} \sum_{n=1}^{N} [C'(m, n) - S'(m, n)]^2; \text{ for } i = 1, 2, 3(\text{color channels}) \tag{5.13}$$

$$PSNR_{ED} = 10 \log_{10} \frac{3}{\sum_{i}^{3} ED_i} \tag{5.14}$$

Where $C'(m,n) - S'(m,n)$

refers to the values of the individual pixels as seen in edge maps in relation to the reference and distorted images. These values are considered for every color channel with the variables $i = 1, 2, 3$. In relation, M and N refer to the amount of columns and rows present in the image.

To address the problem posed, parameters that are called "chromosomes", composed of simple data strings, undergo translation. The process starts with the initial step involving various characteristics that are obtained with the aim of undertaking random pioneer generation of the society. This is followed by measuring the value of relevant proportionality by determining fitness function. This step is followed by forming the second or next generation based on certain selection criteria and processes. This is also done through genetic operators based on characteristics that are formerly set. For each of the individual selections, parents are chosen in pairs. This way of selection is made in order to come up with the component that is considered to be most appropriate; because of the randomization, the components that are considered weakest are given a chance to be selected. In addition, there is also a bypassing seen among the local solutions. Nonetheless, the present study used the tournament method to undertake this process.

In here, an interaction of the two chromosomes and their contents are seen to obtain newborn chromosomes. Specifically, these two original chromosomes undergo generation process and produce the other two. In this way, a combination of two best chromosomes would also yield an excellent pair. However, mutations could also occur during the process. If this happens, the succeeding generation could be bred wherein the new ones will be having different characteristics as the original ones.

5.3 Experimental Results

To undertake this study, a development of a full environment aimed to test the algorithm was created. This environment was created using a series of C language routines. For instance, a complete compression decompression algorithm was used through the Visual C++ environment, while the GA and arithmetic coding were accompanied by C programs. The comprehensive experiments included a set of 2000 images which came from the Corel database. These images have resolutions and sizes that vary from one another. In particular, this chapter discusses only six images which were named Airplane, Baboon, House, Lenna, Pepper, and Tiffany. The images included in the testing or in the entire experiment are images with 24 bit color RGB with a size of 512×512. In here, the metadatas, which are either image of a text, were tested for the experiment using varying sizes.

A comparative approach was used in verifying the proposed model's performance. This involved two approaches as discussed earlier in this section. For the first approach, a mapping function that is GA-based was used in the process of embedding data, specifically in discrete wavelet transform coefficients placed in 4×4 blocks as applied to the cover image (Ghasemi et al., 2012). The second one applied the Syndrome-Trellis Codes. The second approach is optimal for embedding as well whilst the Human Visual System (HVS) that is considered as near-optimal especially when applied for lessening the impact when used in integer lifting wavelet transform domain embedding (Pan et al., 2011). For this research, the two approaches are respectively referred to as DWT-GA and DWT-HVS.

The proposed method is generated by using 10 chromosomes produced through a clustering of random numbers with the aim of obtaining the earliest population. Within every generation three main operators are expected to be obtained, which will reflect the best solution expected. Processes included here are crossover, mutation and reproduction. An evaluation of the generated chromosomes follows the process. The evaluation is done according to the values of the PSNR-HVS. However, survival will only depend on the

presence of the top 10 PSNR-HVS with the highest values in order to be considered for the next or new generation or population. The final generation will undertake a selection of the chromosomes with highest PSNR-HVS value. The selection and its evaluation is done according to the computation time, PSNR value and histogram error.

Moreover, the stego image's imperceptibility is evaluated through different measures such as HVS based PSNR (PSNT-HVS), Peak Signal to Noise Ratio (PSNR), Structure Similarity Index Measure (SSIM), and Universal Quality Index (UQI). This is followed by a decomposition of host image through a bi-orthogonal 9/7 DWT leading to the yielding of five levels. A computation of the NVF in 4×4 image windows as well as an assumption of the noises as white Gaussian noises are done in this stage.

The computation of the maximum allowable embedding rate amplitude of all pixels was performed by considering Equation 5.7. This is done simultaneously with the maintenance of the meta-data's invisibility. The maximum embedding rate of Lena is shown in Figure 5.7. In here, the regions allowing bigger data hiding amplitude are represented by bright parts. This is done in order to conduct the process of embedding while denoting dark parts of the regions and allowing data hiding, specifically those with smaller amplitude to be embedded. The estimated outline of Lena is seen in Figure 5.7. To illustrate, the embedding of the meta-data's higher amplitude is permitted to be embedded in Lena's hair regions as an illustration of the complex texture regions or edge regions.

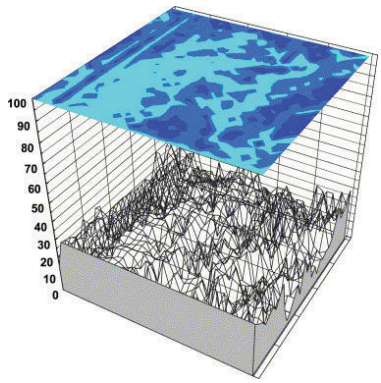

Fig. 5.7: Maximum embedding rates in Lenna

(a) The cover images (Lenna, Pepper, Airplane, Baboon, House and Tiffany)

(b) The stego images embedding 10%

(c) The stego images embedding 30%

(d) The stego images embedding 50%

Fig. 5.8: Different cover images with different embedding rates

5.3.1 Imperceptibility Evaluation

The process of concealing data has the tendency to yield some noise in relation to the obtained stego object. To produce a better output, a degradation of the statistical means must not be evident because of the noise. At the same time the noise should not also degrade the perceived quality. When cover image and stego image are compared and the degradation could not easily be noticed, it can be said that an imperceptible system is successful. The evaluation of stego image's imperceptibility when subjected to different rates for embedding could be done through PSNR, PSNR-HVS, SSIM, and UQI.

When these techniques were applied to images at 10%, 30% and 50%, a high and therefore acceptable rate was obtained. Table 5.2 illustrates this result. With this result, a noteworthy improvement was seen from the proposed method when it is compared to the other methods including the DWT-HVS based and the optimized DWT.

All images were also tested using histogram analysis (HA). This is done to provide a graphical representation in relation to the image's general distribution. For every entire value, the amount of pixel is designed by the HA. The histogram for a particular image could also show how total distribution can be judged. The histograms of the images in Airplane, Baboon, House, Lenna, Peppers, and Tiffany are illustrated in Figure 5.9. As can be seen in the illustration, histograms specifically for stego and cover images showing an almost indistinguishable character. This shows that the proposed model offers a more robust technique in contrast to statical attacks.

Table 5.2: The quality performance for various embedded rates for the proposed method and other embedding techniques

		Proposed		DWT-GA Ghasemi et al. (2012)		DWT-HVS Pan et al. (2011)	
image	Hiding Rate	30%	50%	30%	50%	30%	50%
Lenna	PSNR	57.581	55.487	49.257	42.578	50.487	44.487
	PSNR-HVS	74.368	69.478	62.458	59.365	62.365	53.489
	SSIM	0.9982	0.9932	0.9225	0.8856	0.9257	0.8652
	UQI	0.9956	0.9921	0.9158	0.8515	0.9157	0.8452
Pepper	PSNR	57.357	55.365	48.487	41.158	49.184	43.158
	PSNR-HVS	71.598	68.054	61.484	58.547	62.354	53.487
	SSIM	0.9978	0.9925	0.9152	0.8859	0.9158	0.8745
	UQI	0.9965	0.9915	0.9105	0.8452	0.9258	0.8452
Baboon	PSNR	57.454	55.458	49.354	40.025	52.457	43.258
	PSNR-HVS	73.587	70.358	62.987	58.587	61.678	53.236
	SSIM	0.9973	0.9915	0.9147	0.8849	0.9146	0.8735
	UQI	0.9964	0.9906	0.9116	0.8436	0.9246	0.8441
Airplane	PSNR	57.358	55.546	54.253	52.155	51.258	43.759
	PSNR-HVS	72.898	69.987	60.158	54.487	68.897	53.515
	SSIM	0.9964	0.9925	0.9153	0.8856	0.9158	0.8741
	UQI	0.9951	0.9915	0.9125	0.8425	0.9223	0.8432
House	PSNR	57.455	55.458	54.577	51.585	49.577	41.756
	PSNR-HVS	71.268	69.236	60.489	52.487	55.056	49.364
	SSIM	0.9962	0.9906	0.9134	0.8847	0.9035	0.8715
	UQI	0.9942	0.9892	0.9133	0.8414	0.9122	0.8336
Tiffany	PSNR	57.545	55.354	54.524	52.244	55.632	53.854
	PSNR-HVS	69.661	64.249	60.487	53.324	55.548	46.319
	SSIM	0.9952	0.9904	0.9065	0.8744	0.90654	0.8705
	UQI	0.9949	0.9894	0.9039	0.8411	0.9532	0.8322

5.3.2 Payload Capacity Evaluation

Limits in steganography appear in the broad majority of the pieces used in this research. This shows that inserting a limit has the tendency to be considered with greater regard than steganographic limit mentioned by (Cox et al., 2008). Furthermore,(Venkatraman et al., 2004) mention that an implanting limit or amount is known to be the relationship of measurement to the undetectable data and secure picture . Wang and Wang further state that utilizing steganographic strategies for the purpose of key association could enhance the steganographic limit as well as help to understand the undetectable data possessed by stego pictures (Wang and Wang, 2004). Nonetheless, (Cole and Krutz, 2003) argues that a better method is to implement more information in the concealed image. However, there is a tendency that steganographic limits undergo constraint through the conduct of measurement to assure that information is recorded, as seen by (Artz, 2001; Rabah, 2004). Enhancement of the volume of key information should be considered when developing the steganographic procedure. Here, this key information may be imperceptible but the stego information documents and its characteristics are affected.

The maximum embedding capacity attributed to the various images is shown in Table 5.3. Here, the proposed method, as well as the other steganography techniques using 512x512 image size, are presented. The embedding capacity when seen in data hiding, based on DWT, obtains the proposed model's maximum capacity at about 50% in almost all images. This implies that embedding capacity went through an improvement. The different embedding rates and stego image's imperceptibility are correlated and are shown in the different illustrations (Figure 5.10, Figure 5.11, and Figure 5.12). Results show that a high and satisfactory imperceptibility is obtained, although a decrease in the embedding rate is also seen in the stego image's imperceptibility.

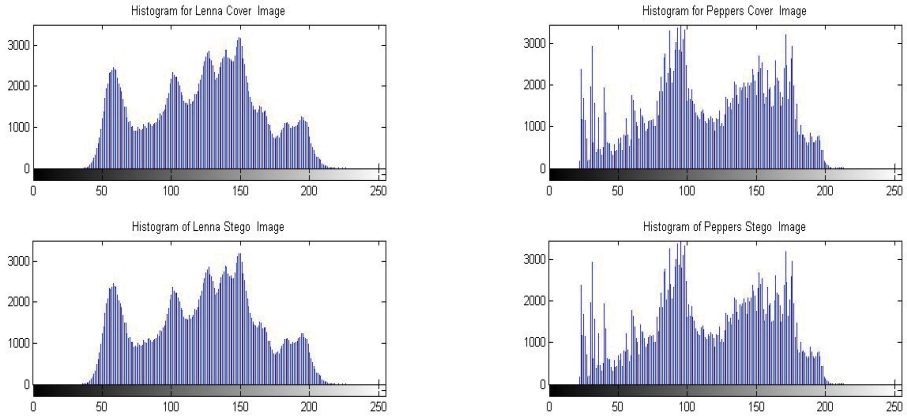

(a) Lenna left, Peppers right and Cover image up, Stego image down

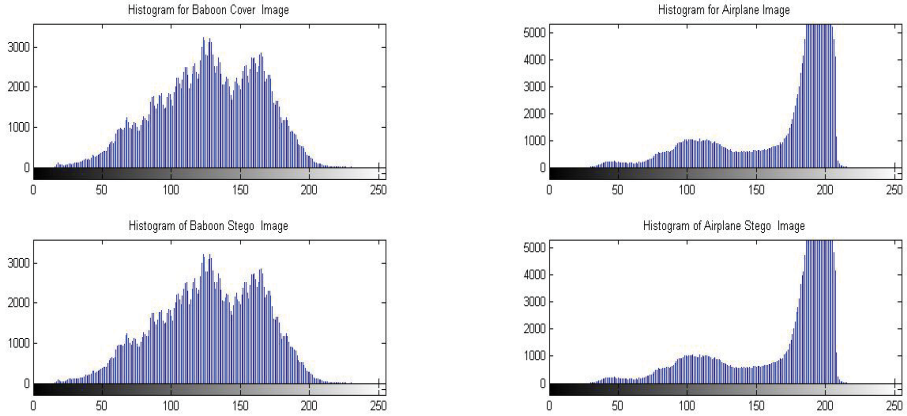

(b) Babbon left, Airplane right and Cover image up, Stego image down

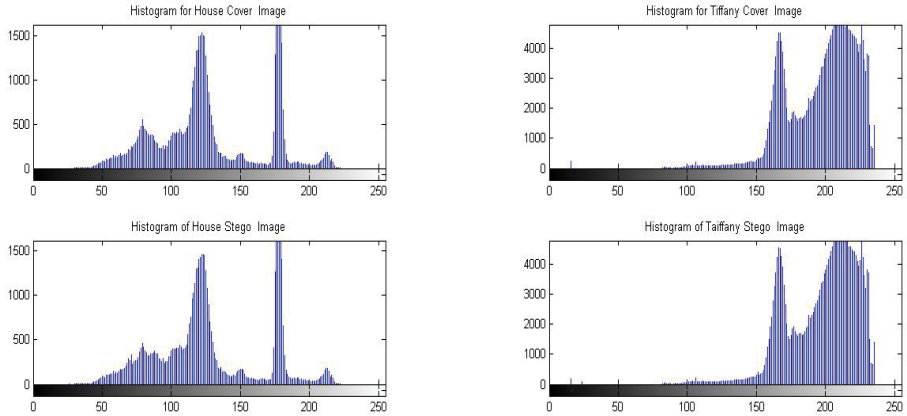

(c) House left, Tiffany right and Cover image up, Stego image down

Fig. 5.9: Histogram analysis

Table 5.3: Maximum embedding capacity

Image	Capacity (bits)
Lenna	349,129
Peppers	350,284
Baboon	347,172
Airplane	346,201
House	335,847
Tiffany	345,503

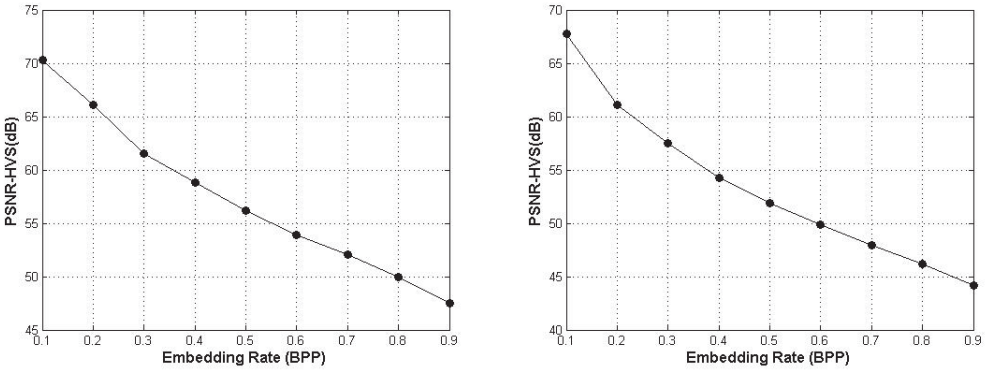

Fig. 5.10: Quality vs. capacity in Lenna left and Peppers right

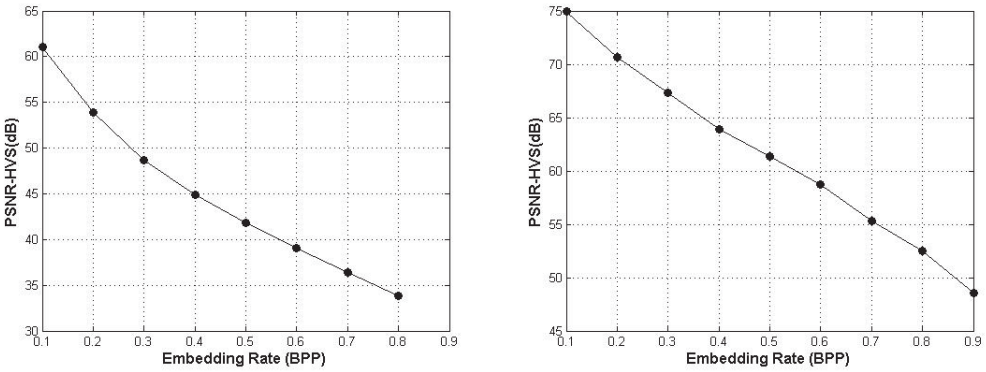

Fig. 5.11: Quality vs. capacity in Baboon left and Airplane right

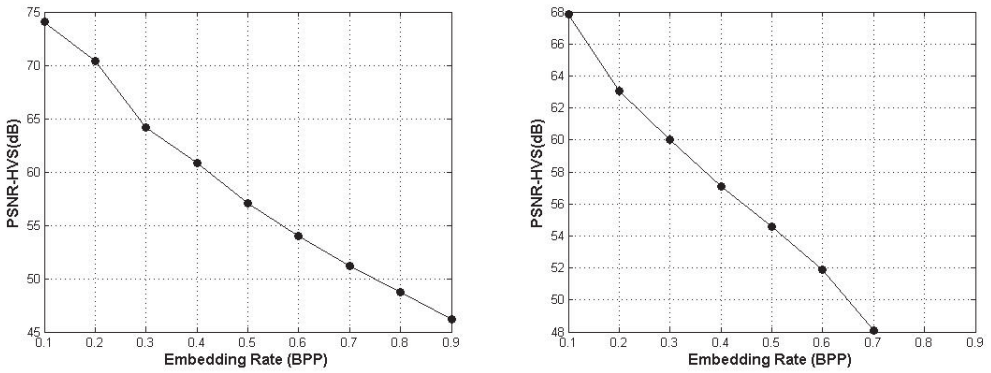

Fig. 5.12: Quality vs. capacity in House left and Tiffany right

5.3.3 Genetic Algorithm Evaluation

Table 5.4: Relation between the number of iteration and imperceptibility

Iteration	PSNR	PSNR-HVS
0	49.358	61.254
25	51.584	63.578
50	53.985	66.584
75	55.754	68.587
100	57.581	71.597

Usually, imperceptibility in techniques that are non-GA also lead to problems. Hence, every possible solution for optimum mapping should undergo testing. If not properly conducted, the overall computation time will be very long and therefore unacceptable. To properly conduct the process of GA, chromosomes, also known as "genes" are represented through the encrypted binary elements. These genes or chromosomes undergo adjustment with the aim of maximizing imperceptibility through the assurance of the best mapping function when used of the cover image as well as the meta-data. This usage should be iterated in an acceptable manner and number. For this research, the balance is made between the GA cost used to undertake the best mapping function selection together with a consideration of the overall completion time.

A selection process of ten entities is made for iteration as seen in the procedure of GA at 300 preparation iterations. This is obtained by doing a crossover proportion (0.25) and the mutation proportion (0.05). As a final step, five individuals having larger PSNR-HVS and PSNR, or those considered at the top are retained to become new individuals and transmitted to the upcoming generation. The imperceptibility increase in relation to PSNR-HVS and PSNR as well as the enhancement of iteration amount are illustrated in Table 5.4.

Furthermore, the crossover is shown in Figure 5.13, where the proposed method's performance is determined against the crossover's probability. In here, the fitness function is seen as maximum as represented by $P_c = 0.438$. On the other hand, the mutation probability is shown in Figure 5.14. In here, a value of 0.902, which is considered as the best one is achieved in the proposed model.

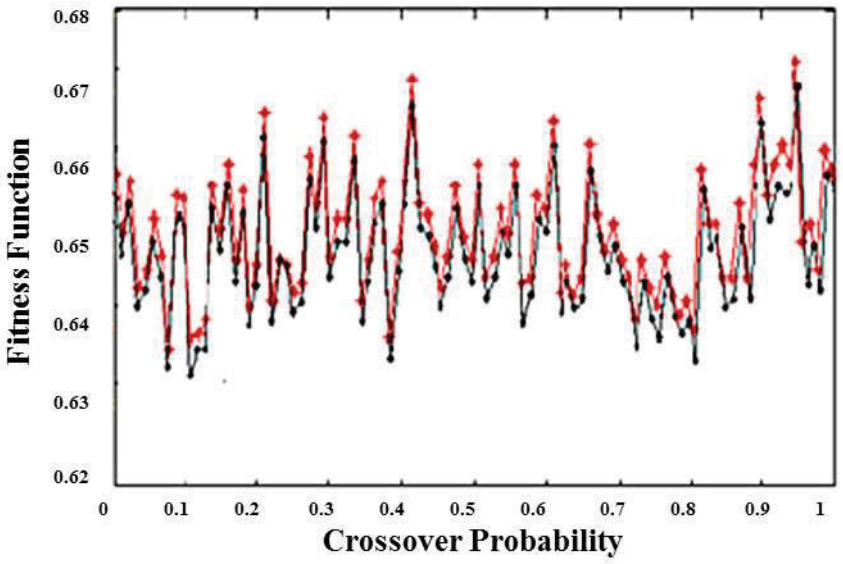

Fig. 5.13: Fitness function evaluation for various crossovers

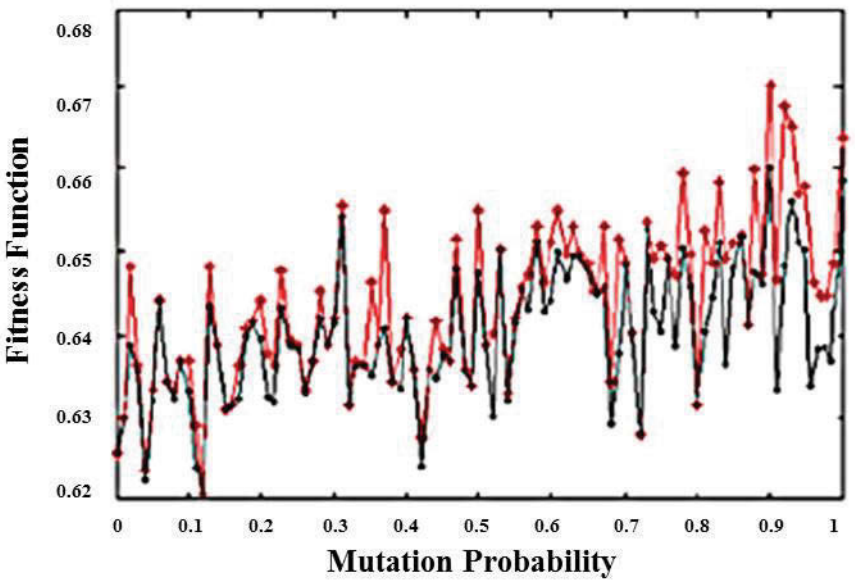

Fig. 5.14: Fitness function evaluation for various mutations

5.4 Conclusion

In steganography, three elements are important for the system's success: security; payload capacity; and imperceptibility. Concealing data as part of the frequency domain could offer a stego image that is more robust but with a very low domain payload capacity. To solve this problem and advance the performance of steganographic methods that are wavelet-based, the human visual sensitivity (HVS) system is incorporated to the existing model to achieve optimum hiding. By utilizing HVS, a balance is attained in relation to the imperceptibility and the capacity of perceptually mapping secret data based on cover image's contents. An evolutionary algorithm is then used here to obtain a better robustness and imperceptibility for the model. This algorithm is applied for all coefficients in order to determine the optimum hiding strength. Furthermore, evaluation of all possible solutions though characteristics of human observation is done by applying a fitness function. As a result, the stego object is seen to be less degraded, while the result of the experiment shows stability among the different characteristics related to

computation time, selectability, and high payload capacity.

Chapter 6

Estimating Optimum Embedding Capacity based on Image Complexity [1]

6.1 The Problem

In steganography, determining the maximum embedding capacity is an important factor to properly choose an appropriate secret message. The process enables a user to reach the capacity through embedding smaller data over and over to reach the optimum capacity of the digital image. Bits per pixel (bpp) was used to express the unit of capacity. The unit of capacity used for data embedding is specifically referred to as the "average capacity" that characterizes image pixels. On the other hand, some assessment measures are used in estimating image quality based on quality degradation, evident after the process of embedding the data. These measures include Peak Signal to Nose Ration (PSNR), Structural Similarity Index Measure (SSIM) and Universal Image Quality Index (UIQI).

However, the process of calculating capacity through steganography is not an easy task because many factors interplay during the calculation. The most essential factors in this complex process include capacity, robustness and quality (Chen et al., 2012). These factors correlate and interconnect with each other in terms of their role in the repetition of hiding bits, generation

[1] Some of the chapter contents have been submitted to *Multimedia Tools and its Applications Journal*

of image quality, and enhancement, among others.

In recent years, there have been a number of discussions regarding the calculation of steganographic capacity. One study by Moulin proposed the use of hiding information in the calculation of the capacity seen through a transmitter and a receiver that makes up a certain information channel (Moulin et al., 2000; Cox et al., 1999). Alternatively, some methods of estimating capacity by using Discrete Cosine Transform (DCT) were discussed by Barni et al. (Barni et al., 1999, 2000). An estimation on the invisible distortion that could be acceptable in every pixel based on neighbor values was coined by Voloshynovisky, calling it the Noise Visibility Function (NVF) (Pereira et al., 6). Other techniques focused on the lessening of distortion by proposing codebooks and coding systems in relation to images generated through steganography (Erez et al., 2005; Yang et al., 2006). Because of the differences in the processes of determining and understanding estimated capacity, the values are also diverse as an effect, ranging from as low as 0.002 bpp to as high as 1.3 bpp (Zhang et al., 2007).

Due to the weaknesses of the HVS and its effect on the algorithm of the system, it is likely to affect changes in the parameters related to the determining degradation and capacity. One example of HVS is Watson's Perceptual model (WPM) which utilizes the measure of perceptual embedding capacity through DCT transformation; it involves measuring the allowable error in every coefficient using non-overlapping blocks through visual sensitivity which corresponds to a parallel DCT basis function. In WPM, the sensitivity determined is based on: frequency sensitivity; luminance masking; and contrast masking.

Moreover, estimating a payload capacity for a specific cover image should ensure imperceptibility to the Human Visual System (HVS). For a balance between maximum capacity and minimum degeneration, there should be an optimum embedding level for each and every coefficient of the selected coefficients of the cover image. In order to achieve optimum embedding level one should consider the hiding capacity as an optimization problem (Khan et al., 2004; Ohnishi and Matsui, 1996; Wang et al., 2001; Fard et al., 2006b;

Dasguptaa et al., 2013; Mandal, 2000; Wazirali et al., 2014; Westfeld and Andreas, 1999).

In this chapter we have proposed an estimation of optimal capacity of steganography techniques that combined Human Visual System (HVS) with Genetic Programing (GP) to produce a proper embedding rate. The process aims to generate an embedding rate that is appropriate for each coefficient. The combination of HVS and GP enables the balancing of hiding capacity and imperceptibility in relation to perceptual mapping of secret data based on the cover image's components. Furthermore, the model is based on the objective of estimating the DCT's embedding capacity through an improved version of the Genetic Algorithm and Watson's Perceptual Model. Therefore, minimum error distortion based on the measurement of image complexity through HVS can be achieved. On the other hand, calculation of proper complexity is done through a combination of WPM and JND. The process is also carried out by calculating optimum hiding threshold, particularly for each cover image coefficient to be able to generate a higher level of robustness and imperceptibility.

6.2 Proposed Model

As mentioned earlier, an estimation of optimum capacity for steganography was proposed by taking into consideration the characteristics of HVS. In estimating the perceptual amount of embedded data, Watson's Perceptual Model is utilized through the cover image contents in the domain of DCT. Also, the Genetic Programing was used in optimizing the contrast sensitivity as well as the texture masking of selected coefficients, luminance masking and their contrast. This is done to perceptually map the obtained data based on the cover image's contents and as a result, paved the way for obtaining improved results.

To clarify, GP is referred to as a type of genetic algorithm that is specialized by considering every individual in the population as a computer program which is represented by a corresponding tree structure. In here, each tree

node has a corresponding operator function such as either +,-, log, sin, or cosine. Moreover, the tree node consists of leaves containing operands (i.e., coefficients, contrast sensitivity, frequency sensitivity, masking, luminance). In the process, a candidate expression is generated by GP to refer to cover image C. The expression is then used in inserting the generated secret message. Furthermore, the evaluation of a candidate expression's performance is made by deriving fitness. The function is understood according to measures of imperceptibility such as Structure Similarity Index Measure (SSIM) and Noise Visibility Function (NVF). This is done in embedding general high energy strength data at a relatively lower visibility cost. The generation will determine the participation of individuals based on their performance, as the weaker individuals are usually eliminated and are not able to participate in the next generation. In here, the stochastic operators of GP are probabilistically applied to create offspring. The process includes selection, mutation and crossover. This goes on throughout generations until the process halts by reaching a certain condition, which has been previously explained. When this condition is attained, the best GP expression present in the final generation is then saved to be used in concealing the images. In here, the individual puts the strength$T_c(u, v, k)$ for every coefficient k back to the cover image C.

An improved version of WPM based on Just Noticeable Differences (JND) will be used. Moreover, to obtain better image complexity, the correlations between different parts of an object in the picture is preserved and stego-image quality is enhanced. For selecting the proper embedding rate, Genetic Programing will be used to select for the right most proper embedding rate for each coefficient. Figure 6.1 illustrates the main architecture of the proposed model.

6.2.1 Segmentation based on the Brightness Distribution

A correlation is seen between various contents of the image and the areas of the various objects. The main difference between the proposed model and that of others such as that of Watson's is the consideration of this correlation. Correlation has been derived because of the process entailed in the division of

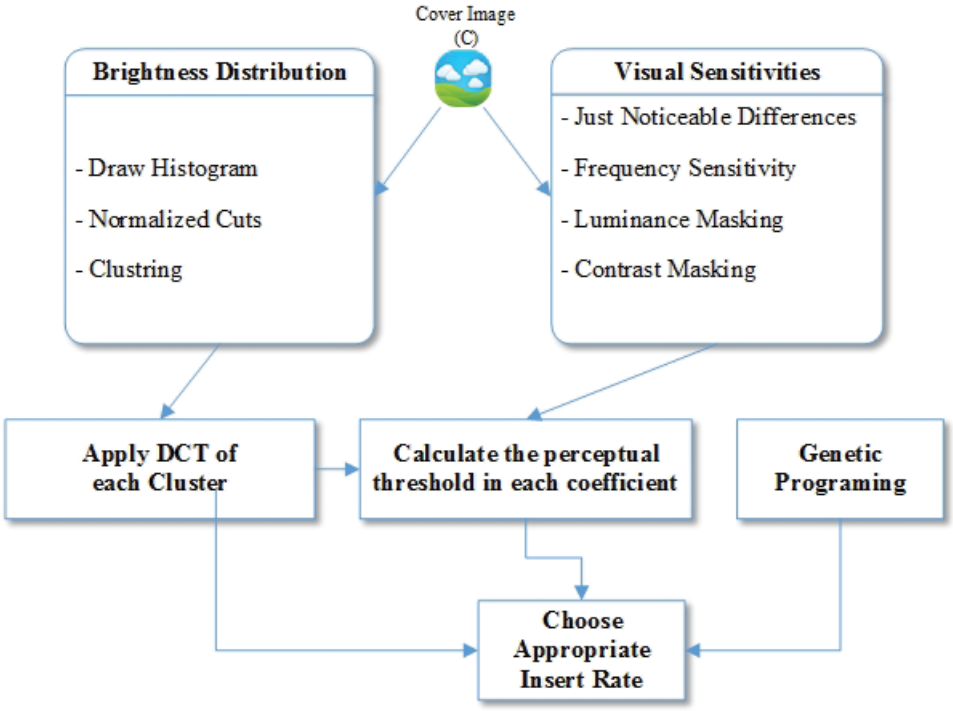

Fig. 6.1: General Architecture of the proposed model

images through the non-overlapping block. In here, each object is placed in a corresponding block, which transmits a message that would refer to a signal insert, making it undesirably placed in the overall object that is noticeable to human visual perception. The adverse effect is prevented through a proper classification of the cover image to sub-images according to the distribution of brightness as emphasized in the proposed method. The steps involved in the segmentation are illustrated in Figure 6.2.

The segmentation is further done by separating the cover image into a color with three channels then drawing the image's histogram. This is followed by the identification of brightness distribution as evidenced in every color channel. Next, the distribution is divided into image cells, which are sub-images having equal size. The work commences by dividing each image cell in an independent and local manner. K-mean cluster to break down segments with k number through an algorithm known as normalized cuts. The process of clustering is primarily concerned with the division of the input

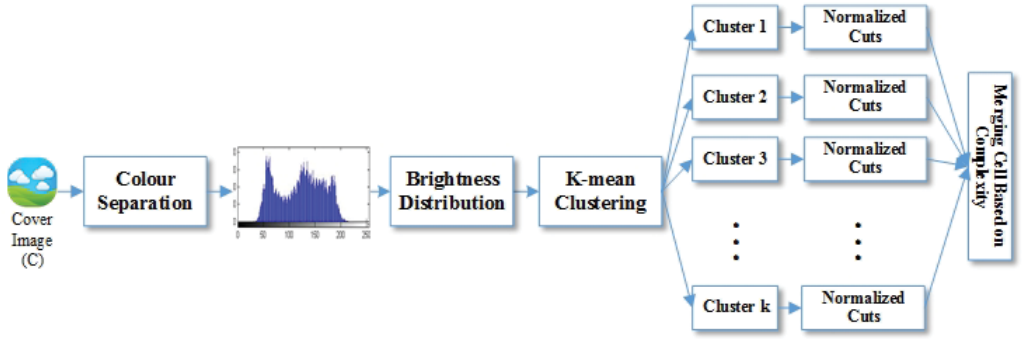

Fig. 6.2: Segmentation Phase Diagram

dataset connection and with the recovering of data points for the clusters or groups. K-means clustering refers to an algorithm that is able to group large-scale data sets in a more efficient manner. This is also a classical clustering method known to have low complexity and intuitive character, which makes it a suitable choice for this work. In addition, an evaluation is also made in terms of deriving cell segmentation done in each image cell. Hence, the image cell's compatibility and its values are checked, while over-segmentation only occurs based on the compactness of an image cell. Nonetheless, over-segmentation positively contributes to the generation of better segmentation by decreasing the slope seen in object margins that are segmented where most of the cell segmentation is performed in an independent manner. This process signals the start of merging of the segmented groups obtained from image cell processing together with the other segments. The calculation of a normalized cut is determined based on overall dissimilarity in the different image cells and the image cell's similarity.

On another note, the areas in an image that are homogenous and are seen to hold common features are clustered as a single image cell. After this, characterization of each segment through the use of nodes is done. These nodes are seen to hold the pixel's mean value with color brightness which is also positioned in the segment's central parts. The created segments originating from the cell stage of the image cell is represented by the nodes' total number as derived from the process. For example, every 40 nodes corresponds to 40 segments from the image cells. Subsequently, the normalized cuts algorithm

proceeds in relation to computed nodes. The final step would then entail the merging of image cell segments according to attributes of centroid position and color values, particularly if similar properties are seen from the nodes.

6.2.2 Image Transformation

One way to transform an image from the spatial domain into the frequency domain is the Discrete Cosine Transform (DCT). This technique is performed through a sub-band generation in according to visual quality. In here, the sub-bands could either be low, middle or high based on transform components. The importance of the image's visual parts is based on the frequency of sub-bands, where low sub-bands comprise the most essential parts while those with high frequency contain the unimportant parts. These unessential parts are then eliminated by using compression or noise attachment. In comparing the two frequencies, middle frequency sub-bands are found to be ideal in relation to embedding of secret data because image visibility is not affected at this level. The equations below describe DCT transform as well as the corresponding inverse of it.

$$C(u,v,k) = \alpha_u \alpha_v \sum_{i=0}^{L-1} \sum_{j=0}^{L-1} \alpha(i,j,k) cos \frac{\pi(2i+1)u}{2L} cos \frac{\pi(2j+1)v}{2L} \quad 0 \leq u,v \leq L-1 \tag{6.1}$$

$$\alpha_u = \begin{cases} \frac{1}{\sqrt{L}} & u = 0 \\ \sqrt{\frac{2}{L}} & 1 \leq u \leq L-1 \end{cases} \qquad \alpha_v = \begin{cases} \frac{1}{\sqrt{L}} & v = 0 \\ \sqrt{\frac{2}{L}} & 1 \leq v \leq L-1 \end{cases}$$

In this equation C(u, v, k) is DCT coefficients for k block.

IDCT transform:

$$C'(u,v,k) = \alpha_i \alpha_j \sum_{v=0}^{L-1} \sum_{u=0}^{L-1} b(i,j,k) cos \frac{\pi(2i+1)u}{2L} cos \frac{\pi(2j+1)v}{2L} \quad 0 \leq i,j \leq L-1 \tag{6.2}$$

$$\alpha_u = \begin{cases} \frac{1}{\sqrt{L}} & u = 0 \\ \sqrt{\frac{2}{L}} & 1 \leq u \leq L-1 \end{cases} \qquad \alpha_v = \begin{cases} \frac{1}{\sqrt{L}} & v = 0 \\ \sqrt{\frac{2}{L}} & 1 \leq v \leq L-1 \end{cases}$$

The coefficient of quantized DCT is composed of DC coefficients, AC coefficients and zero AC coefficients (Figure 6.3). The DC coefficient is characterized by a block's mean luminance that changes based on perceptual artificial "blockiness". On the other hand, AC coefficient is broken down into two types: zero AC and non-zero AC coefficients. The former is constantly seen at the high and middle frequency. If modifications to these occur, the structure of continuous zeros is broken, which provides a hint relating to presence of secret bits based on abrupt non-zero values. In contrast, the non-zero AC coefficients are seen along the middle and low frequencies. Despite the disruption occurring in these coefficients, visual quality of the image is not adversely affected as compared to other DC members. With these characteristics, it is proper to say that the most suitable choice in conveying secret bits is through non-zero AC coefficients.

6.2.3 HVS Based Complexity

As metioned in section 6.1, three fundamental properties relating to human vision are: frequency sensitivity; luminance sensitivity; and masking effects. These are used to attain maximum threshold and minimum hiding error when DCT coefficients are used in every block. To explain, frequency sensitivity is characterized by the understanding of the sensitivity of the human eye

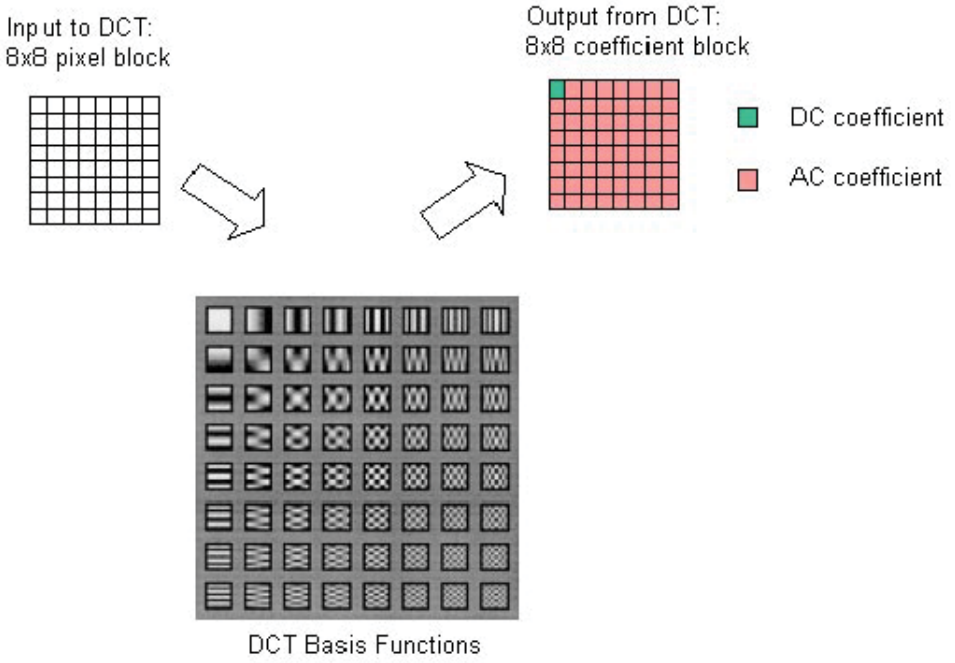

Fig. 6.3: DCT transform

in relation to different spatial frequencies. On the other hand, luminance sensitivity is used in gauging the impact of a noise's detectability threshold when a constant background is present. Moreover, it is referred to as a frequency sensitivity correction based on changes occurring in the background luminance. Whilst the impact of visibility decreases in a signal when another signal is present, this is called "masking". The other signal that influences the decreasing visibility is referred to as a "masker". Two types of masking exist: self-masking and neighborhood masking. When the masked signal and masking process occur in an image within similar location, orientation and spatial frequencies, this is referred to as "self-masking". On the contrary, when the location, orientation and spatial frequencies in an image are close, it is referred to as "neighborhood masking".

In order to measure the distortions that every DCT coefficient is able to resist, an improved version of the Watson's Perceptual Model is put forth. In here, scaling of maximum threshold, seen as a visible embedding error in every coefficient of DCT in each block, in each area, and in analogous areas, is

done. Related visual sensitivity in relation to function-based discrete cosine transform is also considered.

The first step is to join Just Noticeable Differences (JND) with frequency sensitivity. The calculation of IND is given in Equation 6.3 where ω, μ are horizontal and vertical spatial frequency. T_{min} is the least threshold resulting at the spatial frequency $f_{T_{min}}$, S indicates the angle of the rounded line, and η is the WPM constant.

$$T_{JND}\frac{T_{min(\omega^2+\mu^2)^2}}{\alpha_u\alpha_v((\omega^2+\mu^2)^2-4(1-\sigma)\omega^2+\mu^2)}10^{S(log\sqrt{\omega^2+\mu^2}-\log f_{T_{min}})} \quad (6.3)$$

Furthermore, T_{JND} thresholds are used to enhance the JND of frequency sensitivity in Watson's model in DCT as given in Equation 6.4

$$T^f(u,v,k) = T(u,v).\left(1+\frac{\gamma.T_{ROI}(\xi,f,x_k)}{100.\max T_{ROI}}\right) \quad (6.4)$$

where T_{ROI} is the weighted threshold based on region of interest (ROI). T_{ROI} is a concept used to integrate capricious density on HVS, x_k is the pixel x in the block k, γ donates the effect of HVS based on region of interest and ξ is the observing distance calculated in image light.

$T^f(u,v,k)$ are additionally rectified by luminance sensitivity masking based on Equation 6.5

$$T^L(u,v,k) = T^f(u,v,k).\left(\frac{C_{DCT}(0,0,k)}{\nu_{0,0}}\right)^{a^T} \quad (6.5)$$

where $C_{DCT}(0,0,k)$ is the DC coefficient for position k, $\nu_{0,0}$donates the DC coefficient related to the average luminance of the display, and a^T is the variable that control the intensity of brightness sensitivity.

Additional modification of $T^L(u,v,k)$ by contrast masking which can be evaluated as Equation 6.6:

$$T_c(u,v,k) = T^L(u,v,k).\max\left[1, \left(e^{\frac{-\pi((u-u_m)^2)}{\left(\beta.\max(1,\sqrt{u^2+v^2})\right)}} \frac{C_{DCT}(u,v,k)}{T^L(u,v,k)}\right)^{\phi(k)}\right] \tag{6.6}$$

where β is the model parameter and $\phi(k)$ manage the amount of masking impact and it can take various spatial frequencies and various blocks. $\phi(k)$ can takes the value from 0 to 1. NVF can be used to control this value as it can takes value range of 0,1. Values near to 1 indicates flat region and values near to 0 indicate textured regions. Therefore, $\phi(k)$ can be calculated as in the given Equation 6.8. Where η indicates the maximum value reflect the robustness of embedded data. NVF is described in Equation 6.7 and $NVF_P$is the NVF of edge region. Moreover, σ_x^2 is the image's local variance when a centering of the window on the pixel having coordinates (m,n).

$$NVF(m,n) = \frac{1}{1+\mu\sigma_x^2(m,n)} \tag{6.7}$$

$$\phi(k) = \begin{cases} \frac{\eta}{3L^2} \sum_{u=1}^{L}\sum_{v=1}^{L}(1-NVF(u,v,k)) & if \sum_{u=1}^{L}\sum_{v=1}^{L}(1-NVF_p(u,v,k)) < L^2 \\ \frac{\eta}{L^2} \sum_{u=1}^{L}\sum_{v=1}^{L}(1-NVF(u,v,k)) & if \sum_{u=1}^{L}\sum_{v=1}^{L}(1-NVF_p(u,v,k)) = L^2 \end{cases} \tag{6.8}$$

Therefore, the value of $T_c(u,v,k)$ provide an estimation of the allowable payload capacity. Various factors influence the value of the estimated capacity these include: local variance; the amount of masking impact; region of in-

Table 6.1: GP parameter sitting

Objective	To provide optimum embedding level for selected coefficient
Fitness function	SSIM
Selection	Generational
Population size	300
Initial population	Ramped half and half
Tree depth	6
Crossover rate	0.25
Mutation rate	0.05
Termination	120 Generation
Survival mechanism	Keep best

terest; viewing distance; average luminance of the display; and intensity of brightness sensitivity; all effect the estimated capacity in different ways.

In the proposed complexity measurement, GP is used to derive a mathematical concept to analyze the hidden dependencies of the coefficient in order to make a balance between imperceptibility and capacity. GP returns the embedding strength for each coefficient represented by $T_c(u, v, k)$. This $T_c(u, v, k)$ is used to produce optimum perceptual embedding level.

A candidate expression is utilized to embed the secret message in the least significant bits in a cover image. Structural Similarity Metric (SSIM) is used as a fitness function to evaluate the performance of the imperceptibility and the payload capacity. These calculations examine each candidate solution to provide a trade off between conflicting properties. The individuals with highest results are selected for the next generations. Genetic operators are utilized to develop the new generation. These processes are repeated until the stopping criteria is achieved. Table 6.1 shows the GP parameter sitting of this experiment.

6.3 Experimental Results

This section presents the three most popular algorithms used in steganography or hiding data: Least Significant Bits (LSB); Discrete Cosine Transform

(DCT); and Discrete Wavelet Transform (DWT). These three function in various domains forming the association between embedding artifacts and estimating capacity present in an image.

For this experiment, 2000 images were used. These images originated from the database of Corel. However, only 6 images will be mentioned for results analysis and used to average the whole dataset. By applying the proposed model, the maximum resolution and size for each image was yielded. Subsequently, the images were hidden by applying LSB, DCT and DWT for a steganographic result. Furthermore, SSIM was used to compare and contrast visual qualities of the stego and host images. Additionally, Mean Square Error (MSE) and Universal Quality Index (UQI) were also used for this purpose as they take structural image similarity as part of the Human Visual System (HVS) into consideration. Similarly, it also offers a more optimized result over other methods like the PSNR.

6.3.1 Capacity Evaluation

One crucial criterion is the achievement of stenography implementation is the concept of payload capacity. Embedding capacity is referred to as the maximum number of bits which may be embedded through a particular cover image where quality of the image is not degraded or compromised. Embedding rate is different according to regions as seen in the model that is being proposed. Hence, measuring image complexity should be done in every region as it is crucial in this process. As a consequences, less complex regions have the tendency to hide less data while more data will be hidden in regions that are more complex. This is illustrated in Table 6.2, Table 6.3, Table 6.4 and Table 6.5, showing the relationship seen between HVS parameters and estimated capacity. Specifically, the maximum rate of test image embedding is shown in Table 6.2. In here, maximum capacity varies based on the texture and content of the image. In relation, the 8X8 block provides maximum embedding capacity as seen in Table 6.3. The relation between estimated capacity and local variance are correlated, as seen in Table 6.4. Lastly, when the ROI value is seen to be high, the related capacity is however seen to

Table 6.2: Maximum embedding capacity in bits

Test Image (256x256)	Optimum Capacity (bits)		
	LSB	Stegangraphy method in Chapter 4	Stegangraphy method in Chapter 5
Lenna	586,432	877,558	752,584
Baboon	558,258	823,587	787,558
Pepper	552,448	821,87	752,558
Airplane	525,587	836,587	784,258
House	554,258	836,558	784,245
Tiffany	532,587	825,587	721,589
Average of Corel Database	558,258	812,487	791,258

Table 6.3: The effect of different block sizes

LxL	2x2	4x4	8x8	16x16	32x32
Lenna	615,474	684,484	825,145	675,184	584,481
Baboon	552,487	687,788	752,488	674,589	495,477
Pepper	535,587	612,879	815,595	625,484	548,497
Airplane	462,578	685,574	765,219	643,892	526,854
House	525,845	562,544	897,231	632,889	432,892
Tiffany	432,587	697,945	758,712	621,897	413,857
Average of Corel Database	552,548	608,484	821,384	625,789	495,258

be decreasing. This is illustrated in Table 6.5 where estimated capacity is evident according to region of interest.

6.3.2 Imperceptibility Evaluation

Stego image imperceptibility is a crucial factor for any steganogrpahic system. Therefore, keeping high imperceptibility while estimating the perceptual embedding capacity is very significant. In fact, there is a relation between embedding capacity and resulting degradation of the stego image. According to the results of this research, steganography degradation is mainly influenced by the perceptual threshold of the estimated capacity.

The performance and estimating capacity are based on the proposed method. Figure 6.4 shows the relation between HVS based estimation capacity and

Table 6.4: The effect of different local variance

Local variance σ_x^2	10	8	6	4	2
Lenna	415,587	458,892	584,158	625,148	671,587
Baboon	405,574	445,588	536,577	615,874	665,981
Pepper	411,484	459,573	548,279	622,984	674,579
Airplane	415,985	452,985	536,974	635,587	685,255
House	428,971	442,589	548,978	642,589	662,589
Tiffany	425,985	458,985	558,126	658,492	658,432
Average of Corel Database	415,784	458,699	548,598	642,589	675,896

Table 6.5: The effect of ROI

γ[%]	0	30	60	90	120
Lenna	675,764	558,279	449,473	355,646	246,463
Baboon	755,543	537,974	459,756	367,457	266,575
Pepper	635,219	534,978	452,574	378,474	256,367
Airplane	686,821	546,126	438,477	375,347	256,346
House	646,463	546,643	428,700	356,458	203,363
Tiffany	653,376	524,646	467,747	346,743	267,363
Average of Corel Database	658,484	534,778	456,800	356,853	275,463

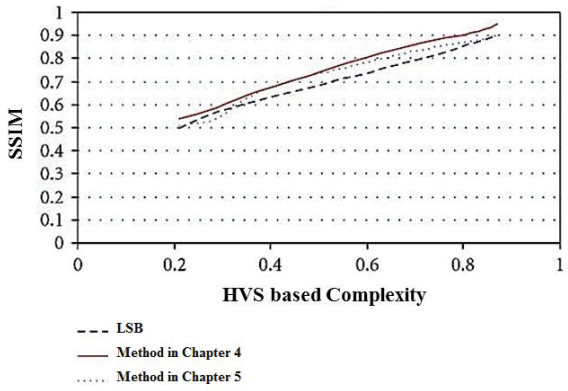

(a) SSIM Vs HVS Complexity

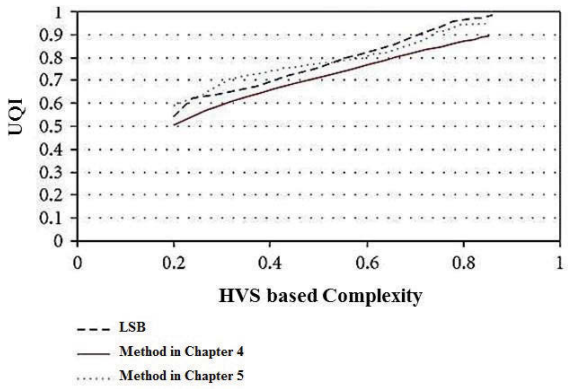

(b) UQI Vs HVS Complexity

Fig. 6.4: The relation between image complexity and image degradation

the various quality degradation metrics (SSIM and UIQI) averaged on 2000 images as mentioned before. LSB, stegangraphy method in Chapter 4 based on optimum edge embedding and the steganography method in Chapter 5 based on perceptual threshold of DWT have been used as hiding schemes. Over all the test images, with the increase of image complexity, the amount of quality degradation decreased. Therefore, it is important to choose a cover image with high complexity features to ensure high quality of the stego image.

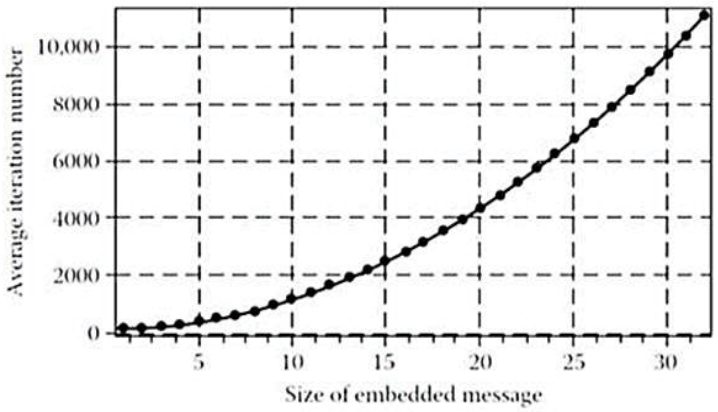

Fig. 6.5: Relation between capacity and the number of iterations

6.3.3 Genetic Programing Evaluation

As seen in the GP-based algorithm used in this chapter, the size of the embedded message as well as the position of the embedding is closely related to the complexity of the algorithm. This relationship is presented in Figure 6.5 where the embedded message and required iterations are embedded through a zigzag order from DC component to the cover image's LSB. In here, an increase in the embedded message, particularly the stego-image, effects the number of required iterations in the GP-based algorithm.

The use of GP enhances the chance of statical quality detectability. The differences between the cover image and the resulted stego image have been considered in GP training. These distortions have been reduced as best as possible. Figure 6.6, Figure 6.7 and Figure 6.8 show the corresponding differences between cover image and stego image after 50, 200 and 300 generations respectively. Accordingly, the differences have been reduced with the increased number of GP training which indicates the highly effective use of genetic programing in this experiment.

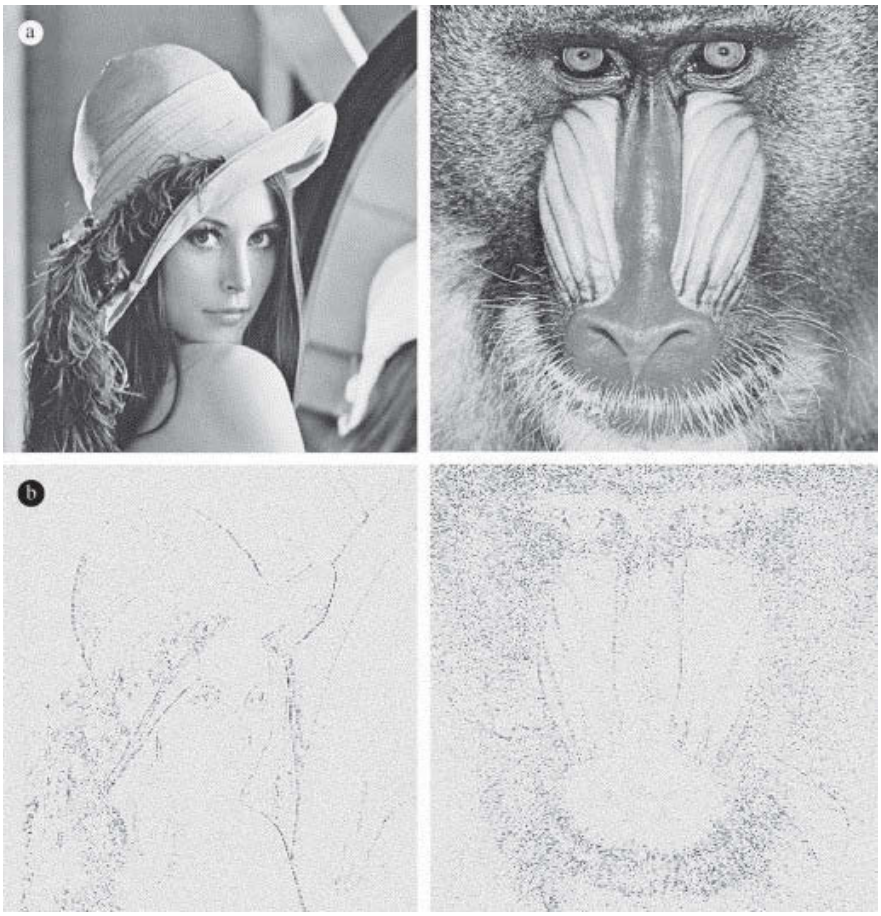

Fig. 6.6: Differences between cover and stego image after 50 generations

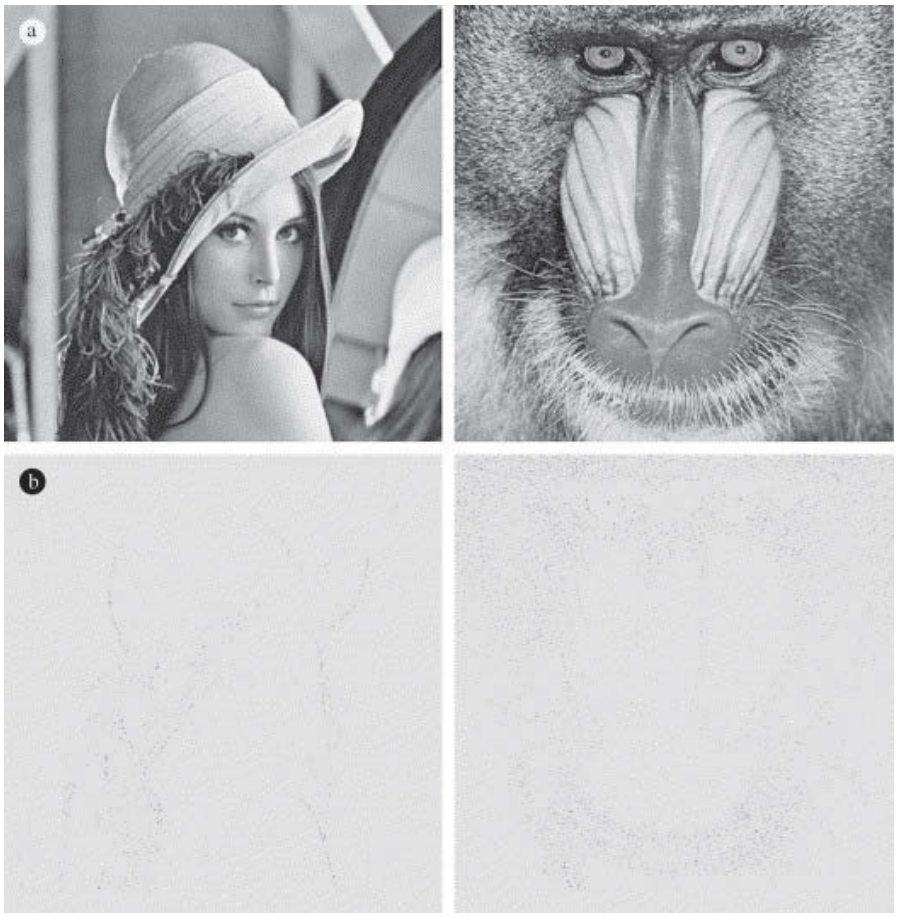

Fig. 6.7: Differences between cover and stego after 200 generations

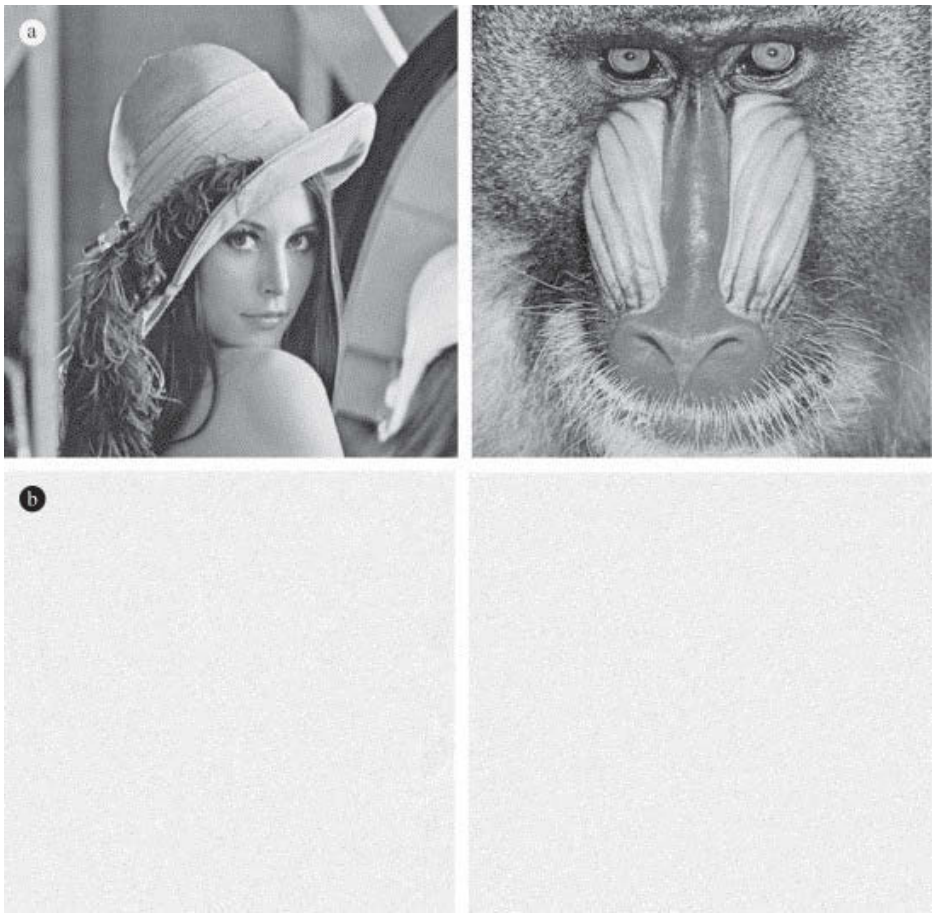

Fig. 6.8: Differences between cover and stego after 300 generations

6.4 Conclusion

Steganography is concerned with the hiding capacity of a digital image's components by finding the amount of information that could be hidden without noticeable distortions while maintaining a standard robustness. The Chapter presented a new method of computing the concept of embedding capacity through image complexity by applying HVS. This is a response to studies on image complexity, especially using HVS. The image degradation was also calculated by using UQI and SSIM. These are used with varying success hiding algorithms based on LSB, DWT and DCT domain used to measure quality.

Chapter 7

Anticipatory Quality Assessment Metric (AQAM) [1]

7.1 The Problem

The main goal of hiding data is to conceal the very existence of the hidden information. Therefore, there is a significant demand for steganographic approaches that can ensure imperceptibility of such information. Measuring the imperceptibility of the stego file is essential for most approaches dealing with image steganography. It can be determined by subjective or objective evaluation as stated in Chapter 2. The most accurate and reliable way to determine the visual quality of such stegoe file would be by human visual evaluation (subjective evaluation) (Yan et al., 2013) and (Zhang et al., 2014). However, this type of evaluation is, time consuming, expensive, and can not be part of an automatic system. For these reasons, researchers used objective evaluation for assessing quality of the image as it based on mathematical equations and provides faster results. However, there are a limited corresponding evaluation parameters available. Most of the studies use the Peak Signal to Noise Ratio (PSNR) as a metric for imperceptibility evalua-

[1] Evaluation of current quality assessment metric has been published in Asia-Pacific Conference on Computer Aided System Engineering (APCASE), 2015 entitled "Objective Quality Metrics in Correlation with Subjective Quality Metrics for Steganography" IEEE. Moreover, Anticipatory Quality Assessment Metric (AQAM) paper has been submitted for publication in *Journal of Information Hiding and Multimedia Signal Processing*

tion, although it could provide less accurate results than the Human Visual System (HVS) evaluation.

The simplest and most extensively utilized objective quality assessment parameter is the Mean Squared Error (MSE), calculated by averaging the squared concentration alterations of cover and stego image pixels. MSE and PSNR are attractive parameters since they are modest to compute, have pure physical connotations, and are statistically suitable in the perspective of optimization. However, PSNR measures the mathematical differences between the cover image and the stego image and does not take into account the characteristic of human visual system (HVS). Therefore, they have poor correlation with the perceived quality by the Human Visual System (HVS) (Wang et al., 2003; Wang, Bovik, Sheikh and Simoncelli, 2004). In the last few decades, extensive work has gone into developing advanced quality assessment methods that effectively use the features of (HVS).

The author of this thesis has analyzed the correlation between subjective and objective evaluation (Wazirali et al., 2015). On these experiments, a comparative study of the existing image quality metrics is performed for the steganographic images. The image quality score for commonly used objective quality metrics in the field of steganography has been compared with the subjective assessment performed by 500 observers. It was found that the selected objective metrics has a poor correlation with the subjective assessment, and may fail to accurately evaluate the performance of a steganographic algorithm. The HVS based metrics have better correlation compared to the standard pixel based metrics such as MSE and PSNR; this shows the effectiveness of using features of HVS in the quality assessment metrics. Figure 7.1 plots the main image quality metrics (objective evaluations) with Mean Opinion Score (subjective evaluation) conducted by 500 observers for degradation evaluation. Poor correlations were obtained between MOS and error based metrics such as PSNR and MSE. However, the objective quality metrics derived from the HVS features have a good relationship with the subjective assessment as compared to standard MSE and PSNR (Al-najjar and Soong, 2012; Babu, 2005; Wazirali et al., 2015). The outstanding quality of the image index de-

picted has the greatest correlation to the subjective score because of its loss of cover and stego images. This is due to the capacity to detect luminance distortion. In addition, the study concludes, that the human eye is depicted to be less sensitive to a blue color and more sensitive to green. (Wazirali et al., 2015). Therefore, it is significant to involve the human perception characteristics to assess the performance of any quality assessment metric. As such, not only color sensitivity should be considered but also brightness, contrast and image complexity are important factors.

Based on this analysis, it is essential to develop a predictive quality metric that is objectively assess the image quality on a similar way to the subjective evaluation. This chapter focuses on predicting the subjective quality using anticipatory objective. Anticipatory Quality Assessment Metric (AQAM) is an objective assessment metric that simulate the judgment of human perception. The primary objective of this chapter is to develop a systematic method of using HVS for image quality assessment.

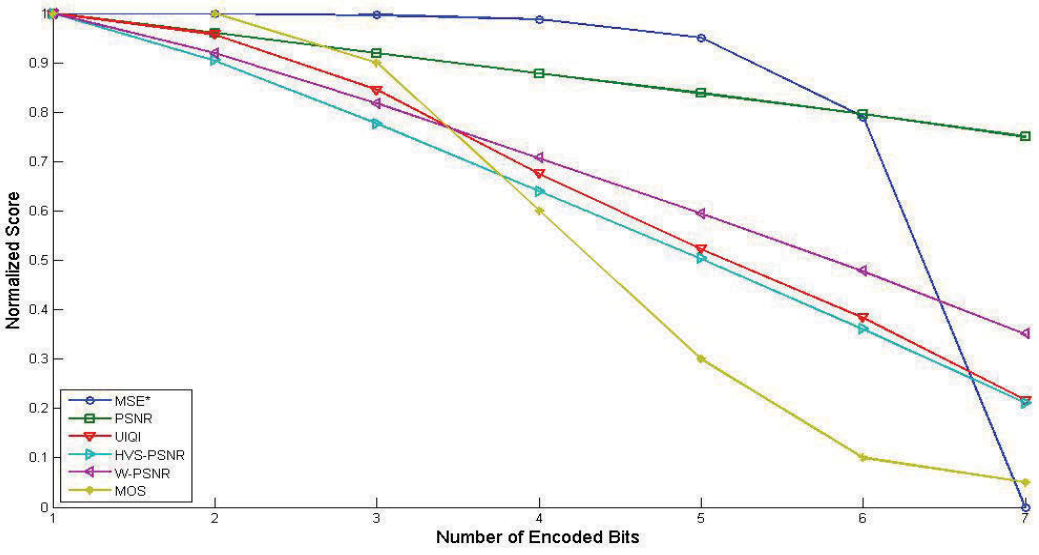

Fig. 7.1: Normalized subjective and objective score

7.2 Anticipatory Quality Assessment Metric

The Anticipatory Quality Assessment Metric (AQAM) parameters determine the quality of the image by applying the underlying principles of Human Visual System. AQAM emphasizes distortion which can be identified by a human observer. Therefore, this method creates a model using the local image properties based on the strategies implemented by HVS. The intensity and edge point of zero-crossing based on wavelets are the main strategies of this study. The intensity of the image is identified from the sharp regions. The details which are found in the sharp region of that photo is resolvable at multiple levels determining the sharp variations in image edge points.

The distortions impact on the contrast points in the photo changing structural data contact. The Noise Visibility Function (NVF) is applied to achieving edge areas in any image analyzed in the multi-level wavelet domain. It generates the information containing various sub-bands.

Zero crossing is a local structure categorized by a set of pixels demonstrating the sharp intensity of variations in the neighborhood. To achieve this, the edge data is extracted from the photo by applying the Laplacian Methods or a gradient. The main function of NVF is the estimation of the regional complexity by carrying out analysis in every region of the local image. The method that is proposed here estimates the quality of the perceptual image by using local image and intensity properties in the wavelet domain.

Frequency data is used for the quality perception of the linear spatial that is mined from the three levels of wavelet. Calculations are made for logging energies of the sub-bands and a weighted geometric mean provide a base for the sharpness estimation. Finer scales (high frequency bands) deliver a bigger result with the reduction in the sharpness numerical value. The intensity of the cover and the stego image is achieved through calculation. In order to find the accurate information of the whole process the similarity in sharpness of the cover and stego images are estimated.

Consequently, the wavelet of the image provides the high frequency sub-bands at i^{th} level as: $\{W^i_{LH}, W^i_{HL}, W^i_{HH}\}$.

The sub-band power of $i \in 1, 2, 3$ are computed as:

$$\alpha_x^i = \log_{10}(1 + \frac{\delta(x)}{\varphi_x^i}) \tag{7.1}$$

$\delta(x)$ is the value achieved by summing up the square off coefficients x, where x belong to $W_{LH}^i, W_{HL}^i, W_{HH}^i$. φ_x^i is the total coefficient of sub-band x which related to level i. The number of strength at each stage is measured as:

$$\alpha^i = \frac{\mu(\alpha_{W_{LH}}^i + \alpha_{W_{HL}}^i) + \eta.\alpha_{W_{HH}}^i}{\mu + \eta} \tag{7.2}$$

In the above mentioned equation the constant and variable have some assigned values as follows:

Constant μ is specified a value 0.3, η is assigned as 3. Note: η is allocated to higher value to provide larger weighting for the HH sub-band that has the high frequency mechanism.

The general intensity of a given image in the Equation 7.3 ensures lower measures of low value wavelets. For stego and cover image, intensity are assumed by γ_C and γ_S. The sharpness likeness of the stego and cover images is shown in Equation 7.4. ψ can be any value use for the avoidance of denominator being zero.

$$\gamma = \sum_{i=1}^{3} 2^{3-i}\alpha^i \tag{7.3}$$

$$\omega = \frac{2\gamma_C\gamma_{S+\psi}}{\gamma_C^2\gamma_{S+\psi}^2} \tag{7.4}$$

The cover image is referred to as a quality reference image at hand, using

the current point of view. By applying the Equation 7.5 and **Equation 7.6,** the edge match of each sub-bands of the stego and cover is assessed. It is seen that the higher the alteration, the higher the difference of the edge. The data will remain in the edge points which are normally not displaced due to distortions.

The difference is seen in the Gaussians (DoG) logical model which was anticipated by many in vision science; these are in the receptive fields of X-cells in the Lateral Geniculate Nucleus (LGN) in the thalamus, (Enroth-Cugell, Christina and Robson, 1966; Wandell, 1995). The CSF was later deployed in the band pass filters within frequency domain, called the weighted sum of DoG (or SDoG). The result is to make DoG the creator of bandwidth of the CSF, taking the visual system as a multi-scale analyzer together with ON/OFF cells with required size and Enroth-Cugell Christina and Robson receptive fields (Enroth-Cugell, Christina and Robson, 1966). The equation referring weighted sum of DoG will be:

$$E(C) = \sum_{k} Th_k \lfloor G^{+}_{\sigma k} - G^{-}_{\sigma k} \rfloor (C) \tag{7.5}$$

$$E(S) = \sum_{k} Th_k \lfloor G^{+}_{\sigma k} - G^{-}_{\sigma k} \rfloor (S) \tag{7.6}$$

In the above equation, C and S are considered as the stego and cover images (in luminance units) respectively; G_σ is the normalized Gaussian operator, Standard Deviation (SD) σ, σ^+ and σ^- are the SD of the positive and negative parts of a DoG ($\sigma^- = \lambda\sigma^+$); and Th is embedding threshold use for illustration in the next part.

A DoG is not seen only as a second derivative but it is also used for achieving edge detection with the same superiority as with $\nabla^2 G$ expressed in the forms of coefficient and localization of the negative and positive weights; they are to be same as per equation (as in Equation 7.5 and Equation 7.6).

The edge points numerical value of the stego and cover images are viewed as$E(C)$ and $E(S)$ correspondingly. The cover and stego image edge show structural similarity and are computed as given in equation E_s.

$$E_{s_x} = \frac{\text{sum}(E_x(C) \cap E_x(S))}{\sqrt{\text{sum}(E_x(C)}\sqrt{\text{sum}(E_x(S)}} \tag{7.7}$$

The final relationship of zero-crossing is shown in equation

$$\Delta = \Pi_x E_{s_x} \tag{7.8}$$

In this context, the two features that are the edge and intensity point of zero-crossing are unavoidable for the image quality evaluation. Therefore, the newly born AQAM metric use to asses the perceptual image quality. The proposed quality metric can be calculated as:

$$AQAM = \Delta^{\nu} \cdot \omega^{\nu} \tag{7.9}$$

The value of ν has been taken as 0.8, for it to give the greater geometric weight to intensity since it is the most powerful feature that captures human attention in early vision.

7.3 Experimental Results

Validating the performance of proposed quality metric subjectively is a primary phase. Mean Opinion Score (MOS), may be used for measuring the subjective evaluation. High MOS values indicates that the image is of good quality and nearly identical to the original image. It is worth noting that in this experiment we used MOS as our benchmark to measure the correlation between selected MOS and IQM. For this reason we selected TID2013

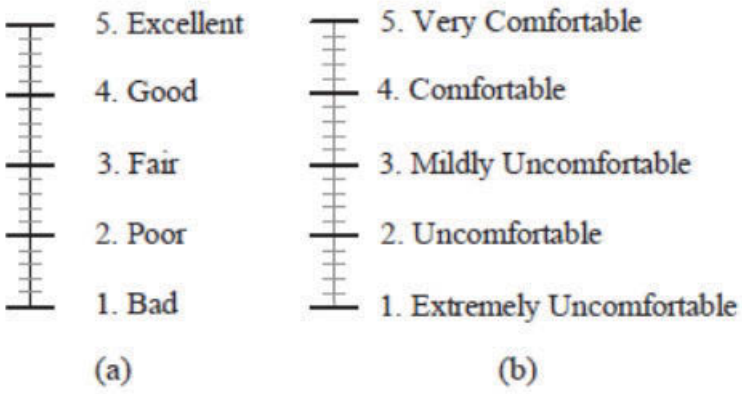

Fig. 7.2: Subjective assessment scale (a) quality and (b) visual comfort

Table 7.1: Steganography approaches

Distortion	Steganography approach
1	Least Significant 4 Bits (2-LSB)
2	Least Significant 4 Bits (4-LSB)
3	Pixel Value Differences (PVD)
4	Steganography method proposed in Chapter 4
5	Steganography method proposed in Chapter 5

(Tampere Image Database 2013) which is a publicly available database Ponomarenko et al. (2013). The MOS on the other hand was obtained from the result of 500 experiments that were conducted by 500 observers from two countries, Saudi Arabia and Australia, delivering MOS which ranges from 1 to 5 as shown in Figure 7.2. The TID2013 consists of 25 cover images, producing 150 stego images from five different steganography approaches. Table 7.1 shows lists of steganography approaches used in the experiment.

The measurements or values produced by each of the selected image quality metrics were correlated with MOS using two different performance measures: Spearman Cank Order Correlation Coefficient (SROCC) Ramsey (1989) and Pearson Linear Correlation Coefficient (PLCC) Lee Rodgers and Nicewander (1988). PLCC was the most commonly used delivering accurate predictions. The prediction accuracy can be quantified by two ways; either by measuring the average error between the algorithm's predictions and MOS values or

Table 7.2: Performance Comparison using PLCC and SROCC

Assessment Metric	PLCC	SROCC
PSNR	0.72896	0.75415
SSIM Wang, Bovik, Sheikh and Simoncelli (2004)	0.81562	**0.93415**
UIQI Wang and Bovik (2002)	0.85952	0.91597
AQAM	**-0.95295**	0.92987

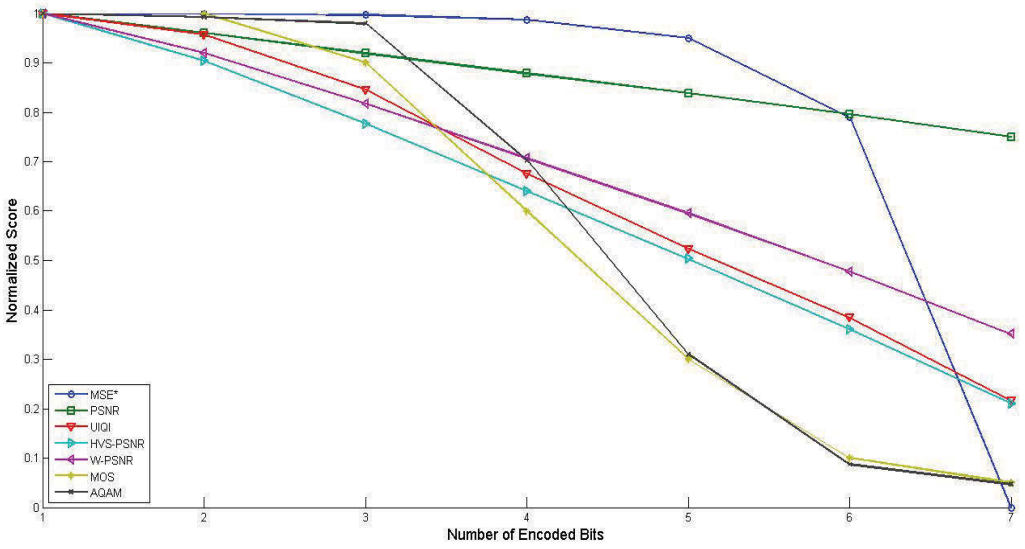

Fig. 7.3: Normalized image metrics with subjective evaluation

by measuring how well an algorithm's predictions correlates with the MOS values. SROCC was employed to assess prediction monotonicity. Thereafter, the prediction monotonicity specifies how well an algorithm predicts the rank ordering of the opinion scores.

The overall PLCC results are obtained from the experiment for the test images and are presented in the scatter plot graph in Figure 7.4. FromFigure 7.4, it is clearly seen that PLCC of PSNR, SSIM, and UIQI metric were positively correlated with MOS. While, the scatter plot graph of AQAM shows a negative correlation between these two variables. The results in Table 7.2 depict a value which is almost equal to -1. From this point of view, we can conclude that the AQAM metric has the highest correlation with MOS

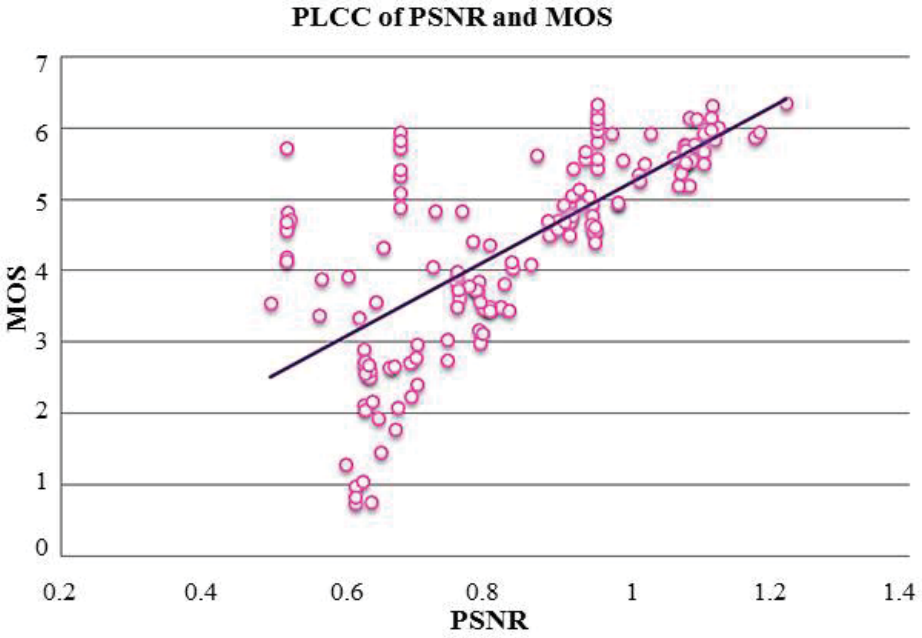

Fig. 7.4: PLCC of PSNR and MOS

readings compared to the other metrics. The main reason why the graph is negative correlates to how the AQAM metrics are calculated. From this it is concluded that the lower the quality of an image, the higher is the AQAM score. Meanwhile, MOS assigns a lower score for lower image quality and a higher score for better image quality. It is seen that the AQAM demonstrated high prediction performance because of the two modeling strategies used by the HVS and by adapting these strategies based on the amount of distortion.

Moreover, Figure 7.3 illustrates the relationship between PSNR, MSE, wPSNR, PSNR-HVS, UIQI and AQAM with MOS based on 500 observers. Most of the metrics deliver good results when the number of encoded bits were low. However, with the increase of the encoded bits, wPSNR, UIQI and PSNR-HVS follow the MOS trajectory in some degree while AQAM perfectly match the MOS.

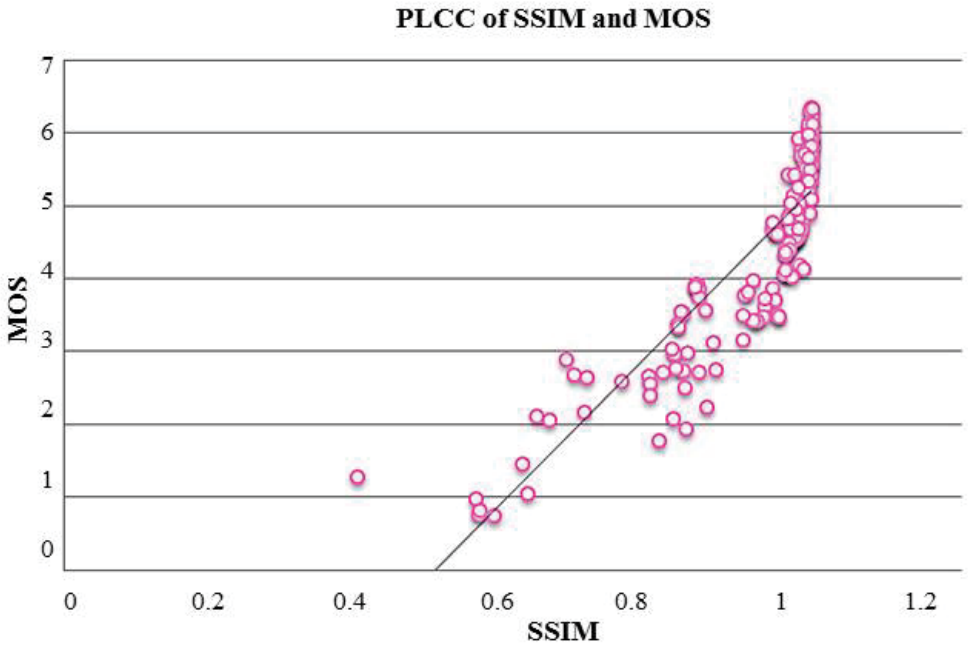

Fig. 7.5: PLCC of SSIM and MOS

7.4 Conclusion

In conclusion, the work presented in the Chapter depicts a simple method used in image quality assessment; it accounts for the most significant features regarding image structural data, the edge point and intensity. From the research conducted, the AQAM method proved to be efficient in the comparative analysis with the other three publicly available image quality assessment databases.

Furthermore, the overall capability of the image quality index (IQM) to predict the quality of image depends on the type of image content and also the level of degradation present. Each IQM has its limitation and strength on estimating image quality. On the other hand AQAM metric provides an excellent correlation with MOS based on PLCC whilst SSIM is the best performing algorithm based on SROCC. The PSNR metric gave the poorest result using both SROCC and PLCC. From the analysis, we conclude that the best metric for the method that uses the properties of HVS is achieved

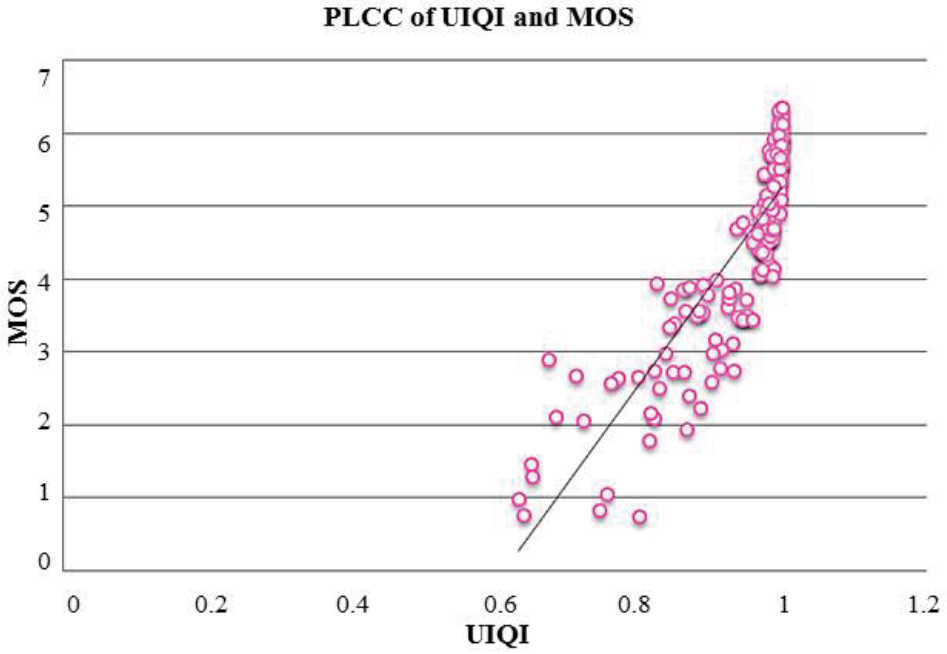

Fig. 7.6: PLCC of UIQI and MOS

through AQAM whereas SSIM is the best method based on the principle of image structure. Alternatively, the performance of SROCC for SSIM is the best, the SROCC of AQAM is acceptable and very close to SSIM performance. It was seen that there were strong monotonic correlations between AQAM and SSIM with MOS. Both of the metrics also demonstrated that they could perform as well as a subjective evaluation process in assessing image quality.

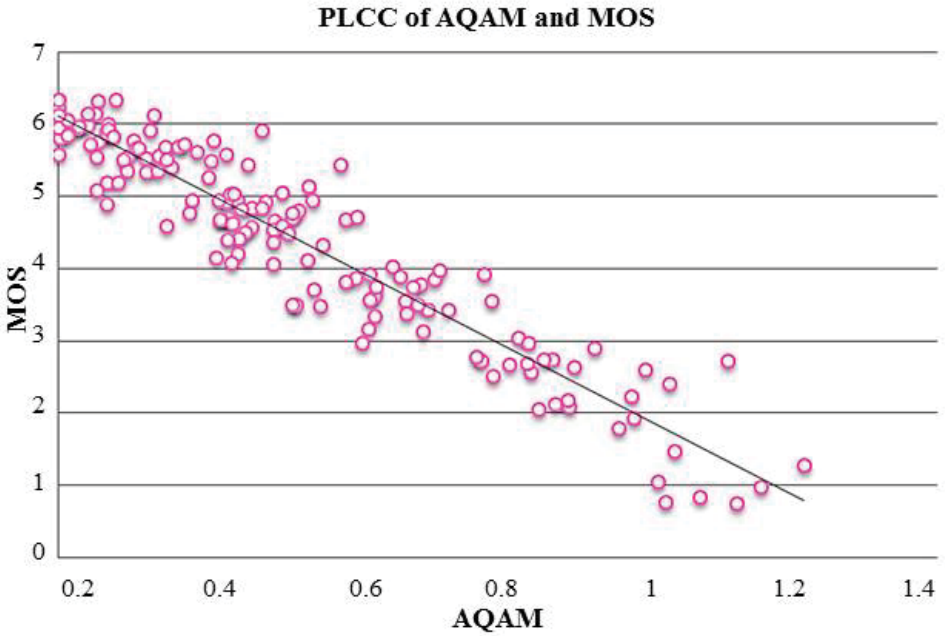

Fig. 7.7: PLCC of AQAM and MOS

Chapter 8

Conclusions and Future Work

8.1 Overview

Future research directions are presented and research conclusions are summarized in this Chapter. The research summary is the result of chapters where research contributions are discussed.

The most important aspects of the stegnographic technique are data capacity and imperceptibility. These two primary factors of digital steganography methods have been addressed and improved experimentally in this thesis. The research goal was to demonstrates effective solutions to address the problem of embedding large payload capacity with minimum distortion delivering multi dimentional information in multimedia objects. In order to improve imperceptibility and enhance steganographic capacity, it is preferred to use potentially all available space of an image to store different messages. A novel steganographic methods have been proposed in this thesis based on the research hypothesis. For enhancing imperceptibility of spatial domain, the method was rely upon a background of edge detection and vision science research. For improving data embedding capacity in frequency domain, the method suggest perceptual threshold for each coefficient. The issue of estimating an accurate embedding rate have been solved using image complexity based on the weaknesses of HVS. A new predictive metric to assess the steganography image imperceptibility have been developed to objectively

measure the stego image quality in a proper time and cost. The development of an image sharing application based on steganography was one of of this thesis objectives to show the effectiveness of steganography. Lastly, important research avenues of future are suggested that would offer more progress to this major area of research.

8.2 Research Findings

Below are the outcomes towards achieving the research aim.

8.2.1 Increase in Capacity of Edge Based Steganography

A high embedding rate and high imperceptibility was achieved by innovative proposed method, validated by the experimental results. The Human Visual System (HVS) in edge regions is less sensitive; for this reason embedding of meta-data was done using edge components. However, since the embedding rate is very limited by the edge-based-steganographic, weaknesses of the Human Visual System (HVS) and Genetic Algorithm (GA) were used as a new idea for the purpose of optimizing the embedding capability in edge portions in this task. The output of simulation test showed that the proposed method provide high quality stego images with minimum distortion along with low and high embedding capacity as indicated on the research hypothesis. Detection of hidden information statically was reasonably resisted and provided the addition of non-linear data distribution.

8.2.2 Define a Perceptual Threshold for Transform Domain

The human visual system (HVS) was used for the purpose of hiding integrated data to the on-hand model to improve the wavelet-based steganographic methods and to resolve selection of proper embedding coefficient with minimum degradation. Based on the contents of the cover image, a balance is achieved with the help of HVS in relation to the capacity of perceptually mapping secret imperceptible data. In order to increase imperceptibility

and robustness of the model, an evolutionary algorithm is used; and for the purpose of finding and hiding strength at the optimum level, and for all coefficients that algorithm are applied. Furthermore, a fitness function was applied to arrive at possible solutions with the help of human observation characteristics. High levels of stability was seen among different characteristics related to time computation, selectability, and payload capacity. The experimental results in Chapter 5 indicate that not only high imperceptibility could be achieved but also ensuring a high embedding rate as demonstrated on the research hypothesis.

8.2.3 Estimate Embedding Rate

The hiding capacity of a digital image's components is the main concern of steganography by identifying the quantity of information which could be hidden without noticeable distortions. Maintaining robustness is highly desirable. The concept of applying HVS to embed capacity through image complexity is a new method presented in this thesis. An estimation of optimum capacity for steganography was proposed by taking into consideration the characteristics of HVS. Watson's Perceptual Model is utilized through the cover image contents. Also, the Genetic Programing was used in optimizing the contrast sensitivity as well as the texture masking of selected coefficients, luminance masking and their contrast. This was done to perceptually map the obtained data based on the cover image's contents and as a result, paved the way for obtaining improved results.

8.2.4 Design an Anticipatory Quality Assessment Metric

The work examined the suitability of most existing objective metrics. It was found poor correlation between objective and subjective assessment, and may fail to accurately evaluate the performance of a steganography algorithm. Hence, it is essential to develop a mathematical metric to simulate the human perception in an acceptable time and cost. Anticipatory Quality Assessment Metric (AQAM) developed to objectively assess the stego image in a way

that simulate the judgment of human perception. AQAM method proved to be an efficient and very close to the subjective evaluation.

8.2.5 Develop a Steganographic Image Sharing App (Case Study)

The capability of steganographic approaches was demonstrated by applying it in a photo App application. Key features of the application are that it is attractive and functional to end users, photo takers; and viewers of the photo. Many tasks can be performed with the help of this application. It is envisaged that they can: create an account; post and share pictures; comment; and search other photos.

This case study emphasizes the development and implementation of a method, within a single image which embeds several hidden messages for the purpose of provide advance data structure of multimedia as shown in the Annex A. . Currently, there are many methods for the same purpose but a key limitation is that storage is very limited, which in turn limits the number of messages. However, the performance is to use potentially use all available space of an image to store different messages.

8.3 Research Contribution

Various new models have been developed and published by a number of indexed publications in high-impact journals and peer-reviewed conferences. The following are the research papers that have been published to achieve the research aim and objectives.

- **Digital Multimedia Archiving based on Optimization Steganography System**, published in *Asia-Pacific Conference on Computer Aided System Engineering (APCASE),* (2014).

The paper provides a mechanism to increase the capacity of spatial domain using score matrix as the method for carrying out the mapping function

procedure. The combination of the secret image and cover image is assessed with the help of the so-called matrix M. To demonstrate the significance of maintaining the cover pixel values at the same level, fewer alterations must be made to the cover image.

- **Bio-informatics with Genetic Steganography Technique**, published as a book chapter in C*omputational Intelligence and Efficiency in Engineering Systems* (2015), Volume 595 of the series Studies in Computational Intelligence pp: 333-345.

The paper utilizes the idea of using score matrix and integrating it with DNA Computing and QR coding. DNA matrix has been used to represent the secret message. After that DNA matrix converted to QR (Quick Response) representation that offers a broad scope of practical usage. In addition, the paper provides an idea of choosing the optimal locations of the QR in order to obtain rightmost position. A new system based on the genetic algorithm has been developed.

- **Hyper Edge Detection with Clustering for Data Hiding,** published in *Journal of Information Hiding and Multimedia Signal Processing* (2016).

The paper presents an effective edge detection method based on gradient, 9x9 mask of LOG and zero crossing in combination with clustering to classify the image to edge and non-edge regions. Different amounts of secret message will be hidden in each cluster after the detection of the edge regions. It declares the stability between stego image imperceptibility and high payload capacity.

- **Data Hiding Based on Intelligent Optimized Edges for Secure Multimedia Communication** published in *Journal of Networks* (2015).

The paper proposes an improvement of the edge-based steganography by incorporating edge detection and vision science research. A Genetic Algorithm

that uses the human visual system characteristics approach for data hiding is presented. Primarily, the approach applies Differences of Gaussian detector which closely resembles the human visual behavior. Secondly, the edge profusion indicates the level of threshold visibility with the help of Genetic Algorithm training. The suggested solution uses Contrast Sensitivity Function (CSF) which produces the edges based on the size of the embedding information.

- **EA based Heuristic Segmentation for Efficient Data Hiding,** *published in International Journal of Computer Applications* (2015).

The paper provides a heuristic approach of choosing the right-most regions for embedding to ensure minimum changes of the stego object. Then, different percentages of secret data will be hidden on the cluster based on the characteristic region. Therefore, the sharp edge region will hide more data while the smooth will hide data. The proposed approach use K-mean clustering to categorized the segmentation and then genetic algorithm will be used to boost the PSNR (peak signal to-noise ratio) value while optimizing high capacity information.

- **The Use of HVS to Estimate Perceptual Threshold for Imperceptible Steganography,** published in the *30th International Conference on Image and Vision Computing New Zealand* (IVCNZ 2015).

The paper presents presents a novel method aimed towards a selection of perceptual embedding threshold in Discrete Wavelet Transform using human visual system characteristics and Genetic Algorithm. This method included an introduction of an optimization model by maintaining a correlation between neighboring areas of the image and the different parts of the object.

- **Estimating Optimum Embedding Capacity based on Image Complexity Using Human Visual System,** submitted to *Multimedia Tools and its Applications Journal* (2016).

The paper considers visual complexity as an important factor to estimate the payload capacity. The propose method estimates image complexity using Human Visual System.

- **Objective Quality Metrics in Correlation with Subjective Quality Metrics for Steganography,** published in *Asia-Pacific Conference on Computer Aided System Engineering* (APCASE), (2015)

The paper provides a review of the existing evaluation metrics that are used to assess the quality of steganography. The examination of the correlation between the existing objective and subjective metrics is also conducted. Pixel differences metrics have a poor correlation with the subjective metrics. Hence the HSV based metrics have better correlation than pixel metrics.

- **Anticipatory Quality Assessment Metric for Steganography Imperceptibility Evaluation,** submitted to *Journal of Information Hiding and Multimedia Signal Processing (JIH-MSP),* (2016)

The paper proposes a predictive quality metric that is objectively assess the image quality on a similar way to the subjective evaluation. The paper focuses on predicting the subjective quality using anticipatory objective. Anticipatory Quality Assessment Metric (AQAM) is an objective assessment metric simulates the judgment of human perception. The primary objective of this paper is to develop a systematic method of using HVS for image quality assessment.

8.4 Future Directions

The tradeoffs between robustness, capacity of payload and imperceptibility in steganographic applications intelligent techniques have shown to be valuable. The future directions which could have an impressive impact on the making of the proposed scheme and embedding more imperceptible with high embedding capacity are discuss below:

The selection of DWT sub-bands, decomposition levels of DWT, and coefficients of DWT for the purpose of embedding messages should be intelligently picked rather finding an optimum level in order to hide the message in wavelet coefficients. The intelligent techniques like GP, PSO, and ACO could achieve this. DWT coefficients should be considered in this way for steganography, rather than using selected band coefficients that are predefined. Different frequency bands in DWT are subjected to many unintentional / intentional attacks, so the resistance of steganographic images against them could be improved by the proper selection of coefficients besides strength alteration. Importantly, the HVS temporal masking phenomenon could be realized as a possible extension of the method. The temporal contrast threshold for a specific temporal frequency is increased because of a variation masking the temporal frequency, which is different in such a scheme. In the temporal direction, the contrast masking would be interpreted as a HVS phenomenon. Because of the increase in contrast threshold, robustness of a steganography scheme in comparison to proposed scheme would be considered better.

In order to prevent attackers to extract and find hidden messages from pictures, future developments of the Photo App is suggested. The represent of the function expansion as a multi-user secret messaging system is recommended. The steganographic method for the purpose of embedding messages would be changed if something was detected.

The photo sharing app can be applied to Facebook or Instagram applications with the development of user account system. It would be useful for Google and other potential web-wide search engines if market was captured by the Photo App. Implementation of a similar system of embedding information about a picture within itself will also influence other developers.

Annex A: Steganographic Multimedia Sharing App User Interface

A1. Overview

The development of an image sharing application is the aim of this project which uses steganography to embed messages into the image that is readable to users through a separate website. Features of the application are attractive to both end users; photo takers and the viewers of the photo. Many tasks users can carry with the help of this application, like; they can create account, post and share pictures, can comment on them and search other photos.

This study is emphasized on the development and implementation of a method, within a single image which embeds several stegnographically hidden messages. Currently, there are many methods for the same purpose but that stores very limited number of messages. However, through this project it is preferred to use potentially all available space of an image to store different messages.

Use of an application with steganographical method is also under the scope of this project, which will give insight into the practicality. Development of prototype, a photo app will be discussed in this section. A number of features are implemented by prototype where steganography is utilized, showing real world working. The design requirements of the application are high such as Architecture and low such as class diagrams.

A2. User Interface Design

The functionality of the user interface and its relation towards the Software Requirements Specifications will be discussed in this section

A2.1 Photo App

Many functions could be accessed from one screen photo app interface. Primarily it was designed for PC or tablet to enable user have quick access over all the functions of the application. Many functions would include, picture taking, picture editing, addition of message on the picture and picture uploading. Photo App user interface during normal function has been shown in Figure 8.1, when a picture has been taken.

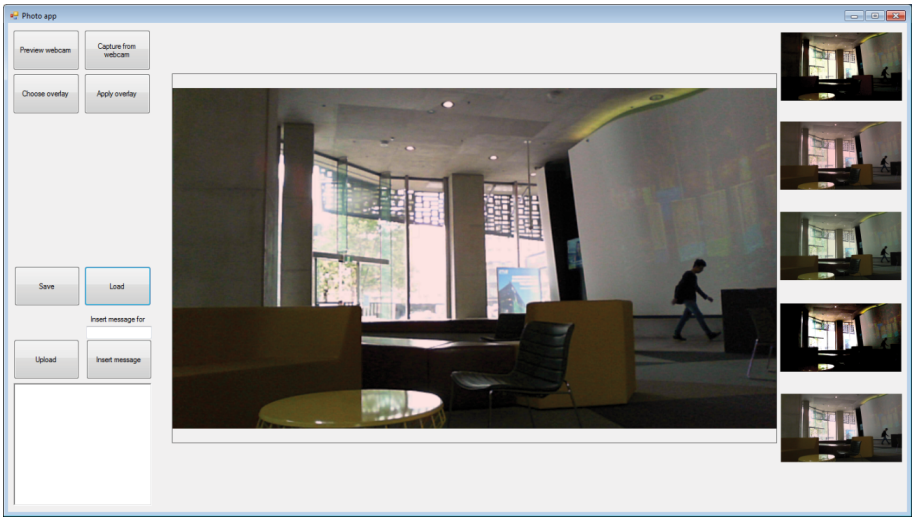

Fig. 8.1: Normal Photo App Screen

A2.2 Taking a picture

As shown in Figure 8.2, two highlighted buttons in the top left corner are used for taking a picture. To check how it looks, user is required to click on 'preview webcam" button. When they are satisfied with the click then they can proceed ahead by pressing "Capture form the webcam" and take a final picture than may get start with editing

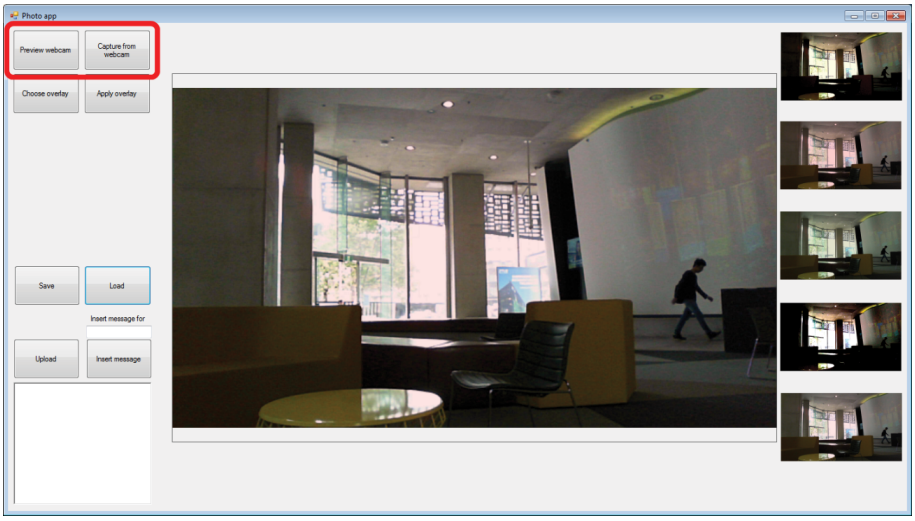

Fig. 8.2: Taking a picture

A2.3 Filters

Photo filters are on the right side of the interface highlighted in the red colour, as shown in Figure 8.3. Filter could be used by user by one click on it and it will change the photo. Filters are considered as basic feature in prototypes, though it could be advanced in future. The image could be restored to its original form when user selects the last filter.

A2.4 Inserting a message

As shown in Figure 8.4, the highlighted controls in the bottom left corner are used for inserting a message. The message is typed in the text box by the user which user wishes to attach with the image by clicking Insert message. This can be done multiple times for multiple users. A scroll bar is used up and down to fit longer messages in the text box. Private message is done in the same way as normal message.

A2.5 Applying an overlay

An image could be pasted over the top of the photo with the help of overlay as shown in Figure 8.5 by selecting one and choosing where to place it. For

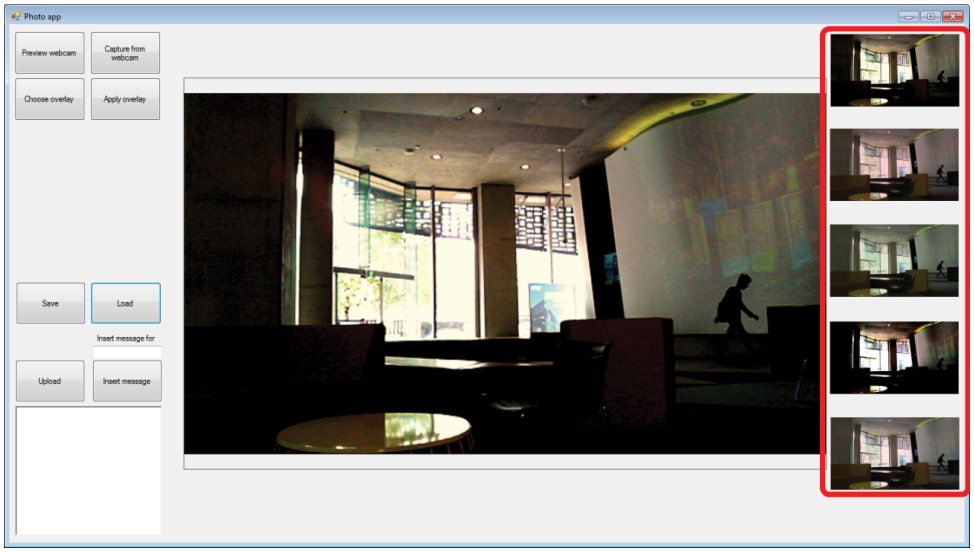

Fig. 8.3: Photo App Filters

choosing and applying an overlay over the photo, there are many buttons which is shown in labeled "1" red box. A movable representation of the overlay that is done by the user is shown in labelled "2", red box. "Choose Overlay" button is clicked by the user to apply, select, and move to the place of choice of user, and then finally "Apply Overlay" button is clicked. A number of overlays applied to the image could be seen in the labelled "3" red box.

A2.6 Saving and loading images

The photo taken by the user could be saved by clicking on "Save" button and also photo could be loaded by clicking on "Load" button", and photo could be selected by users of choice for the purpose of loading into the application. This way pictures could be modified taken by users at a later date, or images could be uploaded by the users which are not taken by their cameras, as illustrated in Figure 8.6.

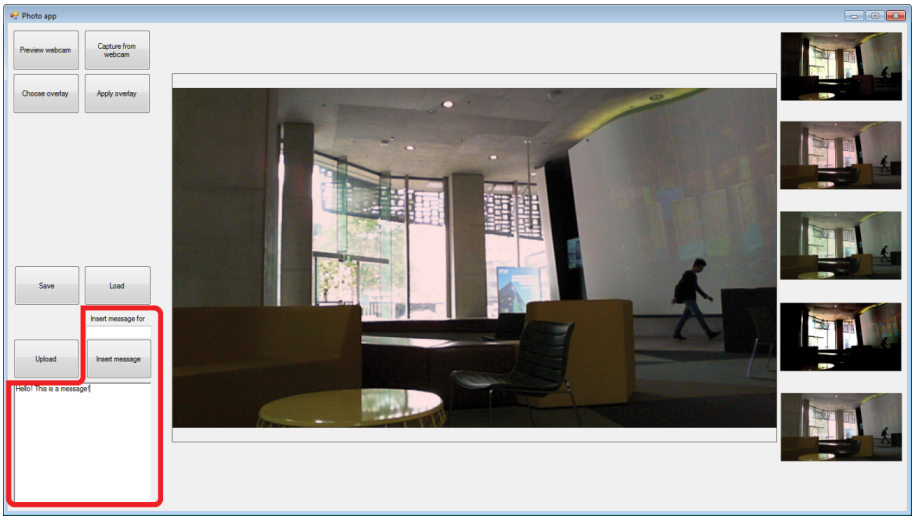

Fig. 8.4: Inserting a message

A2.7 Uploading an image

Figure 8.7shows, images could be uploaded by user to gallery via Photo App. Upload could be done when user has made changes to the photo and inserted messages that user want. The process may take some time, which depends on the speed of internet connection of the user.

The user can upload images to the Gallery via the Photo App (Figure 8.7). Once the user has made the changes to the photo that they want and inserted the messages they want, they can click the "Upload" button to upload the image. This may take a few seconds, depending on the speed of the user's internet connection.

A2.8 Gallery

Previously uploaded pictures could be previewed by the user, is shown in Figure 8.8. Option for the user to login is shown in labelled "1" red box. When users click this, they will be directed to login.php. Users are made enabled for search of images according to the terms of their choice they input. This is done by search bar in red box labelled "2". Results are then displayed in Search.php to users by clicking, "submit". Image preview example is shown

Fig. 8.5: Applying an overlay

in red box labelled "3". Users are taken to Photo.php by clicking on one of these previews which displays full size image where messages are also attached.

A2.9 Login

Where the user can log in to account is illustrated in Figure 8.9. Users will be able to view messages those are directed them in LoggedInGallery.php, once after they enter details like; username and password and click "Submit". Figure 8.10, shows the option of logout instead of login to the account other than this Gallery.php is same almost as LoggedInGallery.php. Users will be logged out when they click on "Logout" button which is highlighted in red coulur and finally will be taken to Gallery.php

A2.10 Search

Where a user is taken after they make a search is shown in figure Figure 8.11. The search engine is a simple mysql query where phrase contained image is looked for, which is a public "message" by user. To get the messages of the

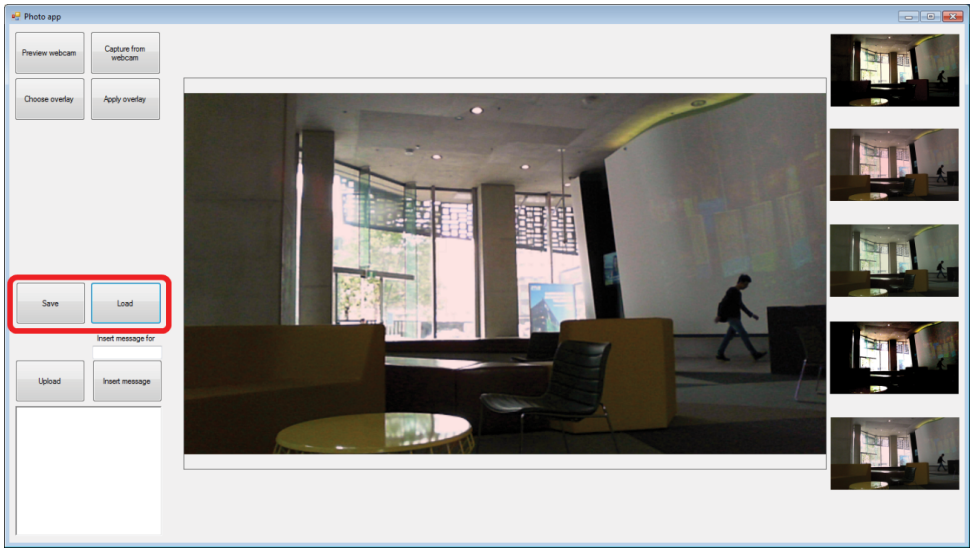

Fig. 8.6: Saving and loading images

public, Index.php is used by server, when images are uploaded and finally added to mysql database. It functions almost same as gallery.

Search of images is possible with the help of above function without storing results in a database. A number of images could be searched with no previous homework through this setup. However, this technique is considerably slower than a database is searched, and for that reason, searching in big scale applications, like a web-wide picture search engine, would be time consuming so prototype, an indexing method is suitable.

A2.11 Register

User can register with a new account which is shown in figure Figure 8.12. Once the name, email address, username and password is entered by user then it will be possible for users to view messages directed to them once they are login to Login.php.

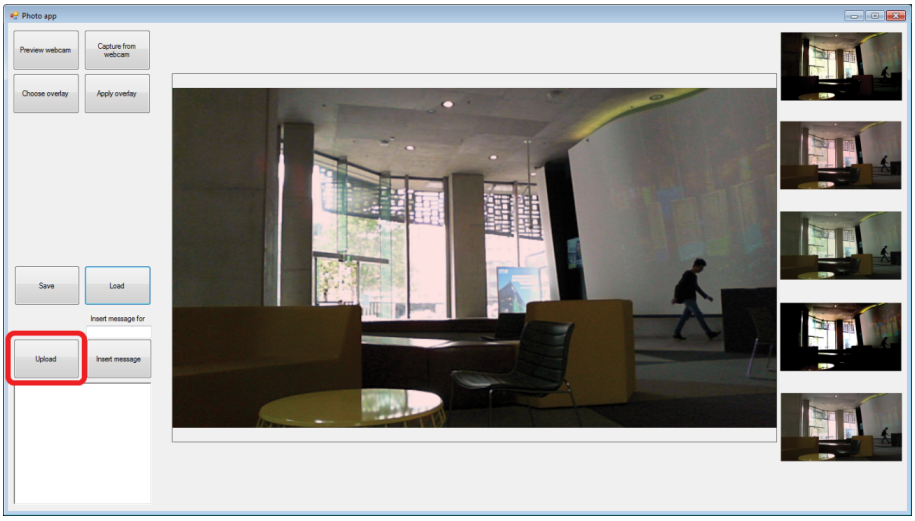

Fig. 8.7: Uploading an image

A3. Conclusion

The power of the steganography as a powerful multimedia tool is clearly shown in this case study which is a successful implementation of the goal of this project. Software Requirement Specifications are fulfilled by Photo App in which utilization of steganography is exposed. Users are made enable due to Photo App for editing photos, adding messages, uploading to gallery where images could be viewed by other users, reading of the messages and finally searching of the images.

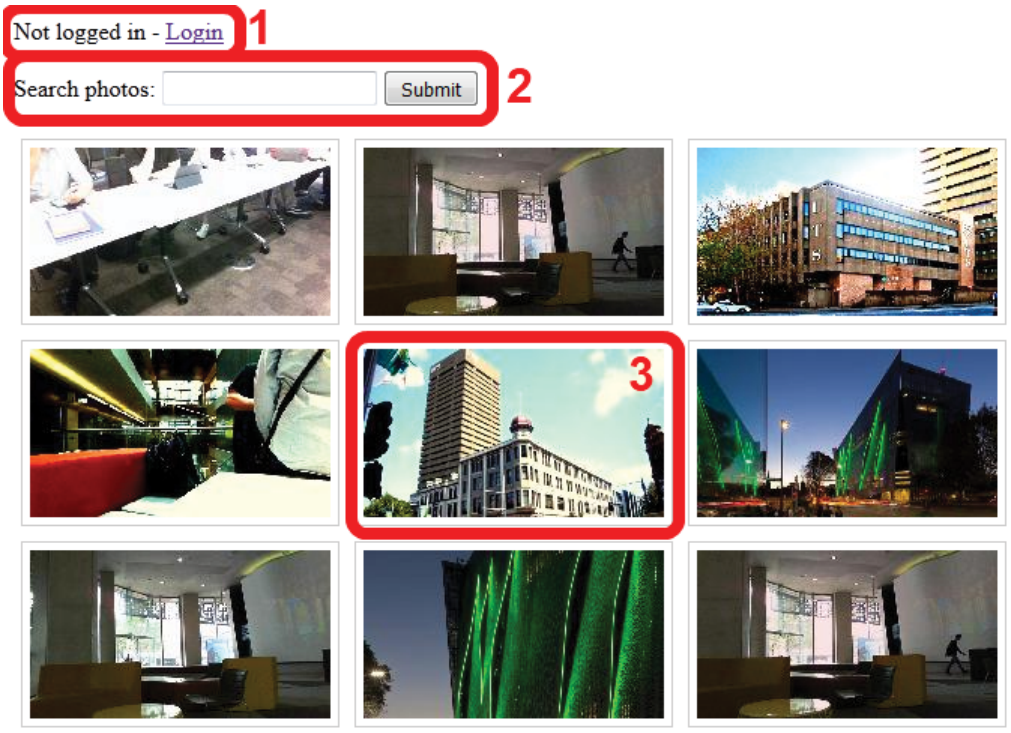

Fig. 8.8: Gallery.php

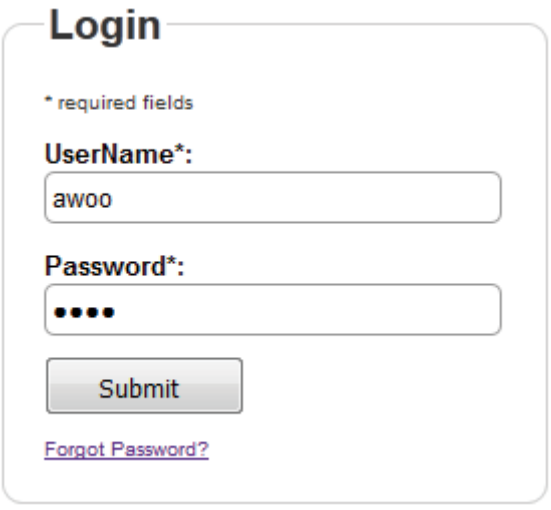

Fig. 8.9: Login.php

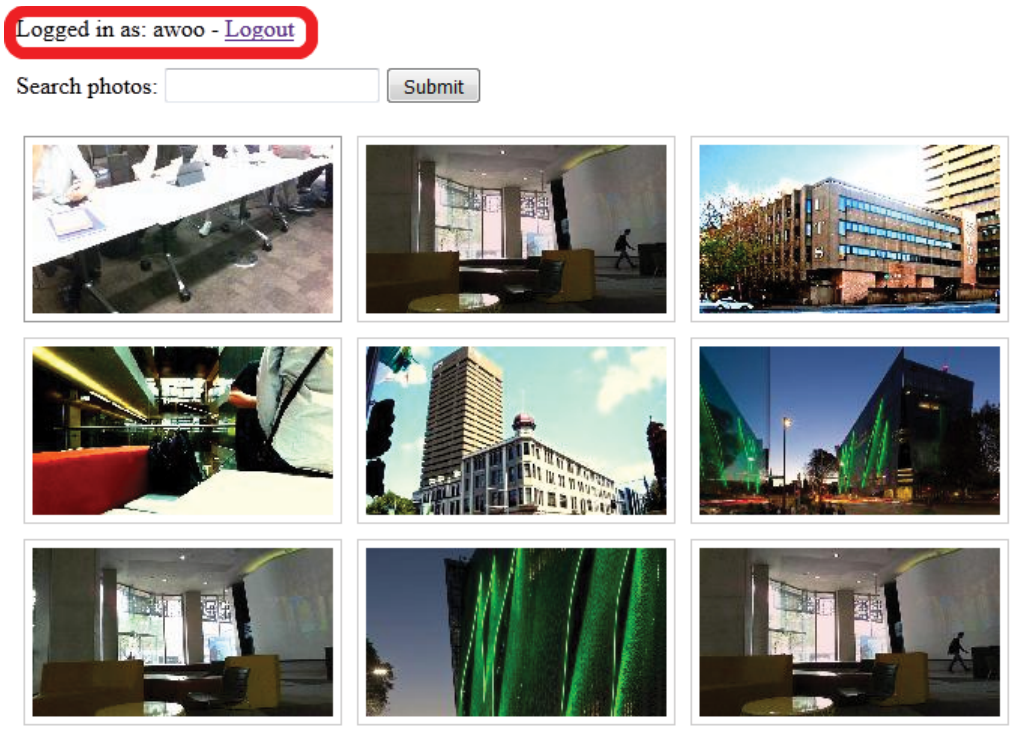

Fig. 8.10: LoggedInGallery.php

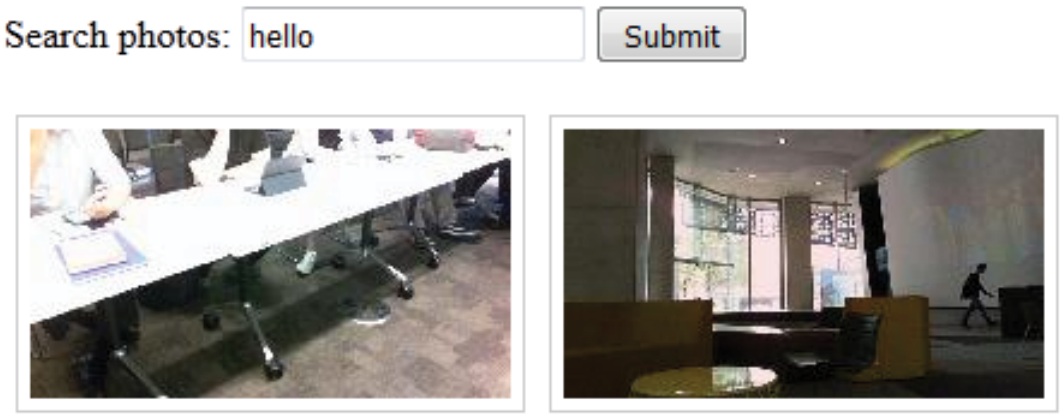

Fig. 8.11: Search.php

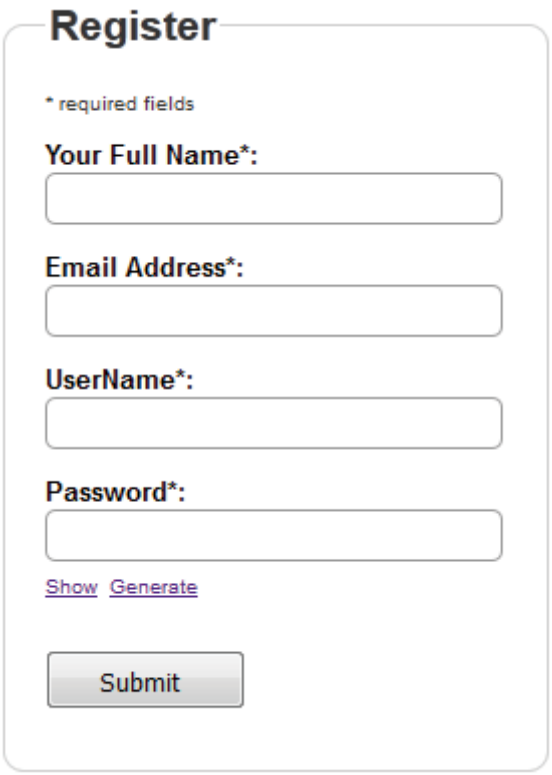

Fig. 8.12: Register.php

Bibliography

Abdul, W., Carré, P. and Gaborit, P. (2010). Human visual system-based color image steganography using the contourlet transform, *IS&T/SPIE Electronic Imaging*, International Society for Optics and Photonics, pp. 75410U–75410U.

Ahmidi, N. (2008). A Human Visual Model for Steganography, *On Canadian Conference In Electrical and Computer Engineering, CCECE 2008.*

Ahumada Jr, A. J. and Peterson, H. A. (1992). Luminance-model-based dct quantization for color image compression, *SPIE/IS&T 1992 Symposium on Electronic Imaging: Science and Technology*, International Society for Optics and Photonics, pp. 365–374.

Al-najjar, Y. A. Y. and Soong, D. C. (2012). Comparison of Image Quality Assessment: PSNR, HVS, SSIM, UIQI, *International Journal of Scientific and Engineering Research* **3**(8): 1–5.

Arora, S. and Anand, S. (2013). A Proposed Method for Image Steganography Using Edge Detection, *International Journal of Emerging Technology and Advanced Engineering* .

Artz, D. (2001). Digital Steganography: Hiding Data within Data, *IEEE Internet Computing* (5): 75–80.

Babu, R. V. (2005). An HVS-Based No-Reference Perceptual Quality Assessment of Jpeg Coded Images Using Neural Networks , *International Conference on Image Processing*, pp. 4–7.

Bae, H. J. and Jung, S. H. (1997). Image retrieval using texture based on dct, *International Conference on Information, Communications and Signal Processing*, IEEE, pp. 1065–1068.

Banzhaf, W., Nordin, P., Keller, R. E. and Francone., F. D. (1998). *Genetic Programming: An Introduction*, San Francisco: Morgan Kaufmann.

Barni, M., Bartolini, F., De Rosa, A. and Piva, A. (1999). Capacity of the watermark channel: How many bits can be hidden within a digital image, *Electronic Imaging'99*, International Society for Optics and Photonics, pp. 437–448.

Barni, M., Bartolini, F., Rosa, A. D. and Piva, A. (2000). Capacity of full frame DCT image watermarks, *IEEE Transactions on Image Processing, 9, no. 8* pp. 1450–1455.

Barten, P. G. (1999). Contrast Sensitivity of The Human Eye and Its Effects on Image Quality, *SPIE Press* **72**.

Basu, A., Saha, A., Das, J., Roy, S., Mitra, S., Mal, I. and Sarkar, S. K. (2015). *Advances in Intelligent Systems and Computing*, Vol. 328, Springer International Publishing.

Bracamonte, J., Ansorge, M. and Pellandini, F. (1997). Adaptive Block-Size Transform Coding for Image Compression, *IEEE International Conference on Acoustics, Speech, and Signal Processing* **4**.

Cachin, C. (1998). An information-theoretic model for steganography, pp. 306–318.

Canny, J. (1986). A Computational Approach to Edge Detection, *IEEE Transactions on Pattern Analysis and Machine Intelligence* **8**(6).

Chan C. K. and Chan L. M. (2004). Hiding Data in Image By Simple LSB Substitution, *Pattern Recognition* **37**: 469–467.

Chang, C. C., Lin, C. C., Tseng, C. S. and Tai, W. L. (2007). Reversible Hiding in DCT-Based Compressed Images, *Information Sciences 177,* **113**: 2768–2786.

Chang, C. C., Lin, C. and Wang, Y. (2006). New Image Steganographic Methods Using Run-Length Approach, *Information Sciences* (176): 3393–3408.

Chang C. C., Y., H. J. and S, C. C. (2003). Finding Optimal Least-Signification-Bit Substitution in Image Hiding By Dynamic Programming Strategy, *Pattern Recognition* **36**: 1583–1595.

Cheddad, Abbas, Condell, J., Curran, K. and Kevitt., P. M. (2010). Digital image steganography: Survey and Analysis of Current Methods, *Signal processing* **90**(3): 727–752.

Chen, C. P., Chen, M. C., Agaian, S., Zhou, Y., Roy, A. and Rodriguez, B. M. (2012). A Pattern Recognition System for JPEG Steganography Detection, *Optics Communications 285,* (21): 4252–4261.

Chen, W. J., Chang, C. C. and Le, T. H. N. (2010). High Payload Steganography Mechanism Using Hybrid Edge , *Expert Systems with Applications* **37**: 3292–3301.

Chou, C. H. and Li, Y. C. (1995). A perceptually tuned subband image coder based on the measure of just-noticeable-distortion profile, *IEEE Transactions on Circuits and Systems for Video Technology* **5**(6): 467–476.

Chu, R., You, X., Kong, X. and Ba, X. (2004). A dct-based image steganographic method resisting statistical attacks, *IEEE International Conference on Acoustics, Speech, and Signal Processing, Proceedings.(ICASSP'04)*, Vol. 5, IEEE, pp. V–953.

Cole, E. and Krutz, R. D. (2003). *Hiding in plain sight: Steganography and the Art of Covert Communication*, John Wiley & Sons, Inc.

Cox, I. J., Miller, M. L., Bloom, J. A., Fridrich, J. and Kalker, T. (2008). *Digital Watermarking and Steganography-Second Edition*, burlington edn.

Cox, I. J., Miller, M. L. and McKellips, A. L. (1999). Watermarking As Communications With Side Information, *Proceedings of the IEEE 87, no. 7*, pp. 1127–1141.

Dasguptaa, K., Mondalb, J. K. and Duttac, P. (2013). Optimized Video Steganography using Genetic Algorithm (GA), *Procedia Technology* **10**: 131–137.

de Garis, H. (1993). Evolvable hardware genetic programming of a darwin machine, *Artificial Neural Nets and Genetic Algorithms*, Springer, pp. 441–449.

Dosselmann, R. and Yang, X. D. (2011). A Comprehensive Assessment of The Structural Similarity Index, *Signal, Image and Video Processing* **5**(1): 81–91.

Egiazarian, K., Astola, J., Ponomarenko, N., Lukin, V., Battisti, F. and Carli, M. (2006). A New Full-Reference Quality Metrics Based on HVS, *CD-ROM Proceedings of The Second International Workshop on Video Processing and Quality Metrics*, pp. 2–5.

Enroth-Cugell, Christina and Robson, J. G. (1966). The Contrast Sensitivity of Retinal Ganglion Cells of the Cat, *The Journal of Physiology 187, no. 3* pp. 517–552.

Erez, U., Shamai, S. and Zamir, R. (2005). Capacity And Lattice Strategies For Canceling Known Interference, *IEEE Transactions on Information Theory* **51**(11): 3820–3833.

Farag, H. and El-Khamy, S. E. (2014). Blind key steganography based on multilevel wavelet and csf, *International Refereed Journal of Engineering and Science (IRJES)* .

Fard, A. M., Akbarzadeh T, M. R. and Varasteh A., F. (2006a). A New Genetic Algorithm Approach for Secure JPEG Steganography, *In 2006 IEEE International Conference on Engineering of Intelligent Systems.*

Fard, A. M., Akbarzadeh T, M. R. and Varasteh A, F. (2006b). A new genetic algorithm approach for secure jpeg steganography, pp. 1–6.

Ghasemi, E., Shanbehzadeh, J. and Fassihi, N. (2012). High Capacity Image Steganography Based on Genetic Algorithm and Wavelet Transform, *In Intelligent Control and Innovative Computing*, pp. 395–404.

Goel, M. M. B., Chaudhari, M. M. and Gode, M. S. A. (2014). A review on data hididng using steganography and visual cryptography, *International Journal of Engineering Development and Research*, Vol. 2, IJEDR.

Gu, Q. and Gao, T. (2009). A Novel Reversible Watermarking Algorithm Based on Wavelet Lifting Scheme, *ICIC Express Letters 3, no. 3* pp. 397–402.

Hashad, A., Madani, A. S. and Wahdan, A. E. M. A. (2015). A Robust Steganography Technique Using Discrete Cosine Transform Insertion, *Enabling Technologies for the New Knowledge Society: ITI 3rd International Conference on Information and Communications Technology.*

Hempstalk, K. (2006). Hiding Behind Corners Using Edges in Images For Better Steganography, *Hamilton: Lotus Press.* .

Holland, J. (1992). *Adaptation in Natural and Artificial Systems: An Introductory Analysis with Applications to Biology*, Control and Artificial Intelligence. second edition. Cambridge, MA: MIT Press.

Hussain, M., Wahab, A. W. A., Anuar, N. B., Salleh, R. and Noor, R. M. (2015). Pixel value differencing steganography techniques: Analysis and open challenge, *IEEE International Conference on Consumer Electronics-Taiwan (ICCE-TW)*, pp. 21–22.

Ji, X.-y., Bai, S., Guo, Y. and Guo, H. (2015). A new security solution to jpeg using hyper-chaotic system and modified zigzag scan coding, *Communications in Nonlinear Science and Numerical Simulation* **22**(1): 321–333.

Jithesh, K. and Kumar, A. S. (2010). Multi layer information hiding a blend of steganography and visual cryptography.

Jung, S. W. and Ko., S. J. (2011). A New Histogram Modification Based Reversible Data Hiding Algorithm Considering The Human Visual System, *Signal Processing Letters, IEEE* **18**(2): 95–98.

Katzenbeisser, S. and Petitcolas, F. A. P. (2000). *Information Hiding Techniques for Steganography and Digital Watermarking*, Artech House.

Ker, A. (2005). Improved detection of LSB Steganography in Gray-scale Image, *Lecture Notes in Computer Science* pp. 97–115.

Khan, A., Mirza, A. M. and Majid, A. (2004). Optimizing Perceptual Shaping of a Digital Watermark Using Genetic Programming, *Iranian Journal of Electrical and Computer Engineering* **3**(2).

Kipper, G. (2004). *Investigator's Guide to Steganography*.

Kumar, R. (2013). HVS Based Steganography, *International Journal of Recent Technology and Engineering (IJRTE)* (2): 43–45.

Lee, I., Kim, J., Kim, Y., Kim, S., Park, G. and Park, K. T. (1994). Wavelet transform image coding using human visual system, *1994 IEEE Asia-Pacific Conference on Circuits and Systems*, IEEE, pp. 619–623.

Lee Rodgers, J. and Nicewander, W. A. (1988). Thirteen ways to look at the correlation coefficient, *The American Statistician* **42**(1): 59–66.

Lee, Y. K. and Chen, L. H. (2000). High Capacity Image Steganographic Model, *IEE Proceedings of Vision, Image and Signal Processing* **147**: 288–294.

Lee, Y. K. and Chen, L. H. (2003). Secure Error-Free Steganography for JPEG Artificial, Images, *International Journal of Pattern Recognition and Intelligence* (17): 967–981.

Li, Q., Yu, C. and Chu, D. (2006). A Robust Image Hiding Method Based on Sign On, Embedding and Fuzzy Classification, *The Sixth World Congress Intelligent Control and Automation, WCICA 2006,*, pp. 10050–10053.

Li, X. and Wang, J. (2007). A steganographic method based upon jpeg and particle swarm optimization algorithm, *Information Sciences* **177**(15): 3099–3109.

Li, Y., Zhu, H., Yu, R., Yang, G. and Xu, J. (2008). An Adaptive Blind Watermarking Algorithm Based on DCT and Modified Watson's Visual Model, *On International Symposium in Electronic Commerce and Security,*, pp. 904–907.

Lie, W. N. and Chang, L. C. (1999). Data hiding in images with adaptive numbers of least significant bits based on the human visual system, *International Conference on Image Processing*, Vol. 1, IEEE, pp. 286–290.

Lu, Y. h., Kong, J., Li, S. h. and Qin, J. (2007). An image steganographic method with noise visibility function and dynamic programming strategy on partitioned pixels, *International Conference on Computational Intelligence and Security Workshops*, IEEE, pp. 680–684.

Luo, W., Huang, F. and Huang, J. (2010). Edge adaptive image steganography based on lsb matching revisited, *IEEE Transactions on Information Forensics and Security* **5**(2): 201–214.

Malhotra, N. and Tahilramani, N. (2013). Survey On Information Hiding Techniques And Analysis of Quality Assessment Parameters, *International Journal of Emerging Technology and Advanced Engineering* **3**(12).

Mandal, J. (2000). A Genetic Algorithm based Steganography in Frequency Domain (GASFD), *India: Springer-Verlag* .

Mannos, J. L. and Sakrison, D. J. (1974). The Effects of a Visual Fidelity Criterion of The Encoding of Images, *IEEE Transactions on Information Theory* **20**(4): 525–536.

Marini, E., Autrusseau, F., Callet, P. L. and Campisi, P. (2007). Evaluation of Standard Watermarking Techniques, *Security, Steganography, and Watermarking of Multimedia Contents IX* **6505**: 1–10.

Marr, D. and Hildreth., E. (1980). Theory of Edge Detection, *Proceedings of the Royal Society of London B: Biological Sciences 207*, pp. 187–217.

Martin, M. B. (1999). *Applications of Multiwavelets to Image Compression*, PhD thesis, Virginia Tech.

Martin, R. and Cochran, D. (1994). Generalized wavelet transforms and the cortex transform, *Conference on Signals, Systems and Computers*, Vol. 2, IEEE, pp. 1105–1108.

Marvel, L. M., Jr, C. G. B. and Retter, C. T. .-. (1998). Reliable Blind Information Hiding for Images, *Second International Workshop on Hiding* **1525,**: 48–61.

Mohanty, A. K., Senapati, M. R. and Lenka, S. K. (2013). A novel image mining technique for classification of mammograms using hybrid feature selection, *Neural Computing and Applications* **22**(6): 1151–1161.

Moulin, P., Mihcak, M. K. and Lin, G. I. A. (2000). An Information-Theoretic Model For Image Watermarking And Data Hiding, *Image Processing* **3**: 667–670.

Nitin, Jain, Meshram, S. and Dubey, S. (2012). Image Steganography Using LSB and Edge Detection Technique, *International Journal of Soft Comput ing and Engineering (IJSCE)* **2**(3).

Nosrati, M., Hanani, A. and Karimi, R. (2015). Steganography in image segments using genetic algorithm, *Fifth International Conference on Advanced Computing and Communication Technologies*, IEEE, pp. 102–107.

Ohnishi, J. and Matsui, K. (1996). Embedding a Seal Into a Picture Under Orthogonal Wavelet Transform, *Proceedings of the Third IEEE International Conference on Multimedia Computing and Systems* pp. 514–521.

Osberger, W. and Maeder, A. J. (1998). Automatic identification of perceptually important regions in an image, *Fourteenth International Conference on Pattern Recognition*, Vol. 1, IEEE, pp. 701–704.

Pan, F., Jun Li, X. L. and Guo, Y. (2011). Steganography Based On Minimizing Embedding Impact Function and HVS, *In International Conference on Electronics, Communications and Control (ICECC)*, pp. 490–493.

Pereira, S., Voloshynoskiy, S. and Pun, T. (6). Optimal Transform Domain Watermark Embedding Via Linear Programming, *Signal processing 81* pp. 1251–1260.

Ponomarenko, N., Ieremeiev, O., Lukin, V., Egiazarian, K., Jin, L., Astola, J., Vozel, B., Chehdi, K., Carli, M., Battisti, F. et al. (2013). Color image database tid2013: Peculiarities and preliminary results, *4th European Workshop on Visual Information Processing*, IEEE, pp. 106–111.

Ponomarenko, N., Lukin, V., Egiazarian, K., Astola, J., Carli, M. and Battisti, F. (2008). Color Image Database For Evaluation of Image Quality Metrics, *IEEE 10th Workshop on Multimedia Signal Processing* pp. 403–408.

Prateek, P. S., Bharadwaj, S. and Gupta, V. B. (2012). A HVS based Perceptual Quality Estimation Measure for Color Images, *ACEEE International Journal on Signal and Image Processing (IJSIP)* **03**(01).

Rabah, K. (2004). Steganography- The Art of Hiding Data, *Information Technology Journal* **3**: 245–269.

Raja, K., Kumar, K., Kumar, S., Lakshmi, M., Preeti, H., Venugopal, K. and Patnaik, L. M. (2007). Genetic algorithm based steganography using wavelets, *Information Systems Security*, Springer, pp. 51–63.

Ramsey, P. H. (1989). Critical values for spearmans rank order correlation, *Journal of Educational and Behavioral Statistics* **14**(3): 245–253.

Roy, R. and Laha, S. (2015). Optimization of stego image retaining secret information using genetic algorithm with 8-connected psnr, *Procedia Computer Science* **60**: 468–477.

Sajasi, S. and Moghadam, A. M. E. (2015). An adaptive image steganographic scheme based on noise visibility function and an optimal chaotic based encryption method, *Applied Soft Computing* **30**: 375–389.

Shi, Y. (2005). Image Steganalysis Based on Moments of Characteristic Functions Using Wavelet Decompositions Prediction-Error Image and Neural Network, *Berlin: Springer-Verlag* .

Simra Pal Kaur and Singh, S. (2012). A New Image Steganography Based on 2k Correction Method and Canny Edge Detection, *International Journal of Computing and Business Research* (2229 - 6166).

Spector, L. (1997). A Comparison of Crossover and Mutation in Genetic Programming, *New York: Grin Verlag* .

Stoica, A., Vertan, C. and Fernandez Maloigne, C. (2003). Objective And Subjective Color Image Quality Evaluation For Jpeg 2000 Compressed Images, *International Symposium on Signals, Circuits and Systems, SCS* **1**: 137–140.

Su, C. C., Moorthy, A. K. and Bovik, A. C. (2015). Visual quality assessment of stereoscopic image and video: Challenges, advances, and future trends, *Visual Signal Quality Assessment*, Springer, pp. 185–212.

Tan, K. T., Ghanbari, M. and Pearson, D. E. (1998). An Objective Measurement Tool for MPEG Video Quality, *Signal Processing* (70): 279–294.

Trochim, W. (2014). Application of Genetic Algorithm in Steganograpy.

Tseng, H. W. and Chang, C. C. (2004). Steganography using JPEG-Compressed and Images , *The Fourth International Conference on Computer Information Technology* pp. 12–17.

Uhrina, M., Hlubik, J. and Vaculik, M. (2013). Correlation between Objective and Subjective Methods Used for Video Quality Evaluation, *Digital Image Processing and Computer Graphics* **11**: 135–146.

Van Nes, F. L., Bouman, M. A. et al. (1967). Spatial modulation transfer in the human eye, *JOSA* **57**(3): 401–406.

Venkatraman, S., Abraham, A. and Paprzycki, M. (2004). Significance of Steganography on Data Security, *The International Conference Information Technology: Coding and Computing*, pp. 347–351.

Voloshynovskiy, S., Herrigel, A., Baumgaertner, N. and Pun, T. (2000). A Stochastic Approach To Content Adaptive Digital Image Watermarking, *Information Hiding* pp. 211–236.

Vose, M. D. (1999). *The Simple Genetic Algorithm: Foundations and Theory*, Vol. 12, MIT press.

Wandell, B. A. (1995). *Foundations of Vision*, Sinauer Associates,.

Wang, H. and Wang, S. (2004). Cyber Warfare: Steganography vs. Steganalysis, *Communications of The ACM* (47): 76–82.

Wang, R., Lin, C. and Lin, J. (2001). Image Hiding By Optimal LSB Substitution And Genetic Algorithm, *Pattern Recognition 34* **3**: 671–683.

Wang, R. Z. and Chen, Y. S. (2006). High-Payload Image Steganography Using Two-Way Block Matching, *IEEE Signal Processing Letters* **13**: 161–164.

Wang, S., Yang, B. and Niu, X. (2010). A secure steganography method based on genetic algorithm, *Journal of Information Hiding and Multimedia Signal Processing* **1**(1): 28–35.

Wang, Z. and Bovik, A. (2002). A Universal Image Quality Index, *Signal Processing Letters* **4**: 81–84.

Wang, Z., Bovik, A. C., Sheikh, H. R. and Simoncelli, E. P. (2004). Image Quality Assessment: From Error Visibility to Structural Similarity, *Image Processing, IEEE Transactions* **13**(600-612).

Wang, Z., Sheikh, H. R. and Bovik, A. C. (2003). *Objective Video Quality Assessment. The Handbook of Video Databases: Design and Applications.*

Wang, Z., Simoncelli, E. P. and Bovik., A. C. (2004). Multiscale Structural Similarity for Image Quality Assessment, *Conference on Signals, Systems and Computers*, pp. 1398 – 1402 Vol.2.

Watson, A. B. (1987). The cortex transform: Rapid computation of simulated neural images, *Computer Vision, Graphics, and Image Processing* **39**(3): 311–327.

Wazirali, R. A. and Chaczko, Z. (2015a). The Use of HVS to Estimate Perceptual Threshold for Imperceptible Steganography, *The 30th International Conference on Image and Vision Computing New Zealand (IVCNZ 2015)*, IEEE.

Wazirali, R. A., Chaczko, Z. and Kale, A. (2014). Digital Multimedia Archiving Based on Optimization Steganography System, *2014 Asia-Pacific Conference on Computer Aided System Engineering (APCASE)*, IEEE, pp. 82–86.

Wazirali, R. and Chaczko, Z. (2015b). Data hiding based on intelligent optimized edges for secure multimedia communication, *Journal of Networks* **10**(8): 477–485.

Wazirali, R. and Chaczko, Z. (2015c). EA Based Heuristic Segmentation For Efficient Data, *International Journal of Computer Applications* **118**(5).

Wazirali, R. and Chaczko, Z. (2016). Hyper Edge Detection with Clustering for Data Hiding, *Journal of Information Hiding and Multimedia Signal Processing (JIHMSP)* .

Wazirali, R., Slehat, S., Chaczko, Z., Borowik, G. and Carrion, L. (2015). Objective quality metrics in correlation with subjective quality metrics for steganography, *Asia-Pacific Conference on Computer Aided System Engineering (APCASE*, IEEE, pp. 238–245.

Wen Jan Chen Chang, Chen, C. and Ngan, H. (2010). High Payload Steganography Mechanism Using Hybrid Edge Detector, *Expert Systems with Applications 37* .

Westfeld, A. and Andreas, P. (1999). Attacks on Steganographic Systems and Genetic Algorithms Application, *New York: Lotus Press.* .

Wu, D.-C. and Tsai, W.-H. (2003). A Steganographic Method For Images By Pixel Value Differencing, *Pattern Recognition Letters 24* pp. 1613–1626.

Wu, H. R. and Rao, K. R. (2006). *Digital Video Image Quality and Perceptual Coding*, crc press edn.

Wu, N. I. and Hwang, M. S. (2006). Data Hiding: Current Status and Key Issues, *International Journal of Network Security* **4**: 1–9.

Yan, X., Wang, S., Li, L., El Latif, A. A. A., Wei, Z. and Niu, X. (2013). A new assessment measure of shadow image quality based on error diffusion techniques, *Journal of Information Hiding Multimedia and Signal Process (JIHMSP)* **4**(2): 118–126.

Yang, C. H., Weng, C. Y., Wang, S. J. and Sun, H. M. (2008). Adaptive data hiding in edge areas of images with spatial lsb domain systems, *IEEE Transactions on Information Forensics and Security* **3**(3): 488–497.

Yang, Y., Sun, Y., Stankovic, V. and Xiong, Z. (2006). Image Data Hiding Based on Capacity Approaching Dirty Paper Coding, *In Proceedings of SPIE* **6072**: 429–439.

Youssef Bassil (2012). Image Steganography based on a Parameterized Canny Edge Detection Algorithm , *International Journal of Computer Applications* **60**(4).

Yu, J.-G., Yoon, E.-J., Shin, S.-H. and Yoo, A.-Y. (2008). A new image steganography based on 2k correction and edge detection, . *Fifth International Conference on Information Technology: New Generations*, IEEE, pp. 563–568.

Yu, L., Zhao, Y., Ni, R. and Zhu, Z. (2009). Pm1 steganography in jpeg images using genetic algorithm, *Soft Computing* **13**(4): 393–400.

Yu, Y. H., Chang, C. C. and Hu, Y. C. (2005). Hiding Secret Data in Images via Predictive Coding , *Pattern Recognition* (38): 691–705.

Zhang, F., Zhang, X. and Zhang, H. (2007). Digital Image Watermarking Capacity and Detection Error Rate, *Pattern Recognition Letters* **28**(1): 1–10.

Zhang, W., Li, L., Zhu, H., Cheng, D., Chu, S. C. and Roddick, J. F. (2014). No-reference quality metric of blocking artifacts based on orthogonal moments, *Journal of Information Hiding and Multimedia Signal Processing* **5**(4): 701–708.

Zhang, X. and Wang, S. (2004). Vulnerability of pixel-value differencing steganography to histogram analysis and modification for enhanced security, *Pattern Recognition Letters* **25**(3): 331–339.

Zhang, X. and Wang, S. (2005). Steganography Using Multiple-Base Notational System and Human Vision Sensitivity, *IEEE Signal Processing Letters,* **12**: 67–70.

Zhu, G. and Sang, N. (2008). An Adaptive Quantitative Information Hiding Algorithm Based on DCT Domain of New Visual Model, *International Symposium on Information Science and Engieering*, pp. 540–550.

Zollner, J., Federrath, H., Klimant, H. and Pfitzmann, A. (1998). Modelling the security of steganographic Systems, *New York: Lotus Press.* .